FY16-17
PGA 582-16-61114-02
Task 3.1

Final Report

Photochemical Modeling of 2017 for the Killeen-Temple-Fort Hood Area

PREPARED UNDER A GRANT FROM THE
TEXAS COMMISSION ON ENVIRONMENTAL QUALITY

The preparation of this report was financed through a contract from the State of Texas through the Texas Commission on Environmental Quality.
The content, findings, opinions and conclusions are the work of the author(s) and do not necessarily represent findings, opinions or conclusions of the TCEQ.

Prepared for:
John Weber
Central Texas Council of Governments
2180 North Main Street
Belton, Texas 76513

Prepared by:
Jeremiah Johnson, Zhen Liu,
Sue Kemball-Cook, Andrew Wentland,
Jaegun Jung, Ross Beardsley,
Ling Huang and Greg Yarwood
Ramboll Environ
773 San Marin Drive, Suite 2115
Novato, California, 94998
www.environcorp.com
P-415-899-0700
F-415-899-0707

September 2017

RAMBOLL ENVIRON

CONTENTS

APPENDICES

TABLES

FIGURES

LIST OF ACRONYMS AND ABBREVIATIONS

APCA	Anthropogenic Precursor Culpability Assessment
AQS	Air Quality System
BCs	Boundary Conditions
BS	Barnett Shale
CAMS	Continuous Air Monitoring Station
CAMx	Comprehensive Air quality Model with extensions
CASTNET	Clean Air Status And Trends Network
CMAQ	Community Multiscale Air Quality Model
CTAIR	Central Texas Air Information and Research
CTCOG	Central Texas Council of Governments
BPA	Beaumont-Port Arthur Area
DDM	Direct Decoupled Method
DFW	Dallas-Fort Worth Area
DV	Design Value
DVC	Current year Design Value
DVF	Future year Design Value
ECS	Equipment Concentration Site
EGU	Electrical Generating Unit
EI	Emissions Inventory
EPA	Environmental Protection Agency
GEOS	Goddard Earth Observing System
GOM	Gulf Of Mexico
HGB	Houston-Galveston-Brazoria Area
HGBPA	Houston-Galveston-Brazoria-Beaumont-Port Arthur Area
HOTCOG	Heart Of Texas Council of Governments
HPMS	Highway Performance Monitoring System
H.R.	U.S. House of Representatives
HS	Haynesville Shale
ICs	Initial Conditions
KTF	Killeen-Temple-Fort Hood
LAI	Leaf Area Index
LI	Local Increment
MADIS	Meteorological Assimilation Data Ingest System
MATES	Military Equipment and Training Site
MATS	Modeled Attainment Test Software
MB	Mean Bias
MDA8	daily maximum 8-hour average
ME	Mean Error
MEGAN	Model of Emissions of Gases and Aerosols from Nature
MOZART	Model for OZone and Related chemical Tracers
MPE	Model Performance Evaluation

MSKF	Multi-Scale Kain Fritsch
MW	MegaWatt
NAAQS	National Ambient Air Quality Standard
NAM	North American Model
NCAR	National Center for Atmospheric Research
NCEP	National Centers for Environment Prediction
NETX	NorthEast Texas
NMB	Normalized Mean Bias
NME	Normalized Mean Error
NNA	Near Non-Attainment Area
NO	Nitric Oxide
NOAA	National Oceanic and Atmospheric Administration
NOx	Oxides of Nitrogen
NRT	Near Real-Time
OA	Organic Aerosol
O&G	Oil and Gas
OSAT	Ozone Source Apportionment Technology
PBL	Planetary Boundary Layer
ppb	parts per billion
PRISM	Parameter-elevation Relationships on Independent Slopes Model
Q-Q	Quantile-Quantile
RE	Ramboll Environ
RMSE	Root Mean Squared Error
RPO	Regional Planning Organization
RRF	Relative Response Factor
RRTM	Rapid Radiative Transfer Model
RRTMG	Rapid Radiative Transfer Model for GCM applications
SCR	Selective Catalytic Reduction
SIP	State Implementation Plan (for the ozone NAAQS)
TCEQ	Texas Commission on Environmental Quality
tpd	tons per day
TSTC	Texas State Technical College
TUV	Tropospheric UltraViolet radiative transfer model
TXDOT	Texas Department of Transportation
UAA	Unmonitored Area Analysis
UCM	Urban Canopy Model
U.S.	United States of America
USAEC	United States Army Environmental Command
VMT	vehicle miles traveled
VOC	Volatile Organic Compound
WRF	Weather Research and Forecast model
YSU	Yonsei University WRF planetary boundary layer parameterization

1.0 EXECUTIVE SUMMARY

In this report, we summarize the development of a 2017 ozone model for the Killeen-Temple-Fort Hood (KTF) 7-county area, and report on the application of the model to evaluate: (1) the local emissions source categories that make the largest contributions to ozone at the Killeen Skylark (Continuous Air Monitoring Station [CAMS] 1047) and Temple Georgia (CAMS 1045) monitors; (2) ozone sensitivity to emissions from the Panda Temple power plant and Fort Hood military base; and (3) ozone impacts in the KTF area as a result of oil and gas (O&G) production in the major shale regions in East Texas as well as local O&G production in the KTF counties. We used TCEQ's latest 2017 future year photochemical modeling platform to address issues relevant to ozone formation within and transport into the KTF area in 2017 and evaluated the models' skill in simulating ozone in Central Texas using a 2012 historical modeling episode. We found that the model showed improved skill in simulating ozone at the Killeen monitor – particularly in reducing persistent overestimates of ozone – relative to the original phase of 2012 modeling conducted in 2015.

The main results of the CAMx modeling of 2017 were:

- KTF area emissions of ozone precursors (oxides of nitrogen [NOx] and volatile organic compounds [VOC]) are projected to decrease between 2012 and 2017.
- KTF area ozone design values are projected to decrease between 2012 and 2017.
- The Killeen monitor model-projected design value for 2017 is 67.5 ppb, which attains the 2015 NAAQS of 70 ppb.
- For CAMS 1047, the contribution of ozone and ozone precursors transported into the KTF area (63.9 ppb) to the 2017 design value is far larger than the contribution of ozone from local KTF emissions sources (3.6 ppb).
- The largest contributions to CAMS 1047 design value from local KTF area emissions are from on-road mobile sources such as cars and trucks (1.3 ppb).
- The combined contribution from Eagle Ford, Haynesville and Barnett Shale O&G sources to the 2017 Killeen monitor ozone design value is 0.9 ppb, which exceeds the contribution of KTF Area O&G emissions sources (0.1 ppb).
- The impact of the Panda Temple EGU on the 2017 design value at CAMS 1047 is less than 0.1 ppb. The maximum impact on KTF area ozone design values is 0.2 ppb near Belton.
- The impact of the Fort Hood military base on the 2017 design value at CAMS 1047 is 0.1 ppb. The maximum impact on KTF area ozone design values is 0.7 ppb near Fort Hood.
- The 2017 modeling showed ozone formation in the KTF area is limited by the amount of available NOx. This finding is consistent with previous KTF studies.

- KTF area emission reduction efforts should continue to focus on NOx reductions rather than VOC reductions.

We recognize that Rider 7 funding is no longer available for photochemical modeling to support future air quality planning and make no recommendations for further model development at this time. However, the 2017 modeling platform uses an emission inventory that is applicable to the present day and could be used in the near term by Central Texas Air Information and Research (CTAIR) Advisory Committee for air quality planning.

- We recommend using the 2017 ozone model to quantify ozone impacts of new/proposed emissions sources or changes in emissions from existing sources.
- Analysis of high ozone days when monitored ozone at CAMS 1047 and CAMS 1045 exceed the 2015 National Ambient Air Quality Standard for ozone (70 ppb) continues to be important in understanding the causes of high ozone at the monitor. High ozone day analysis can also identify days which may be excluded from the design value calculation under the EPA's Exceptional Events Rule[1], potentially lowering the design values at the Killeen Skylark and Temple Georgia monitors.
- As of the writing of this report, the 2017 design value for CAMS 1047 stands at 67 ppb. The 2017 design value for CAMS 1045 stands at 69 ppb. Both design values are below the 2015 National Ambient Air Quality Standard for ozone (70 ppb). If design values in the KTF area were to approach 70 ppb in the future, routine daily photochemical modeling designed to identify the influence of exceptional events on KTF area ozone would be important. Ozone impacts from wildfires, stratospheric ozone or international transport could all be modeled with a short lag time (on the order of 2-3 days) and could be used as a possible screening tool for exceptional events. Ramboll Environ has developed a modeling platform for TCEQ to support this type of analysis.

[1] The Exceptional Events Rule states that if an exceedance of the ozone NAAQS can be shown to be caused by an uncontrollable, unusual event such as a wildfire or stratospheric ozone intrusion, the exceedance day may be excluded from the calculation of the monitor's ozone design value, potentially lowering the design value and even changing nonattainment status to attainment.

2.0 INTRODUCTION

The Central Texas Council of Governments (CTCOG) area is comprised of San Saba, Mills, Lampasas, Hamilton, Coryell, Bella and Milam Counties. This region, referred to as the Killeen-Temple-Fort Hood (KTF) region hereafter, lies on the central Texas plain between the major metropolitan areas of Dallas-Fort Worth (DFW) to the north and Austin to the south. A map of the area is shown in Figure 2-1. At the time of the last U.S. Census in 2010, Austin had an estimated population of 810,759[2] and the DFW area had an estimated population of 6,371,773[3] and was the fourth largest metropolitan area in the U.S.[4]. Ozone precursor emissions, primarily as NOx or VOCs, from both Austin and the DFW area have been shown to influence ozone concentrations at the Killeen Skylark monitor within the KTF Area (e.g. Parker et al., 2013). In addition, ozone precursor emissions from other less populous urban areas that are located closer to the Bell County monitors can also influence ozone in the KTF Area. In particular, Killeen, Waco and Temple were estimated by the 2010 Census to have populations of 127,911[5], 124,810[6], and 66,312[7], respectively. Ozone precursor emissions from a variety of different emissions sources (e.g. cars, trucks and industrial facilities) in these urban areas can contribute to ozone concentrations in the KTF Area.

Figure 2-1 shows Interstate highway I-35 intersecting Bell County. I-35 is a major roadway that extends across Texas from Mexico to Oklahoma and passes through Austin and San Antonio as well as Waco and the DFW area. Analysis of the 2006 TCEQ emission inventory for Bell County performed by Parker et al. (2013) suggested that emissions from the heavily-trafficked I-35 highway makes an important contribution to the NOx emission inventory for Bell County.

2.1 Ozone Attainment Status of the KTF Area

In order to protect public health and the environment, the U.S. Environmental Protection Agency (EPA) sets a National Ambient Air Quality Standard (NAAQS) for ground-level ozone. Under the Clean Air Act, the EPA is required to: (1) review the NAAQS periodically, and (2) designate areas as meeting or not meeting the standard within two years of the NAAQS promulgation. Areas that meet the standard are designated as attainment areas, whereas areas that do not meet the standard are designated as nonattainment areas. In 2008, the ozone NAAQS was revised to 75 parts per billion (ppb), and in 2012, the KTF area was designated as being in attainment of the 75 ppb 2008 NAAQS. On October 1, 2015, the EPA lowered the

[2] http://quickfacts.census.gov/qfd/states/48/4805000.html
[3] http://www.census.gov/population/www/cen2010/cph-t/CPH-T-2.pdf
[4] http://www.census.gov/compendia/statab/2012/tables/12s0020.pdf
[5] http://quickfacts.census.gov/qfd/states/48/4839148.html
[6] http://quickfacts.census.gov/qfd/states/48/4876000.html
[7] http://quickfacts.census.gov/qfd/states/48/4872176.html

ozone NAAQS from 75 ppb to a more protective standard of 70 ppb. The EPA has indicated that final attainment designations for the 2015 ozone NAAQS will be based on 2014-2016 data[8].

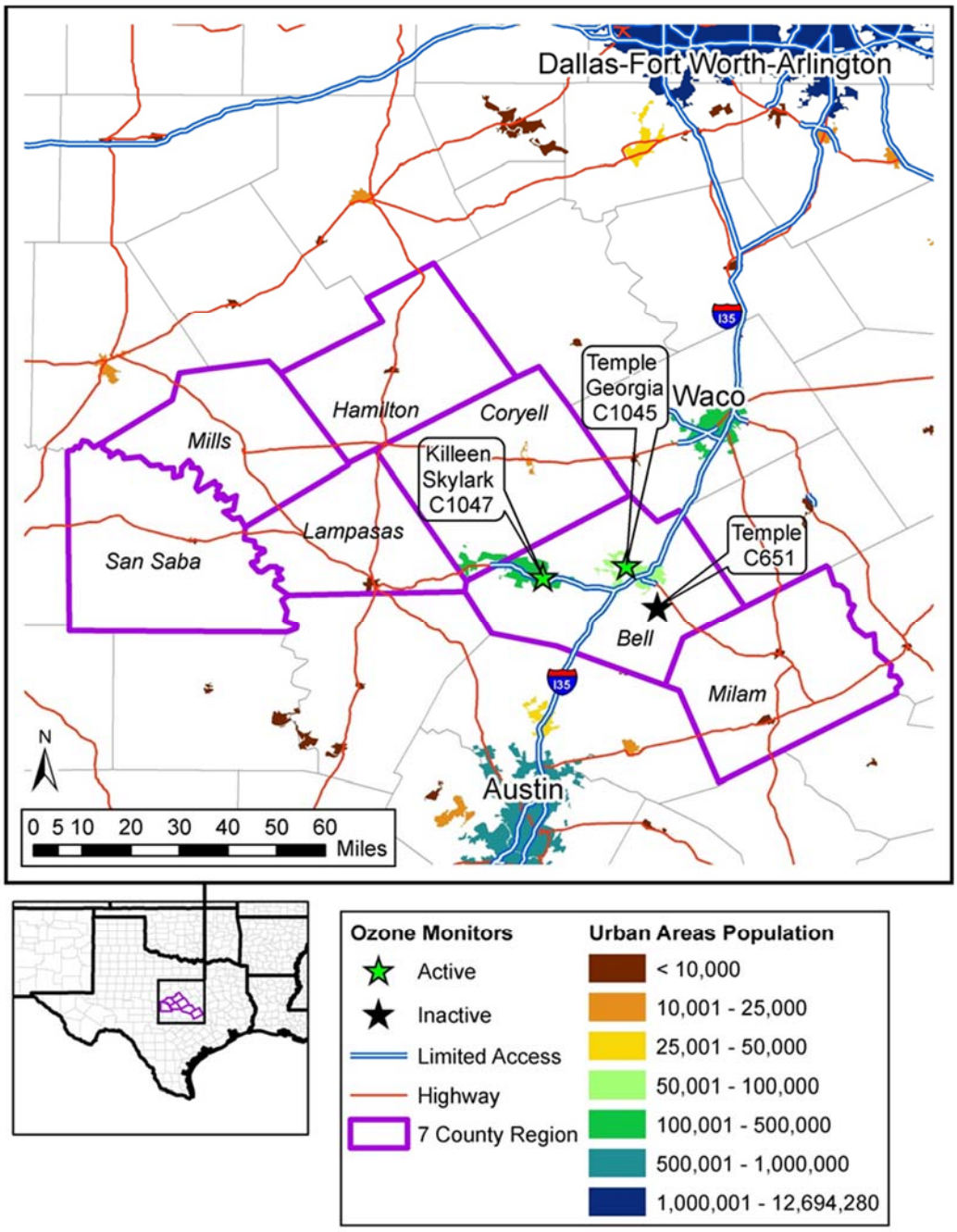

Figure 2-1. The seven county KTF Area, location of CAMS monitors in Bell County, population distributions and major roadways in the surrounding region.

[8] https://www.epa.gov/sites/production/files/2016-02/documents/ozone-designations-guidance-2015.pdf

The metric used to determine attainment of the ozone NAAQS is the 8-hour ozone design value (DV), which is defined as the annual fourth highest daily maximum 8-hour average concentration (MDA8) averaged over three years. A DV of 70 ppb attains the 2015 ozone NAAQS, while a DV of 71 ppb violates the 2015 ozone NAAQS.

Ozone measurements from the Texas Commission on Environmental Quality's (TCEQ's) Continuous Air Monitoring Station (CAMS) in Bell County (Killeen Skylark [CAMS 1047] and Temple Georgia [CAMS 1045]) are used to determine whether the KTF is in compliance with the ozone NAAQS. CAMS 1047 is located at the Skylark Field general aviation airport in Killeen and CAMS 1045 is located about 5 miles ENE of the Temple city center. Ozone monitors nearest to the KTF area and active in 2016 are displayed in Figure 2-2: Waco Mazanec (CAMS 1037), CAPCOG Lake Georgetown (CAMS 690), CAPCOG Hutto College Street (CAMS 6602) and Austin Audubon (CAMS 38). The meteorological monitoring stations at the Waco Regional Airport (KACT) and Burnet County Airport (KBMQ) are also shown. KTF area monitor location and other information are presented in Table 2-1.

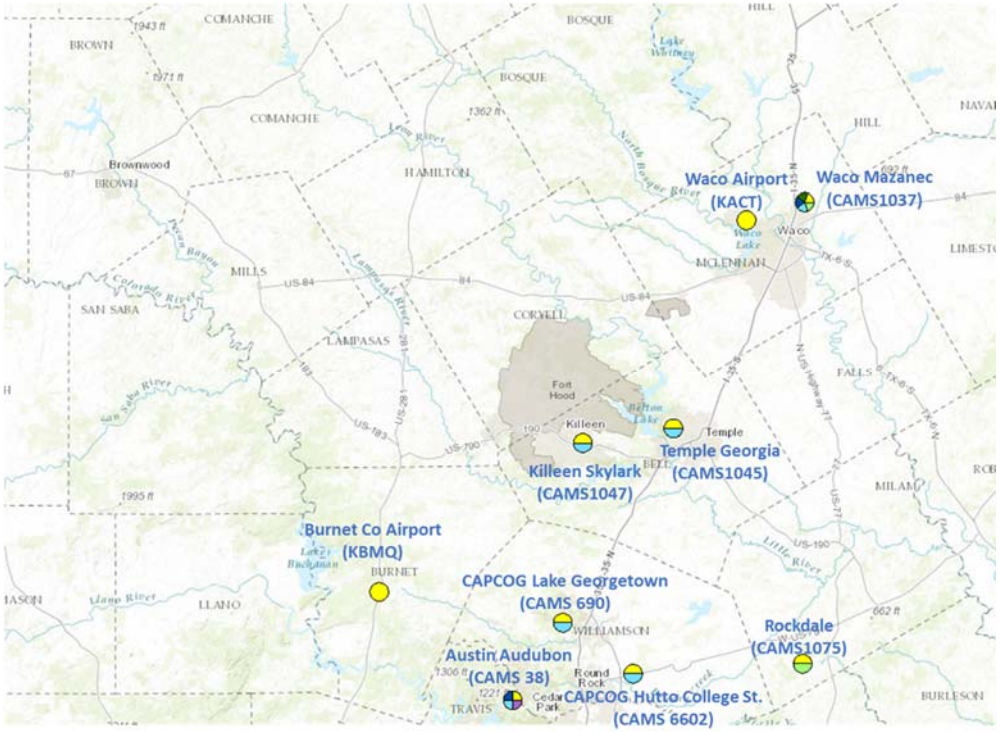

Figure 2-2. Ozone and meteorological monitoring stations active in the KTF area and vicinity during 2017. Adaptation of TCEQ figure[9].

[9] https://www.tceq.texas.gov/gis/geotam-viewer

Table 2-1. Site location and monitoring information for KTF area ozone monitors.

	Killeen Skylark	Temple Georgia
EPA Site Number	480271047	480271045
CAMS	1047	1045
Activation Date	June 11, 2009	October 04, 2013
Current Status	Active	Active
State	Texas	Texas
County	Bell	Bell
City	Killeen	Temple
Address	1605 Stone Tree Drive	8406 Georgia Avenue
ZIP	76543	76502
Latitude	31º 5' 17'' North (31.0880022º)	31º 7' 21'' North (31.1224187º)
Longitude	-97º 40' 47'' West (-97.6797343º)	-97º 25' 52'' West (-97.4310523º)
Elevation	256.0 m	188.0 m
Owned By	TCEQ	TCEQ

On August 3, 2016, the TCEQ approved designation recommendations for the 2015 NAAQS and on September 30, 2016, Governor Greg Abbott provided these recommendations to EPA[10]. TCEQ recommended that KTF Area counties be classified as follows:

- An attainment designation is recommended for Bell County since regulatory ozone monitor data for Killeen Skylark CAMS 1047 in Bell County is certified from 2013 through 2015 as complete and meeting the NAAQS. (The Temple Georgia CAMS 1045 monitor was activated in October 2013 and therefore did not have three complete years of measurements.)
- An unclassifiable/attainment designation is recommended for all other KTF Area counties, which do not have ozone monitors.

The EPA has a statutory obligation to finalize designations by October 1, 2017. In June 2017, the EPA administrator announced he was using his authority to extend the deadline for promulgating designations for the 2015 ozone NAAQS by one year. However, on August 10, 2017 the EPA withdrew the extension[11], therefore, the current deadline for the EPA to promulgate initial designations is October 1, 2017.

[10] September 30, 2016 letter from Texas Governor Greg Abbot to EPA Assistant Administrator Janet McCabe and Regional Administrator Ron Curry: State Designation Recommendations for the 2015 Ozone NAAQS. http://www.tceq.texas.gov/assets/public/implementation/air/sip/ozone/2015Designations/TXRecommendation/2015Ozone_DesignationRecommendation_Submittal_to_EPA.pdf

[11] https://www.gpo.gov/fdsys/pkg/FR-2017-08-10/pdf/2017-16901.pdf

There remains some uncertainty in the designation schedule due to ongoing legislation in the U.S. Congress. On June 8, 2016, the House of Representatives (H.R.) passed the Ozone Standards Implementation Act of 2016 (H.R. 4775)[12]; a parallel bill, the Ozone Standards Implementation Act of 2017 (H.R. 806)[13] was introduced in the House on February 1, 2017. If H.R. 4775 or H.R. 806 becomes law as currently written, the schedule for finalizing designations would be delayed by eight years. States would be required to submit designation recommendations in October 2024 and the EPA would be required to finalize recommendations in October 2025.

At the end of 2016, the 8-hour ozone DV for both CAMS 1047 and CAMS 1045 was 67 ppb[14], which is lower than the 70 ppb 2015 ozone NAAQS. Although the current DV is lower than the NAAQS, it has exceeded 70 ppb as recently as 2014. Figure 2-3 presents DVs for CAMS 1047 and CAMS 1045 from 2009 to 2016 in relation to the historical 8-hour ozone NAAQS. As of the writing of this report on September 1, 2017, the 2017 design values for CAMS 1047 and CAMS 1045 are 67 and 69 ppb, respectively.

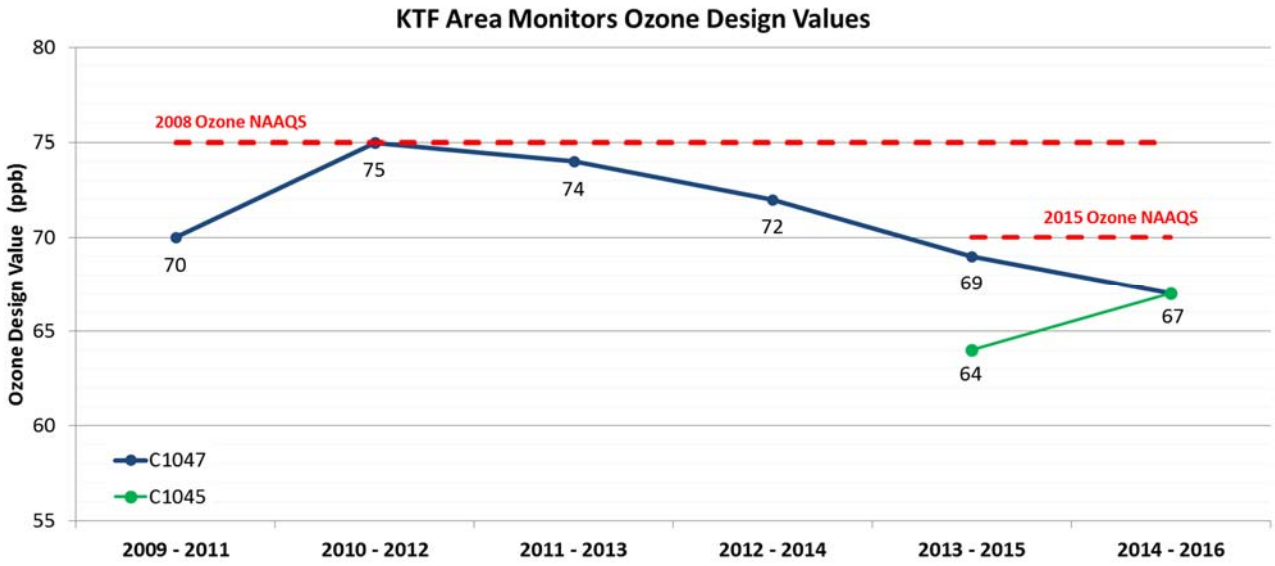

Figure 2-3. Ozone design values for the Killeen Skylark (CAMS 1047) and Temple Georgia (CAMS 1045) monitors during 2009 – 2016.

[12] https://www.congress.gov/bill/114th-congress/house-bill/4775
[13] https://www.congress.gov/bill/115th-congress/house-bill/806
[14] https://www.tceq.texas.gov/cgi-bin/compliance/monops/8hr_attainment.pl

2.2 KTF Area Air Quality Planning

The CTCOG is participating in the U.S. EPA's Ozone Advance Program[15] on behalf of the KTF Area of Central Texas. Air quality planning in Central Texas is led by CTCOG and the Central Texas Air Information and Research (CTAIR) Advisory Committee. CTAIR is a voluntary stakeholder group that was formed in 2016 to fill the need for an organized and comprehensive approach to improving air quality based on regional needs. CTAIR consists of representatives from local government, local business and industry, Texas Commission on Environmental Quality (TCEQ) staff and the general public. More information on CTCOG and CTAIR may be found at https://ctcog.org/regional-planning/air-quality/ and http://ctair.org/.

Since 2014, the KTF area has participated in the TCEQ's Rider 7/8 Air Quality Planning Program for near nonattainment areas. The program is named after the Texas Legislature Rider under which funding was allocated. The name of the program was changed to Rider 7 in 2015 following the 2015 session of the Texas Legislature and renewal of the air quality program under a different Rider. The Rider 7 Air Quality Planning Program was not renewed for the 2018-2019 biennium.

CTCOG joined EPA's Ozone Advance Program in May 2017. Ozone Advance is designed to foster collaboration between the EPA and local governments to reduce emissions of ozone precursors so that current attainment areas can continue to maintain compliance with the NAAQS. As part of its participation in Ozone Advance, CTCOG provided EPA an Ozone Action Plan (Kemball-Cook et al., 2017) that describes the emissions reductions measures and/or programs that have been and will be implemented in the 7-county area and sets a schedule for the implementation of each measure/program[16].

As part of its air quality planning, CTCOG has carried out ozone modeling to understand the formation, transport and fate of ozone in the KTF area- and evaluate the ozone impacts of new emissions sources.

In this report, we describe the development and application of an ozone model for the KTF area for the May – September ozone season for a 2012 historical year and a 2017 future year. This study is intended to address needed improvements in photochemical model performance identified in KTF's previous 2012 modeling and also to improve understanding of ozone formation within and transport into the KTF area in a present-day 2017 emissions scenario.

Section 3 describes the joint (TCEQ and Ramboll Environ) development and final configuration of the 2012/2017 seasonal modeling platform. Further details on model development and evaluation are provided in Appendix A. The 2017 future year modeling scenario was applied to evaluate current year emissions sources that influence KTF area ozone (Section 4). In Section 5,

[15] http://www3.epa.gov/ozoneadvance/
[16] https://www.epa.gov/advance/central-texas

we apply the 2017 model to evaluate ozone impacts of the Panda Temple Power Plant and Fort Hood military base. Section 6 provides a summary of the modeling results and recommendations for future ozone modeling efforts in the KTF area.

3.0 SUMMER 2017 OZONE MODELING PLATFORM

In this section, we present an overview of the development of a Comprehensive Air quality Model with Extensions (CAMx; Ramboll Environ, 2017) summer 2017 ozone modeling platform. The 2017 modeling platform was developed by the TCEQ for State Implementation Plan (SIP) modeling and uses a 2017 future year emission inventory together with weather data for May-September 2012. The model uses emission inputs that are as close as possible to present-day conditions and weather conditions from the 2012 ozone season, which had several extended periods of high ozone in East Texas when high ozone occurred in the KTF area.

Development of an ozone model requires evaluating the model using a historical ozone episode to determine whether the model provides a realistic simulation of the processes that cause high ozone in the area of interest. Once the model has been shown to simulate ozone reasonably well, the model can be used with future year emission inventories. For this modeling, the historical episode was 2012 and the future year was 2017. Previous KTF ozone modeling also used the TCEQ's June 2012 episode.

Previous KTF modeling with the June 2012 episode showed an overall high bias at CAMS 1047, but underestimates of peak ozone on the days when observed ozone was highest (Kemball-Cook et al., 2015). During the 2016-2017 biennium, Ramboll Environ performed extensive evaluation of the June 2012 episode and sensitivity testing to improve model performance in simulating ozone at CAMS 1047. In 2016, the TCEQ expanded the June 2012 episode so that it encompassed the entire 2012 ozone season; this is consistent with current EPA modeling guidance that recommends modeling a full ozone season for air quality planning[17]. Ramboll Environ evaluated the performance of the expanded May-September 2012 model at CAMS 1047 and other monitors in the vicinity of the KTF area and made further efforts to improve the model's ability to simulate KTF area ozone. While the underestimates of peak ozone on days when observed ozone was highest are still found at CAMS 1047, the overall high bias is substantially reduced. We do not anticipate substantial impacts to the source sensitivity and source apportionment analyses resulting from the ozone underestimates.

All model improvement efforts and the final model configuration that was used in the 2017 modeling presented in this report are documented in Appendix A.

Figure 3-1 presents the CAMx modeling domains used for the ozone modeling platform. These domains are the TCEQ State Implementation Plan (SIP) modeling domains, which have been used for previous KTF modeling. The 36 km modeling domain encompasses the continental U.S. and parts of Canada and Mexico. The 12 km grid includes Texas and adjacent states and the 4 km grid is centered on East Texas.

[17] https://www3.epa.gov/scram001/guidance/guide/Draft_O3-PM-RH_Modeling_Guidance-2014.pdf

Figure 3-1. CAMx 36/12/4 km modeling domains developed by TCEQ. TCEQ figure[18].

[18] https://www.tceq.texas.gov/airquality/airmod/data/domain

4.0 2017 OZONE SOURCE APPORTIONMENT MODELING

In this section, we present results of two 2017 ozone source apportionment simulations. In a source apportionment simulation, the photochemical model estimates the contributions from multiple emissions source regions, emissions source types, and pollutant types to ozone throughout the modeling domain. The first simulation was designed to examine ozone impacts from the major emissions sectors within the KTF region, while the other simulation was designed to estimate the ozone impacts of oil and gas development from the major shale regions in East Texas and Louisiana.

This analysis is designed to be relevant to current emissions levels, rather than historical emissions, and so uses a 2017 TCEQ emission inventory. As described in Appendix A, the 2012 historical modeling episode was evaluated against observed data and we determined that the model performs well enough in simulating observed ozone to be used as a tool for understanding KTF area air quality. Then, we used the CAMx model with TCEQ's 2017 emissions modeling platform to conduct a source apportionment analysis for the KTF area. This configuration is a 2017 future year simulation using 2012 as the base year. All CAMx model inputs from the 2012 historical year were held constant for the 2017 future year scenario except for: (1) 2012 anthropogenic emissions inventory was replaced by 2017 anthropogenic emissions and (2) 2012 CAMx model initial conditions and 36 km grid boundary conditions were replaced by 2017 initial and boundary conditions. Both sets of updated inputs were obtained from TCEQ's Houston SIP modeling database[19].

EPA's Modeled Attainment Test Software (MATS) tool was used to project 2017 future year design values (DV) at monitoring locations. We followed EPA's guidance for performing modeled ozone attainment demonstration as outlined in the EPA's current 8-hour ozone and modeling guidance document (EPA, 2014). The MATS tool and ozone DV analysis method is described in Appendix C.

4.1 2017 KTF Emissions Overview

In this section, we summarize the 2017 KTF area emissions inventory used in this study. We present information about emissions in the KTF region as well as oil and gas emissions within and outside the KTF region. This section provides context for the ozone source apportionment analysis presented in Section 4.3 that examines contributions from emissions from local sources in addition to emissions from oil and gas shale regions from outside the KTF region.

We present 2012 and 2017 ozone season average NOx emissions for the 7-county KTF region by anthropogenic source sector (Point, Off-road, Oil+Gas, Area, On-road, and Total) for 2012 (blue) and 2017 (red) in Figure 4-1.

[19] https://www.tceq.texas.gov/airquality/airmod/data/tx2012

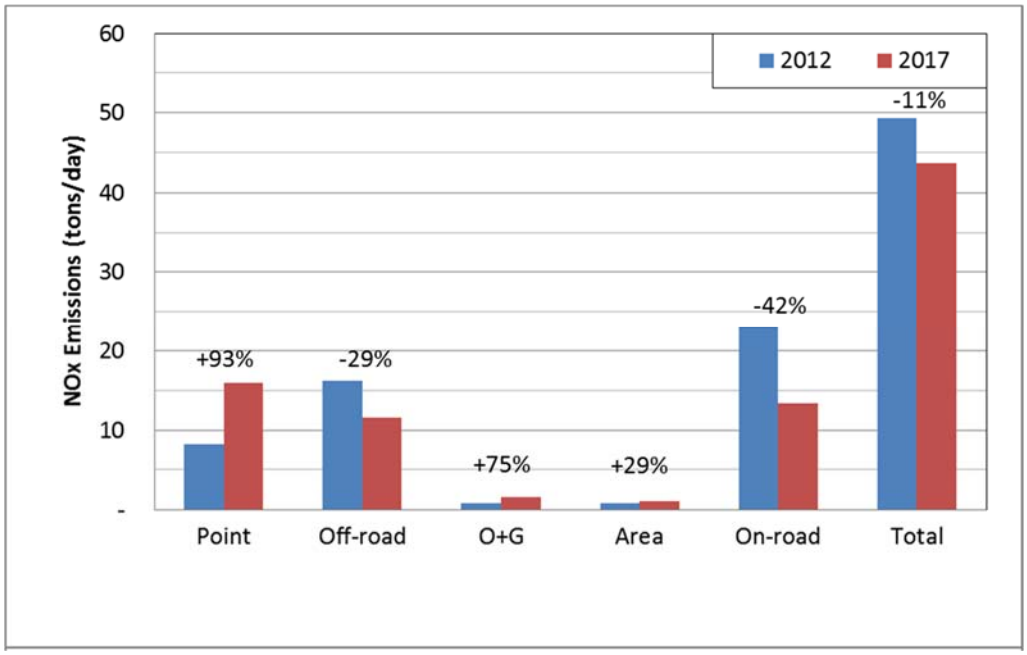

Figure 4-1. Anthropogenic NOx emissions totals (tpd) by source sector for the 7-county KTF region for 2012 (blue) and 2017 (red). Data labels show percent change from 2012 to 2017.

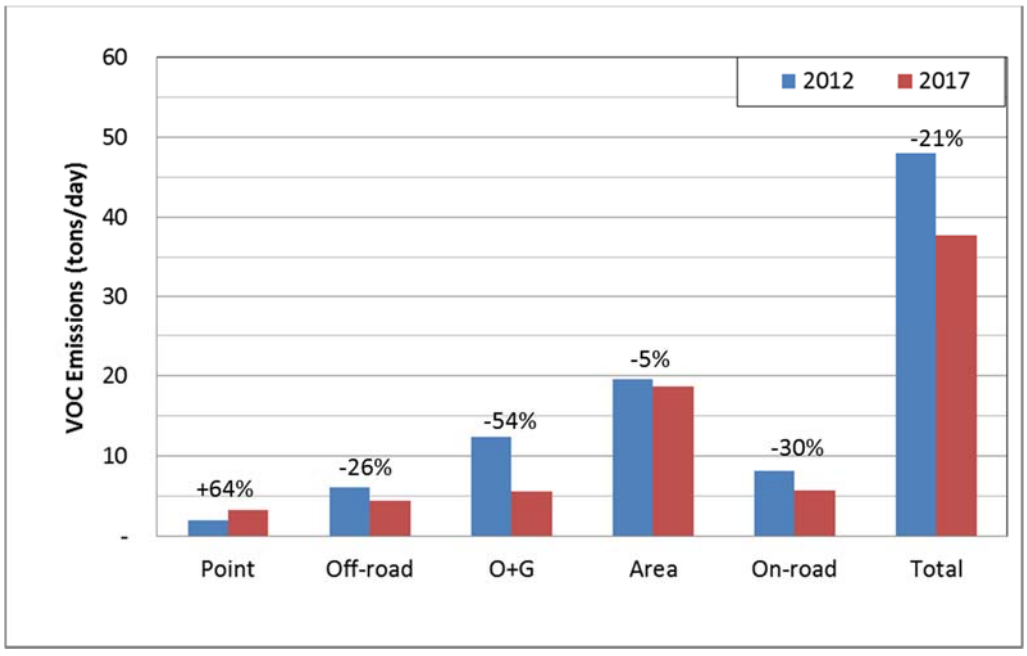

Figure 4-2. Anthropogenic VOC emissions totals (tpd) by source sector for the 7-county KTF region for 2012 (blue) and 2017 (red). Data labels show percent change from 2012 to 2017.

These emissions totals come from TCEQ's latest emissions inventories[20] for 2012 and 2017 developed for the Houston SIP and which we subsequently used for the base and future year modeling conducted in this study. Figure 4-2 presents the same information but for VOC emissions. Despite an overall decrease of NOx emissions from 2012 to 2017 (-11%), point source emissions increase by 93%. Point source NOx emissions for 2012 and 2017 are shown for the largest NOx emitters in the 7-county area in Table 4-1. The largest change in point source NOx emissions is the increase of 4.8 tpd from the Sandow Power Plant in Milam County. The next largest change comes from the Fort Hood military base, which increased by 1.8 tpd from 2012 to 2017. Finally, the Panda Temple Power Plant, which came online in 2014, has 1.1 tpd NOx emissions in 2017. Together these three sources contribute 98.5% of the NOx emissions from point sources located within the KTF region.

Table 4-1. TCEQ 2012 and 2017 NOx emissions for selected large point sources in the KTF 7-county area.

Facility	NOx Emissions (tpd)		
	2012	2017	2017-2012
Sandow Power Plant	7.92	12.73	4.81
Fort Hood Military Base	0.08	1.87	1.79
Panda Temple Power Plant	0.00	1.06	1.06
Total Emissions	**8.00**	**15.66**	**7.66**

We present a map of oil and gas well locations in Texas in Figure 4-3. The KTF region lies to the north and northwest of the Eagle Ford Shale region, which appears as an arc of wells beginning near Laredo, passing south of San Antonio and east of Austin. The Haynesville Shale and Barnett Shale regions lie to the east and north of the KTF region, respectively. The KTF Conceptual Model of Ozone (Kemball Cook et al., 2015; Parker et al., 2013) indicates that on high ozone days at CAMS 1047, these shale regions can be upwind of the KTF area. In Section 4.3, we present an ozone source apportionment analysis that tracks impacts on KTF area ozone from oil and gas emissions in these shale regions.

[20] https://www.tceq.texas.gov/airquality/airmod/data/tx2012

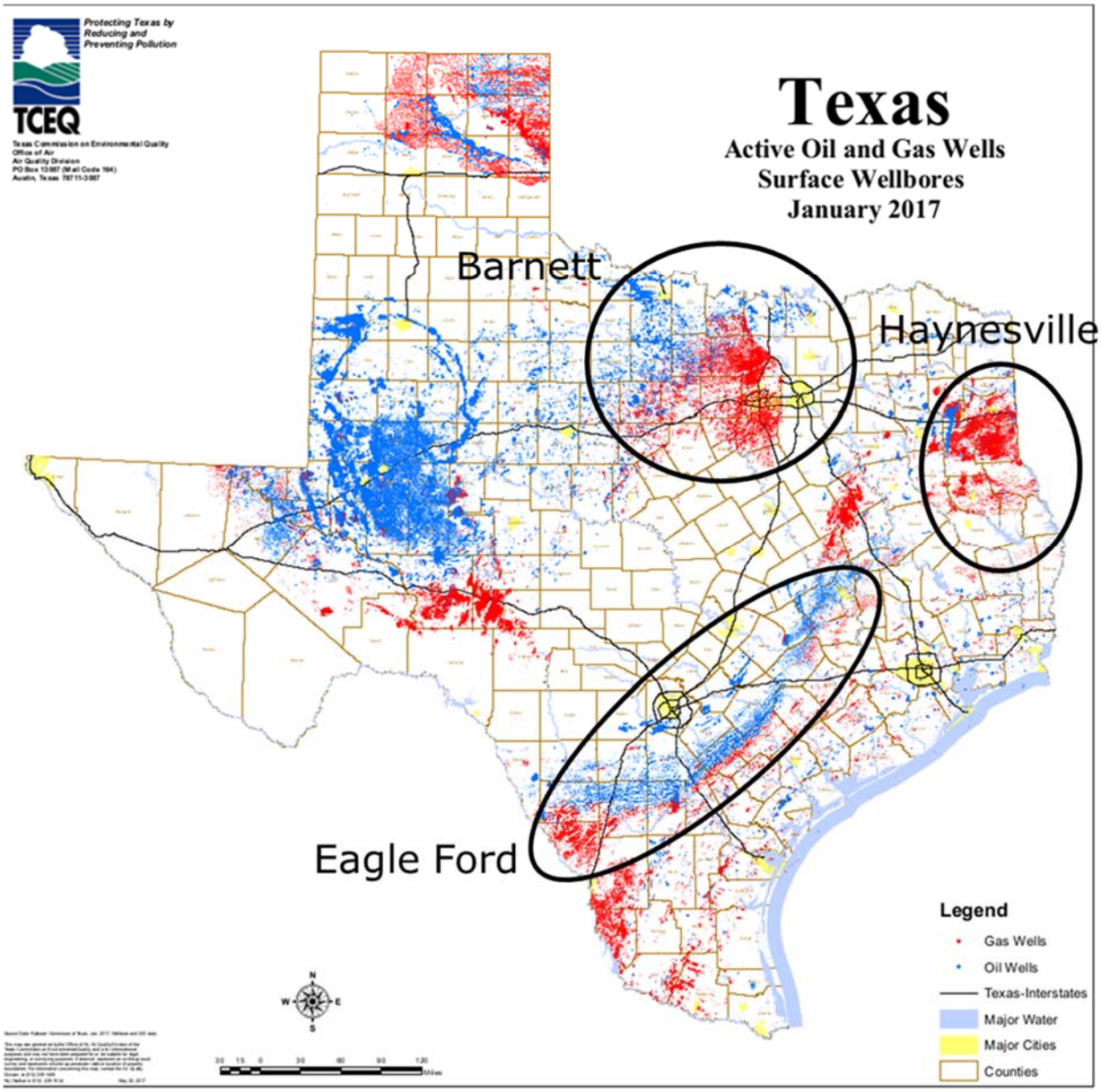

Figure 4-3. Texas active oil (blue) and gas (red) wells in January 2017. Base map generated and provided by TCEQ.

Figure 4-4 presents the same information as in Figure 4-3, but is focused on the 7-county KTF region. According to the map, all of the oil wells (blue) in the KTF region are located in Milam County. There are very few gas wells (red) across the KTF counties, with wells located in Hamilton, Milam and Mills counties.

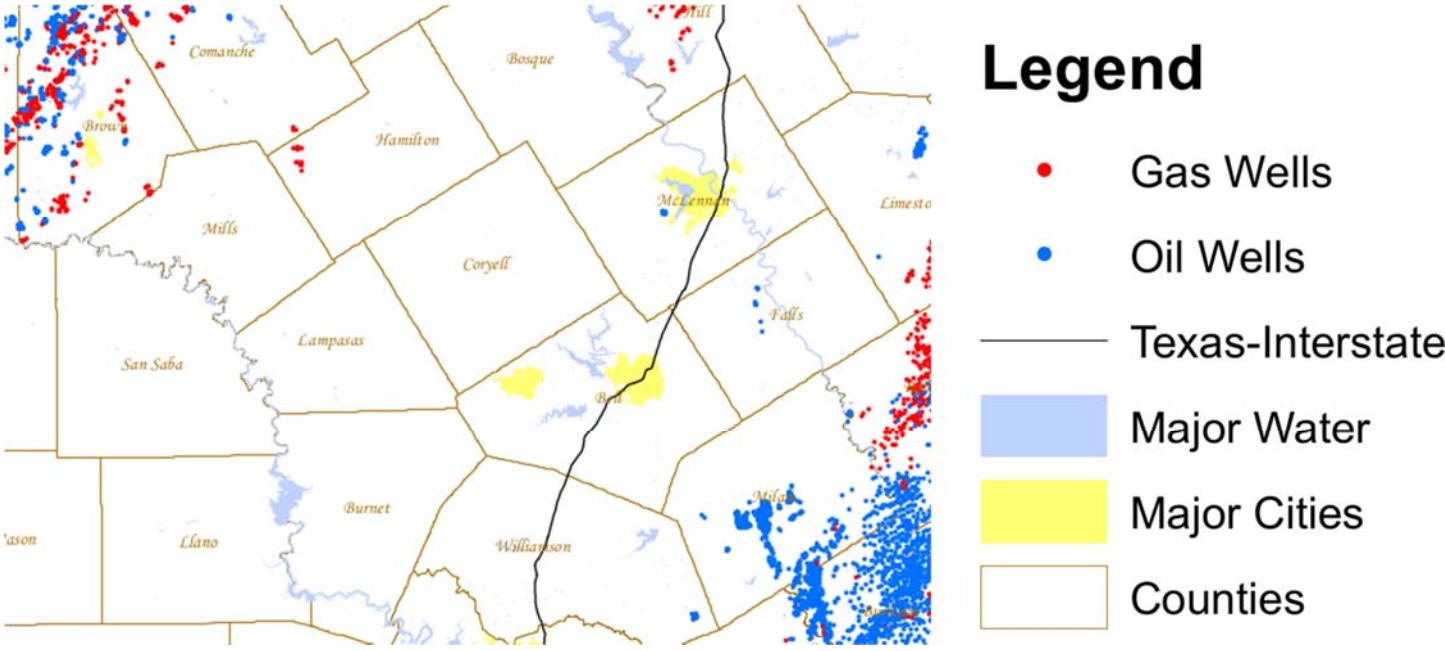

Figure 4-4. Active oil (blue) and gas (red) wells in January 2017 zoomed in to KTF region. Map generated and provided by TCEQ.

TCEQ O&G emissions for the KTF counties for the years 2012 and 2017 are shown in Table 4-2. O&G NOx emissions from the KTF counties are relatively small, with NOx emissions less than 2 tpd for the entire area. O&G VOC emissions are larger (12 tpd) but make up a small fraction of the total KTF area emission inventory (731 tpd), which is dominated by biogenic VOC (683 tpd). Nearly all NOx and VOC emissions occur in Milam County. The reason for the small increase in NOx emissions in Milam County in 2017 relative to 2012 is unclear. We suspect that differences in TCEQ emission estimation methods in the 2012 and 2017 inventories may explain this small increase in NOx emissions despite reductions in both O&G production and VOC emissions.

Table 4-2. O&G emissions for the KTF 7-county area in the TCEQ 2012 and 2017 emission inventories.

	O&G NOx Emissions (tpd)				O&G VOC Emissions (tpd)		
County	2012	2017	2017-2012		2012	2017	2017-2012
Bell	-	-	-		-	-	-
Coryell	-	-	-		-	-	-
Hamilton	0.01	0.01	0.00		0.04	0.03	-0.01
Lampasas	-	-	-		0.01	-	-0.01
Milam	0.91	1.61	0.70		12.28	5.59	-6.69
Mills	-	-	-		0.01	0.01	0.00
San Saba	-	-	-		-	-	-
Total	0.92	1.62	0.70		12.34	5.63	-6.71

4.2 Description of the CAMx APCA Ozone Source Apportionment Tool

The CAMx Anthropogenic Precursor Culpability Assessment (APCA) source apportionment tool uses multiple tracer species to track the fate of ozone precursor emissions (VOC and NOx) and the ozone formation caused by these emissions within a simulation. The tracers operate as spectators to the normal CAMx calculations so that the underlying CAMx-predicted relationships between emission groups (sources) and ozone concentrations at specific locations (receptors) are not perturbed. Tracers of this type are conventionally referred to as "passive tracers," however it is important to realize that the tracers in the APCA tool track the effects of chemical reaction, transport, diffusion, emissions and deposition within CAMx. In recognition of this, they are described as "ozone reaction tracers." The ozone reaction tracers allow ozone formation from multiple "source groupings" to be tracked simultaneously within a single simulation. A source grouping can be defined in terms of geographical area and/or emission category. So that all sources of ozone precursors are accounted for, the CAMx boundary conditions and initial conditions are always tracked as separate source groupings. This allows an assessment of the role of transported ozone and precursors in contributing to high ozone episodes within the KTF area.

The methodology is designed so that all ozone and precursor concentrations are attributed among the selected source groupings at all times. Thus, for all receptor locations and times, the ozone (and ozone precursor) concentrations predicted by CAMx are attributed among the source groupings. The methodology also estimates the fractions of ozone arriving at the receptor that were formed en-route under VOC- or NOx-limited conditions. This information suggests whether ozone concentrations at the receptor may be responsive to reductions in VOC and NOx precursor emissions and can guide the development of additional sensitivity analyses.

APCA differs from the standard CAMx Ozone Source Apportionment Tool (OSAT) in recognizing that certain emission groups are not controllable (e.g., biogenic emissions) and that apportioning ozone production to these groups does not provide information that is relevant to development of control strategies. To address this, in situations where OSAT would attribute ozone production to non-controllable (i.e., biogenic) emissions, APCA re-allocates that ozone production to the controllable portion of precursors that participated in ozone formation with the non-controllable precursor. For example, when ozone formation is due to biogenic VOC and anthropogenic NOx under VOC-limited conditions (a situation in which OSAT would attribute ozone production to biogenic VOC), APCA re-directs that attribution to the anthropogenic NOx precursors present. The use of APCA instead of OSAT results in more ozone formation attributed to anthropogenic NOx sources and less ozone formation attributed to biogenic VOC sources, but generally does not change the partitioning of ozone attributed to local sources and the transported background for a given receptor.

The CAMx APCA source apportionment tool has been improved (Yarwood and Koo, 2015) since it was last deployed for the KTF area. When ozone is transported into NOx-rich areas, such as portions of Central Texas with substantial NOx emissions, it can be converted to NO_2 by reaction with locally emitted NO and later returned as ozone. The new APCA scheme can

correctly attribute this returned ozone to the more distant source region (where the ozone was originally formed) whereas the old scheme would most likely attribute the returned ozone to a local source (Yarwood and Koo, 2015).

4.3 APCA Results

In this section, we describe the local KTF area and transported contributions to ozone at CAMS 1047 and CAMS 1045 and provide a breakdown by emissions source category for the local KTF contribution. In addition, we also examine the oil and gas contribution to ozone at the two monitors from East Texas shale oil and gas development. The KTF area is near the Eagle Ford Shale, which saw rapid development between 2010 and 2015 (see Figure 4-5).

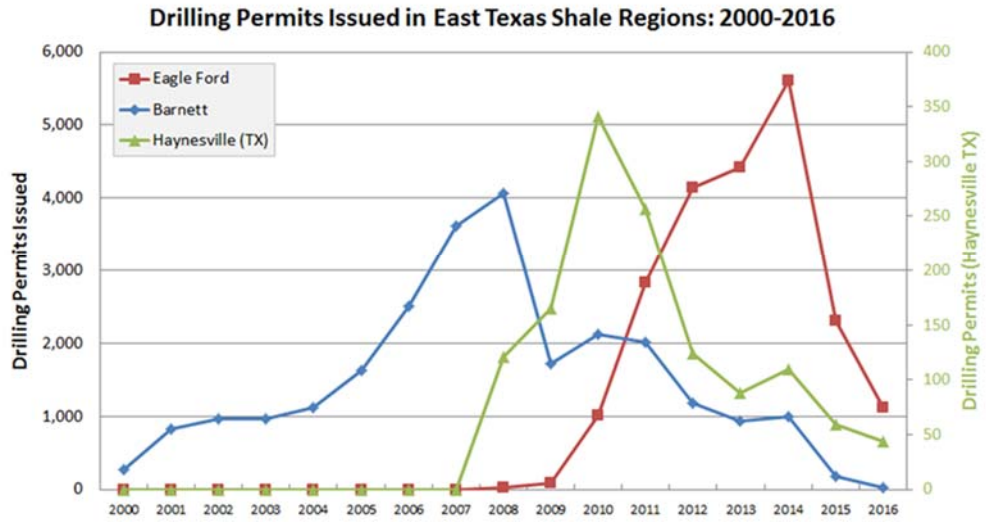

Figure 4-5. Drilling permits for the Eagle Ford and Barnett Shale (Haynesville) plotted on left (right) axis. Haynesville permit data are for Texas wells only, and do not include wells in Louisiana. Figure from Parrish et al. (2017) and data from Texas Railroad Commission[21].

We conducted two separate APCA simulations for May – September 2017, each focusing on ozone contributions from different emissions sources and regions. The APCA source region maps define the areas whose ozone impacts we wish to quantify. Figure 4-6 shows one of the two source region maps used in the APCA analysis. The simulation that used the map in Figure 4-6 was designed to understand the relative importance of local KTF emissions and ozone transport from regions in East Texas in producing high ozone at CAMS 1047 and CAMS 1045. The source region map allows us to determine which regions of Texas and which emissions source categories contribute to ozone at the two monitors through transport of ozone into the KTF area. The map shows the 4 km modeling domain boundary in blue. All areas outside of

[21] http://www.rrc.state.tx.us/oil-gas/research-and-statistics/production-data/historical-production-data/

Texas and the Gulf of Mexico are defined to be part of the “Other” source region. For this analysis, we combined the Mexico and Other regions into a single “non-Texas” region.

The CTCOG/KTF region consists of the KTF 7-county area. The contribution to KTF area ozone from local emissions sources is reckoned using this source region boundary. The HTCG region consists of the HOTCOG 6-county area and includes Waco. Other NNAs such as the Houston-Galveston-Brazoria/Beaumont-Port Arthur (HGBPA) and Dallas-Fort Worth (DFW) areas are broken out as separate source regions. The remaining areas of East Texas are grouped into source regions as follows:

- SAAA: Austin and San Antonio NNAs
- NETX: Northeast Texas (Tyler-Longview-Marshall NNA)
- NNTX: Northeast Texas (excludes NETX)
- SCTX: Victoria/Corpus Christi and rural counties between HGBPA and HTCG areas
- HOOD: Hood County
- WTX: West Texas
- GOM: Gulf of Mexico

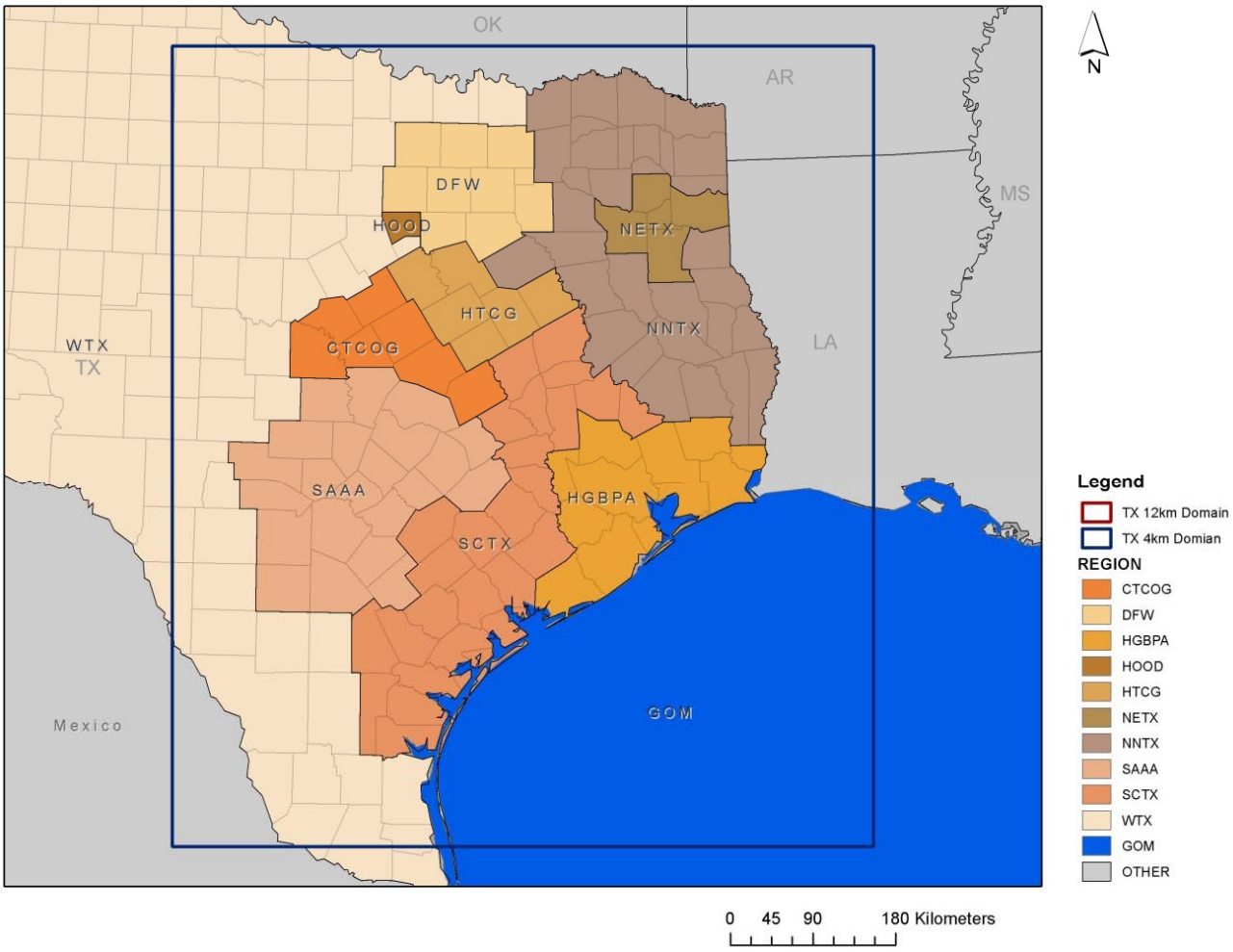

Figure 4-6. 4 km grid APCA source region map.

Figure 4-7 shows the second source region map used in the APCA analysis. The purpose of this source apportionment simulation was to understand the effect of oil and gas emissions from shale regions outside the KTF area on ozone at local monitors. The map shows the outline of the 4 km boundary in blue. This source region map was designed to track oil and gas emissions activity from the four largest gas-producing shale regions in Texas and Louisiana:

- EF1: Eagle Ford Shale #1
- EF2: Eagle Ford Shale #2
- HS: Haynesville Shale (includes part of Louisiana)
- BS: Barnett Shale

All areas outside of Texas and the Gulf of Mexico are defined to be part of the “Other” source region. For this analysis, we combined the Mexico and Other regions into a single “non-Texas” region.

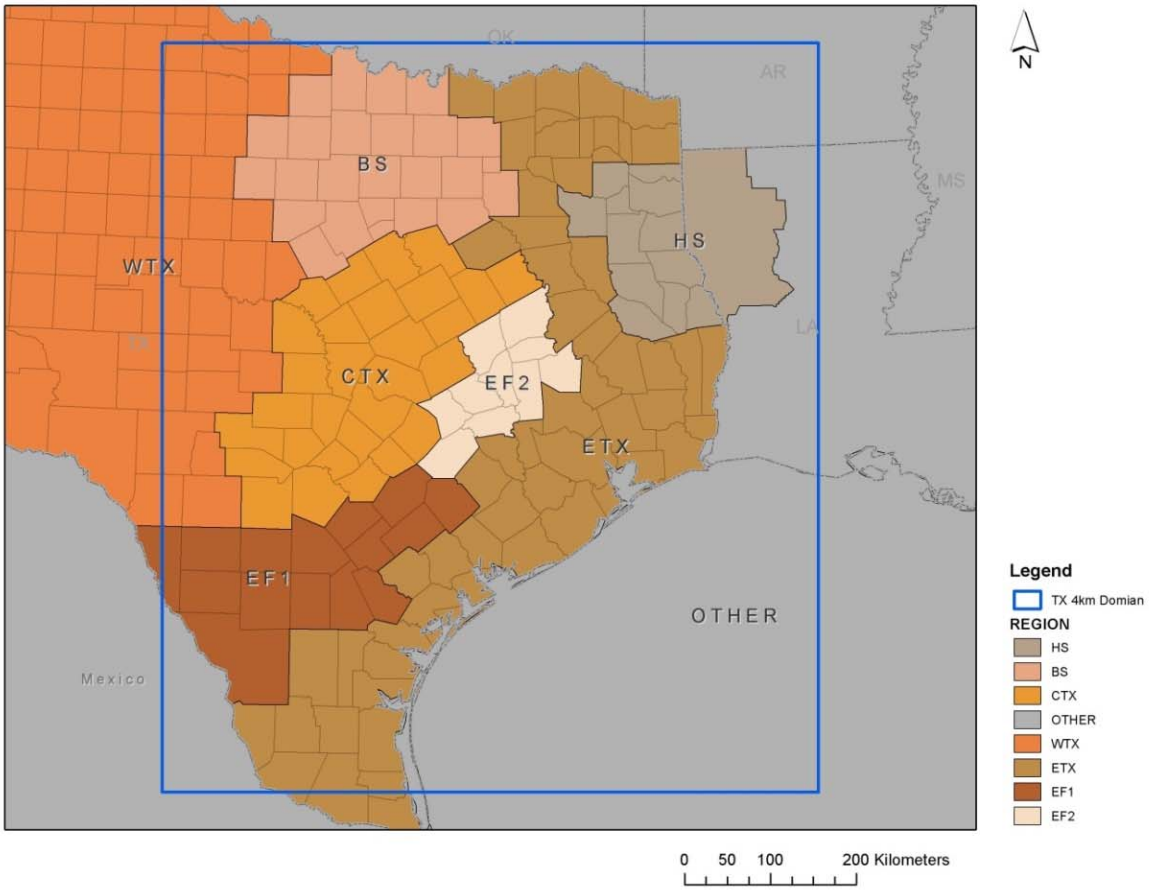

Figure 4-7. 4 km grid APCA source region map for oil and gas basin analysis.

Both APCA source apportionment simulations used the same set of five emissions source categories:

- Natural: biogenic emissions and wildfires
- EGU: electrical generating units (power plants)
- On-road: on-road mobile (cars, trucks, motorcycles, busses, etc.)
- Oil and Gas: oil and gas drilling and production
- Other: non-road/off-road mobile (includes airport, locomotive, low-level shipping), other area, low level point sources, elevated shipping and other non-EGU emissions

4.3.1 Local Contributions to Future Year Ozone Design Values

For ozone analysis, EPA's current recommended procedures for making future year ozone projections involve use of the model in a relative sense to scale observed site-specific current year 8-hour ozone Design Value Concentrations (DVCs) based on the relative changes in the modeled 8-hour ozone concentrations between the current year and the future year. The model-derived scaling factors are called Relative Response Factors (RRFs), and are based on the

relative changes in the modeling results between the current year base case (2012) and the future-year (2017) emission scenarios. These EPA guidance procedures for performing 8-hour ozone DV projections have been codified in the MATS tool.

We supplied the MATS tool with the CAMx ozone source apportionment model output to estimate relative contributions from emissions source regions and source categories to ozone DVFs at CAMS 1047. We utilized this technique in order to estimate each source category's impact on 2017 design values. Because the CAMS 1045 monitor was not in operation during the 2012 base year, it could not be used in this analysis.

We present MATS ozone contribution results at CAMS 1047 in Table 4-3. The 2012 DVC of 73.7 ppb – which exceeds the current ozone NAAQS standard – is projected to be reduced to 67.5 ppb in 2017. As discussed in Section 2, the 2014-2016 design value at CAMS 1047 based on ozone measurements is 67 ppb. We cannot make a direct comparison (model vs. observed) of 2017 ozone design values because the 2017 ozone season is still underway as of the writing of this report. However, the good agreement between the model and observations for this value suggest that the ozone model is capturing the general downward trend in ozone at the Killeen monitor. Because the 2017 ozone model uses an identical configuration as the 2012 model except for model boundary conditions on the 36 km grid and emissions, these two model inputs must be responsible for the ozone decreases represented by the 2017 design value.

Previous KTF ozone modeling has shown that ozone at CAMS 1047 is influenced more strongly by transport than by local 7-county area emissions sources (Kemball-Cook et al., 2015). This study also supports this finding – KTF emissions account for only 3.6 ppb of the 67.5 ppb 2017 projected design value. Therefore, we conclude that the amount of transported ozone has been reduced and is likely responsible for much of the decrease in ozone design value at CAMS 1047. We also note that KTF total NOx emissions in 2017 are reduced about 11% from 2012, so the local contribution to ozone is also reduced.

The total contribution from KTF emissions sources to 2017 ozone DVF at CAMS 1047 is 3.6 ppb. Table 4-3 shows that natural, EGU, on-road and the other (non-road/off-road mobile, other area, low level point sources, elevated shipping and other non-EGU) emissions source categories each contribute from 0.6 to 1.3 ppb. O&G emissions from the KTF region contribute only 0.1 ppb to the Killeen Skylark monitor's 2017 design value.

Table 4-3. 2012 ozone DVC, 2017 ozone DVF and contributions to 2017 ozone DVF from KTF emissions sources at CAMS 1047.

			KTF Local Emissions Contribution to 2017 DVF					
Site name	2012 Observed DVC	2017 Projected DVF	Natural	EGU	On-road	Oil+Gas	Other	Total
Killeen Skylark	73.7	67.5	0.6	0.7	1.3	0.1	0.9	3.6

Figure 4-8 shows MATS spatial maps for the 2017 ozone DVF (top left) and contributions to the 2017 DVF from KTF emissions source categories. KTF EGU contributions are shown in the top right panel, followed by natural sources (middle left), oil and gas (middle right), on-road mobile (bottom left) and other sources (bottom right).

We note that the total ozone 2017 DVF map shows that no part of the 7-county region has a design value above the current ozone NAAQS (red grid cells in top left panel of Figure 4-8 indicate areas with design values exceeding 70 ppb). The EGU contribution map is shown in the top right panel of Figure 4-8. For context, we provide the third quarter (Q3) average 2007-2016 NOx emissions (obtained from EPA's Acid Rain Database[22]) along with the 2017 Q3 average NOx emissions (extracted from TCEQ's 2017 future year emissions inventory) for the three power plants within the KTF region in Figure 4-9. Emissions from the Fort Hood source are not available from EPA, so only the TCEQ 2017 emissions are shown for this facility. We note that the relative magnitude of NOx emissions shown in this plot agrees roughly with the relative magnitudes of ozone impacts from each EGU in Figure 4-8. Specifically, the map shows an ozone maximum associated with emissions from the Sandow Electric Generating Station, a coal-fired power plant in Milam County operated by Luminant. The EGU impacts on ozone DVF are around 5-6 ppb in the immediate vicinity of the power plant. Some parts of Bell County show EGU impacts of greater than 1 ppb, but the EGU contribution from all sources in the KTF region at CAMS 1047 is 0.7 ppb (Table 4-3). EGU contributions exceeding 2.5 ppb exist just outside the KTF region in Williamson County.

[22] Obtained from EPA's Air Markets Program Data tool: https://ampd.epa.gov/ampd

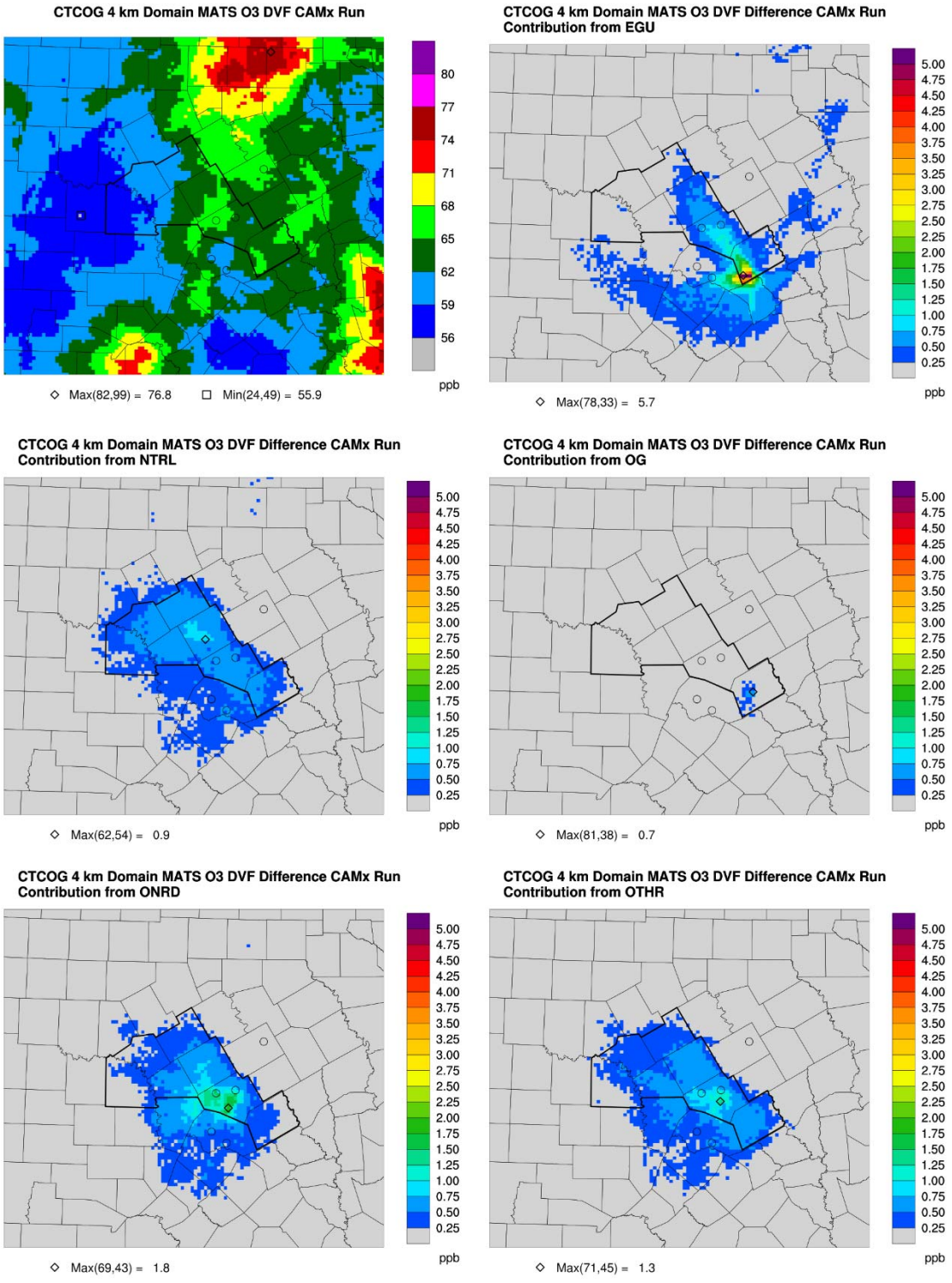

Figure 4-8. 2017 ozone DVF (top left) and KTF contributions to 2017 ozone DVF from EGUs (top right), natural sources (middle left), oil and gas emissions (middle right), on-road mobile (bottom left) and other emissions (bottom right).

In the middle left panel of Figure 4-8, the KTF natural contribution to 2017 ozone DVFs shows areas exceeding 0.75 ppb in Coryell County. Ozone impacts from the natural source category are associated with biogenic soil NOx emissions and wildfires. Near the Killeen and Temple monitors, we find natural contributions around 0.5 ppb. The KTF O&G contribution (middle right panel of Figure 4-8) shows very small contributions (less than 0.25 ppb) everywhere except for Milam County, where the peak impact is 0.7 ppb. This peak coincides with natural gas wells in the area as shown in Figure 4-4. The O&G contributions at the Killeen and Temple monitors are each less than 0.25 ppb.

In the bottom left panel of Figure 4-8, the on-road mobile contribution shows a peak (1.8 ppb) in the vicinity of I-35 and other regions exceeding 1.5 ppb near Highway 190 in Bell County. The contributions at CAMS 1047 and CAMS 1045 are around 1 ppb. Finally, the bottom right panel of Figure 4-8 shows the Other emissions category (primarily composed of non-road/off-road mobile which includes airport, locomotive and watercraft emissions) with a maximum (1.3 ppb) that occurs just south of the Temple monitor near Belton. Areas exceeding 0.75 ppb are located almost entirely in Bell County. The BNSF Temple railyard and lakes with recreational boating in Bell County both contribute emissions to the Other category. Bell County accounts for 41% of all off-road mobile emissions within the KTF area. The Other contributions at CAMS 1047 and CAMS 1045 are slightly less than 1 ppb.

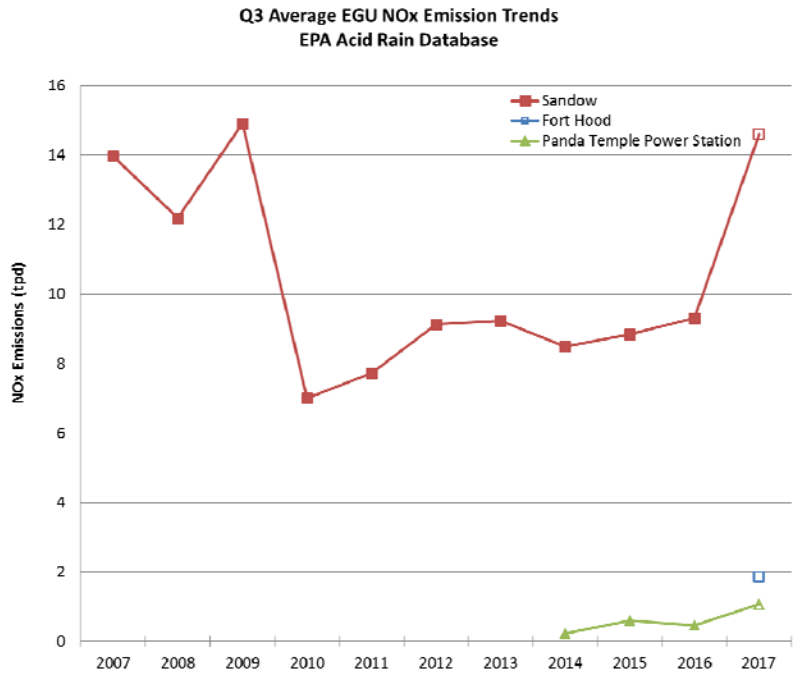

Figure 4-9. Q3 average NOx emissions for 2007-2016 (obtained from EPA's Acid Rain Database) and Q3 average 2017 NOx emissions (obtained from TCEQ's 2017 future year emissions inventory) for the three power plants in the KTF region. Emissions for Fort Hood not available from EPA.

Figure 4-10Figure 4-10 shows 2017 ozone DVF impacts from oil and gas contributions from the three major shale regions in Texas/Louisiana (Eagle Ford, Haynesville and Barnett). We note that all of these shale regions lie outside the KTF area. The Conceptual Model of Ozone Formation in the KTF Area (Kemball-Cook et al., 2015) found that wind direction at C1047 was frequently from the south and southeast (shale regions upwind of Killeen) on days when observed ozone exceeded 60 ppb. Oil and gas production from the Haynesville Shale (0.2 ppb; ENE of Killeen) and Eagle Ford Shale (0.7 ppb; SW of Killeen) result in about a 0.9 ppb contribution at CAMS 1047. Most of the KTF region shows contributions from oil and gas emissions above 1 ppb and a small part of Milam County is above 2 ppb. Figure 4-10 indicates that the KTF area is outside the area of largest ozone impacts from shale gas development in East Texas.

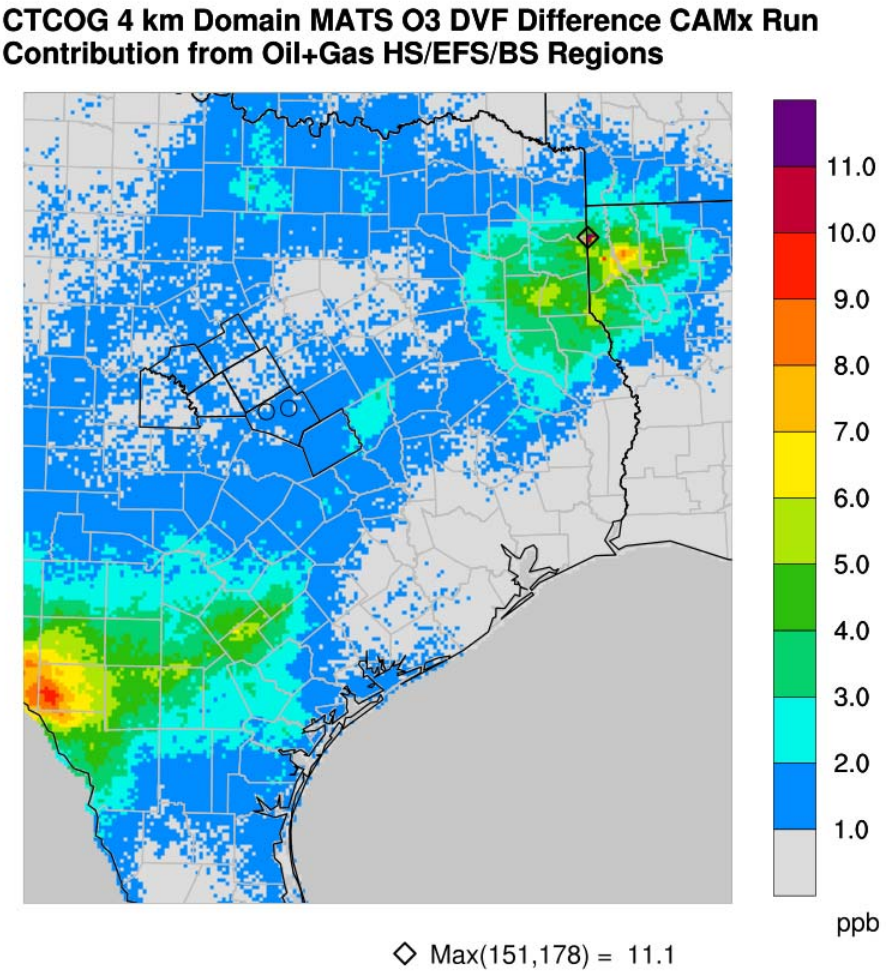

Figure 4-10. Oil and gas contributions from the three major shale regions in Texas/Louisiana (Haynesville, Eagle Ford and Barnett) to 2017 ozone DVF.

Figure 4-11 shows the frequency distribution for impacts on the MDA8 ozone at CAMS 1047 from the same oil and gas shale regions shown in Figure 4-10. We note that the total O&G contribution (green) has the most frequent contribution in the 2-3 ppb range and has a maximum contribution in the 4-5 ppb range. By far, the largest O&G MDA8 contribution at CAMS 1047 comes from the Eagle Ford shale region, which has nearly half of the modeling episode with contributions of 1 ppb or higher. There are only a handful of days throughout the episode where MDA8 ozone contributions from either the Haynesville or Barnett shale regions exceed 1 ppb. This result agrees with our understanding of typical wind patterns on high ozone days. In particular, winds from the south – which bring air from the O&G wells in the Eagle Ford Shale to CAMS 1047 – are frequent on days where observed ozone MDA8 exceeds 60 ppb (Kemball Cook et al., 2015; Parker et al., 2013). In addition, the Eagle Ford Shale region is closer to CAMS 1047 than either the Barnett or Haynesville Shale regions.

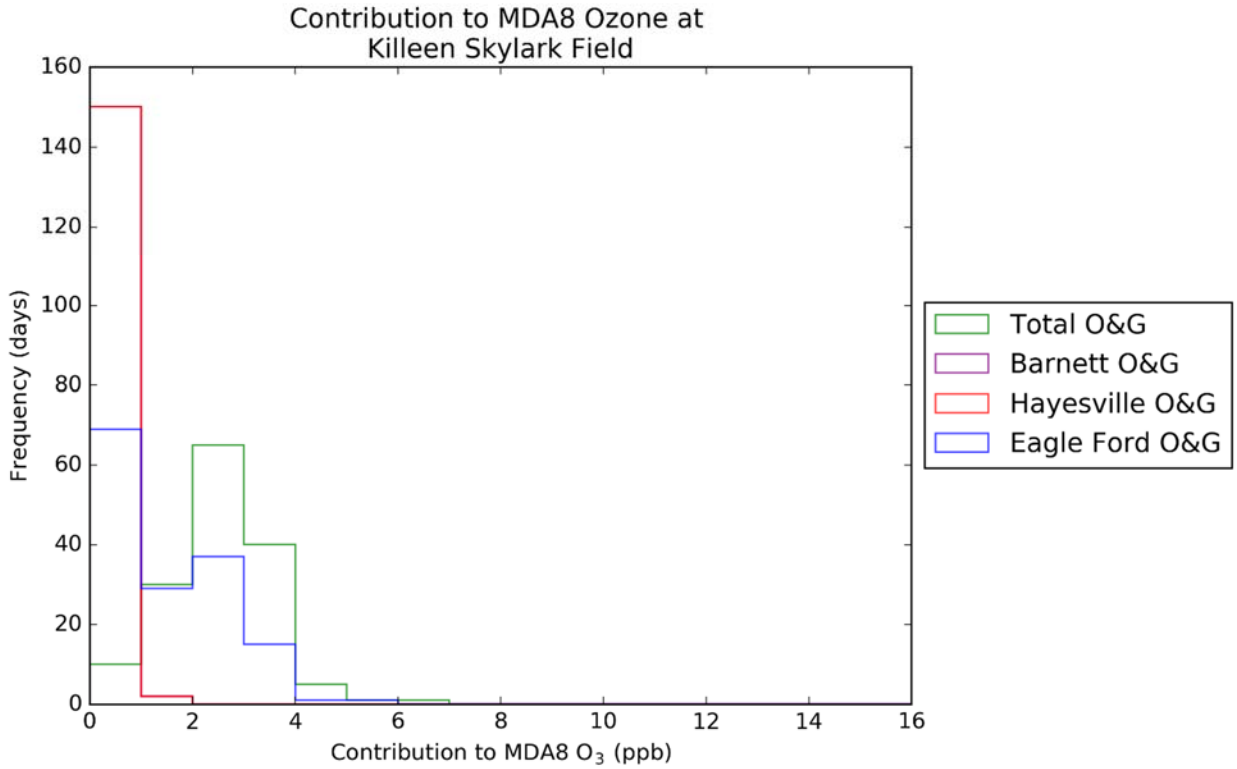

Figure 4-11. Frequency distribution of the projected contributions to 2017 MDA8 ozone concentrations from O&G emissions within the Barnett (purple), Haynesville (red), Eagle Ford (blue) and all (green) shale regions at CAMS 1047.

Figure 4-12 shows the same information as Figure 4-11 but for the Temple Georgia (CAMS 1045) monitor. We find similar O+G impacts as found at the Killeen Skylark monitor, with the most frequent total O+G impacts in the 2-3 ppb range. The Temple Georgia monitor results show more frequent occurrences of 4-5 ppb impacts (about 10 days).

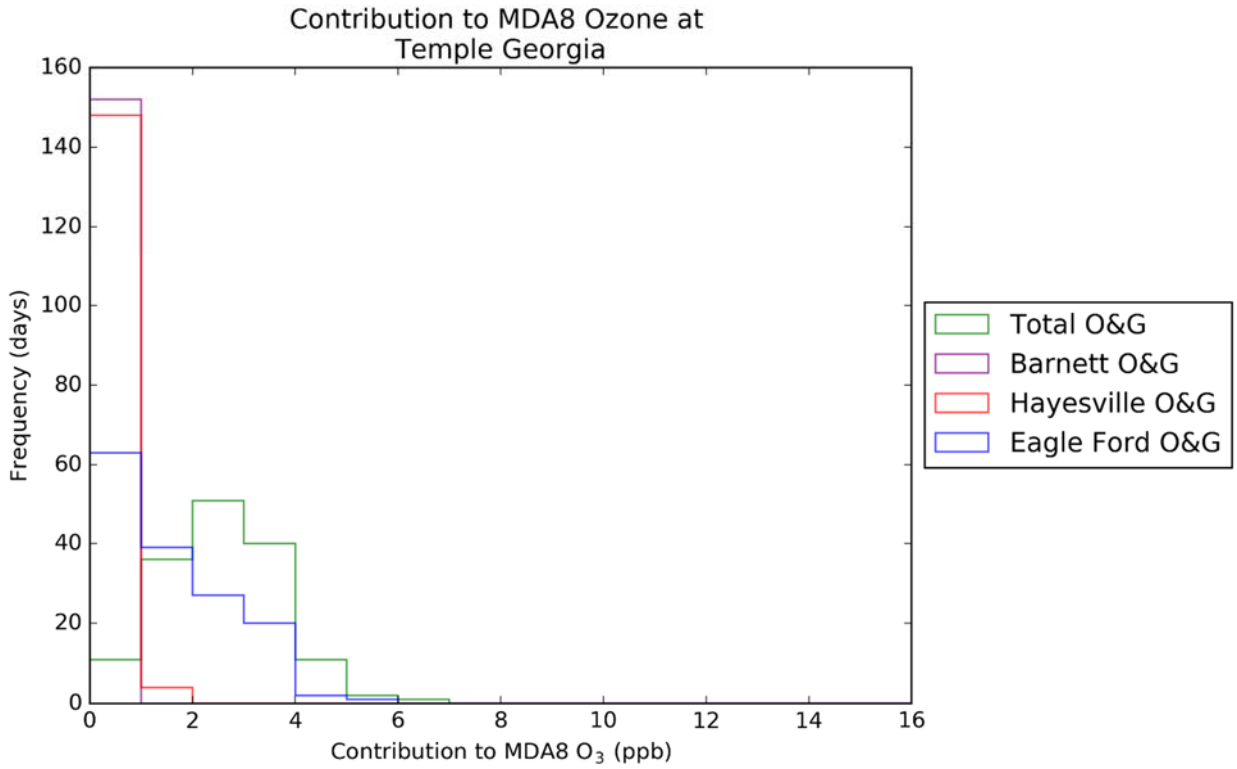

Figure 4-12. Frequency distribution of the projected contributions to 2017 MDA8 ozone concentrations from O&G emissions within the Barnett (purple), Haynesville (red), Eagle Ford (blue) and all (green) shale regions at CAMS 1045.

4.3.2 Source Apportionment Results for CAMS 1047 and CAMS 1045

In order to develop emission control strategies for the KTF area that will reduce the local contribution to ozone, it is necessary to understand how ozone formation in the area depends on the amount of available NOx and VOC. Previous studies have shown that because of an abundance of biogenic VOC emissions in the area, ozone forms under NOx-limited conditions almost exclusively (Grant et al., 2017; Kemball-Cook et al., 2015). Figure 4-13 shows NOx-limited (blue) and VOC-limited contributions from local KTF area emissions to episode average (top) and maximum (bottom) MDA8 ozone at CAMS 1047 for the May-September 2017 modeling period. Consistent with previous KTF modeling efforts (Kemball-Cook et al., 2015), we note that the vast majority of contributions to ozone occur under NOx-limited conditions. Therefore, we expect that NOx emission controls on local sources will be far more effective than VOC emissions controls at reducing local production of ozone at CAMS 1047.

Figure 4-13 also gives a sense of the relative contributions of each source category. The episode average contributions to MDA8 ozone (top panel of Figure 4-13) for Natural, EGU, On-road mobile and Other categories are all between 0.3 and 1.0 ppb. The contribution from oil and gas emissions is much smaller (less than 0.1 ppb). The episode maximum contributions to MDA8

ozone (bottom panel of Figure 4-13) show a similar relationship – the contribution from oil and gas is small (0.3 ppb) compared to the other four categories (1.9 to 5.4 ppb).

Figure 4-14 shows the same MDA8 ozone contributions as in Figure 4-13 but for the Temple Georgia (CAMS 1045) monitor. We note that the episode average contributions to MDA8 ozone at CAMS 1045 (top panel of Figure 4-14) are nearly identical to those at CAMS 1047. In fact, the only emissions category that shows a difference greater than 0.1 ppb is the EGU contribution which is 0.2 ppb greater (CAMS 1047: 0.1 ppb; CAMS 1045: 0.3 ppb). The episode maximum contribution to MDA8 ozone at CAMS 1045 (bottom panel of Figure 4-14) also shows similar results compared to CAMS 1047 – contributions from on-road mobile, O&G and Other are each within 0.2 ppb of the contributions found at the Killeen monitor. The largest discrepancies between the two monitors are found for the natural (CAMS 1047: 3.3 ppb; CAMS 1045: 2.5 ppb) and EGU (CAMS 1047: 1.9 ppb; CAMS 1045: 2.5 ppb) contributions. The natural contribution difference between the two monitors is due entirely to the NOx-limited contribution, suggesting that the CAMS 1047 monitor is influenced more by biogenic soil NOx emissions than at the C1045 monitor. While CAMS 1045 shows the highest contribution of all monitors from KTF EGU emissions (Figure 4-15), two other monitors (Waco Mazanec and Austin Audubon) show higher contributions to their MDA8 ozone from KTF area EGU emissions than the C1047 monitor. We note that the contribution from KTF area EGU emissions to the Waco design value is less than 0.25 ppb. Therefore, we can infer that the episode maximum contribution is not occurring on the highest ozone days.

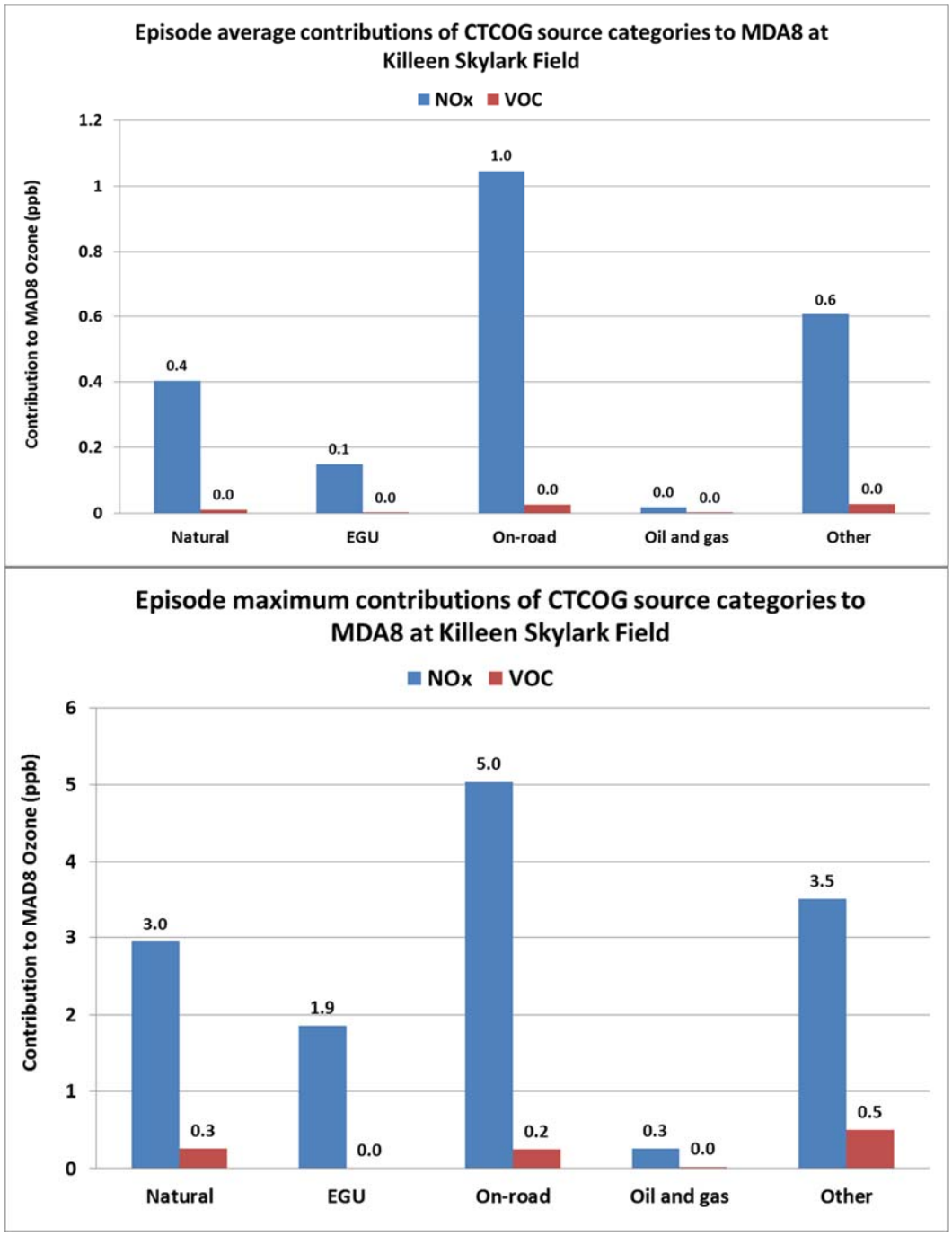

Figure 4-13. Comparison of the NOx vs. VOC-limited contributions to episode average (top) and maximum (bottom) MDA8 ozone at CAMS 1047 during the May-September 2017 period.

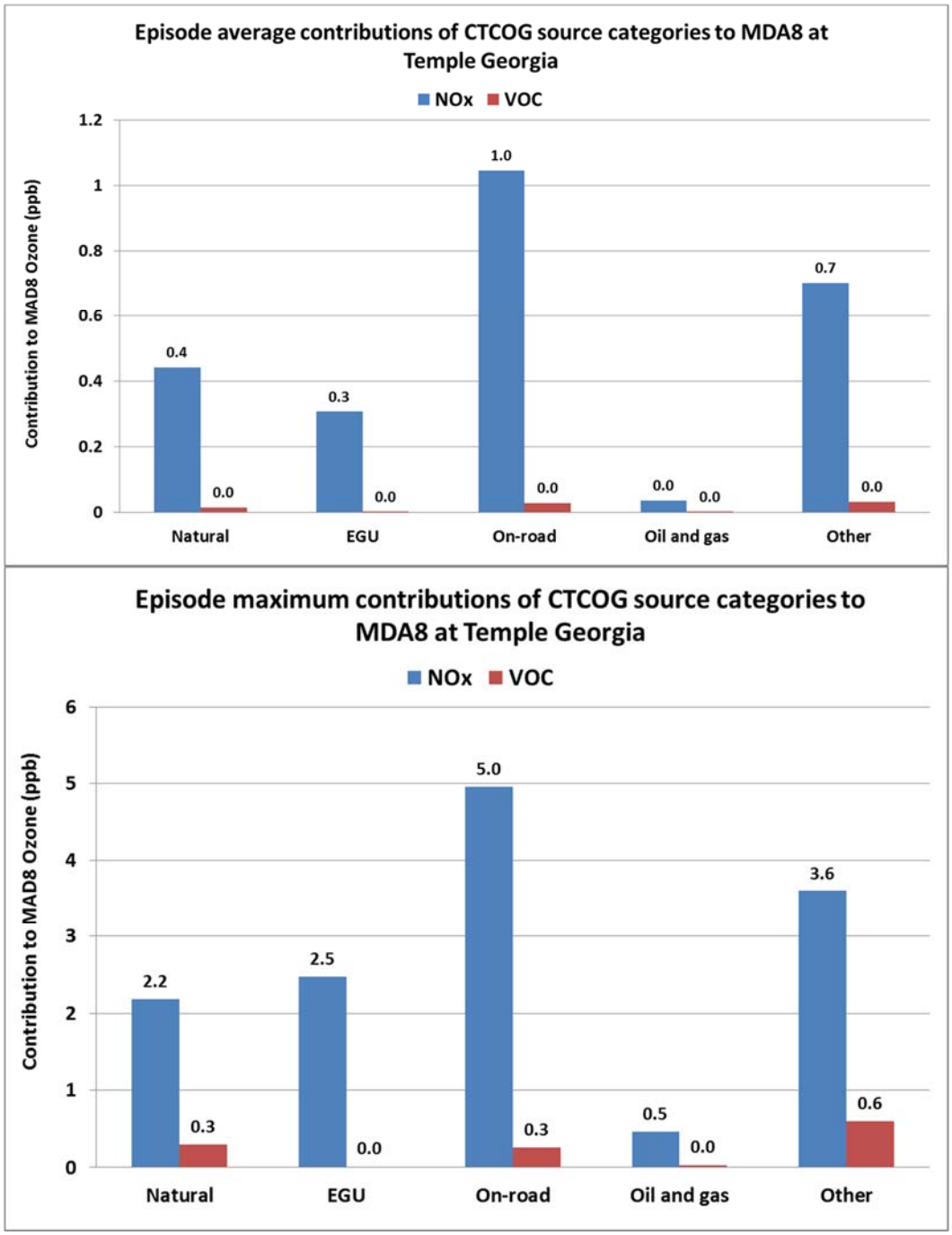

Figure 4-14. Comparison of the NOx vs. VOC-limited contributions to episode average (top) and maximum (bottom) MDA8 ozone at CAMS 1045 during the May-September 2017 period.

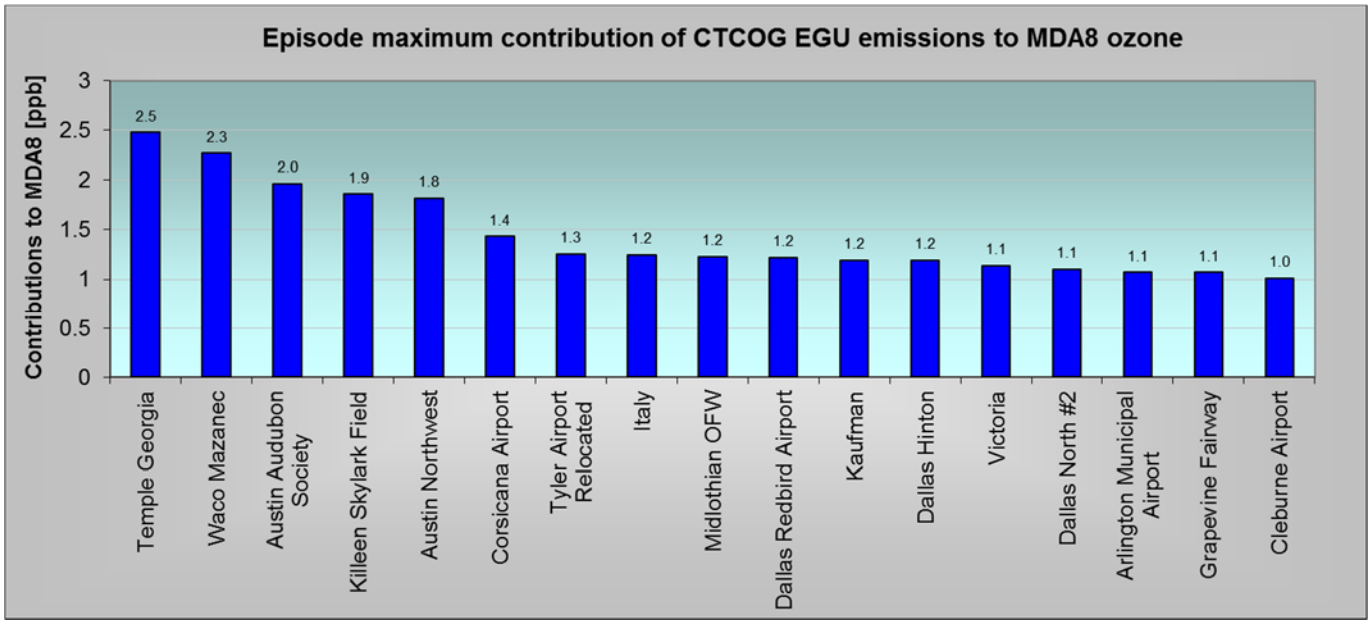

Figure 4-15. May-September 2017 episode maximum contributions from KTF EGU emissions to the Temple Georgia (CAMS 1047), Killeen Skylark (CAMS 1045) and other nearby monitors.

The May-September 2017 modeling episode ozone contributions to CAMS 1047 are broken down by source region in Figure 4-16. The largest contributions for both the episode average (top panel of Figure 4-16) and episode maximum (bottom panel of Figure 4-16) come from the initial and boundary conditions (IC+BC; 19 ppb episode average contribution and 39 ppb episode maximum contribution) and from regions outside Texas (Other; 11 ppb episode average contribution and 38 ppb episode maximum contribution). The IC+BC contribution represents transport of ozone from sources outside the continental-scale 36 km CAMx modeling domain. The contribution from outside Texas represents ozone transport from other U.S. states and portions of Mexico that are within the CAMx modeling domain. The largest episode average contribution from within Texas to the Killeen monitor comes from the adjacent San Antonio/Austin region and is 6 ppb. The next largest contributions come from the GOM (Gulf of Mexico; 2.6 ppb) and adjacent SCTX area (2.5 ppb). The SCTX area is largely rural, but has two coal-fired power plants – Oak Grove and Twin Oaks – located in Robertson County. The KTF area and much of East Texas experiences periods of low ozone associated with transport from relatively clean air from the Gulf of Mexico periodically during the summer ozone season.

We note that for the episode maximum contributions (bottom panel of Figure 4-16), there are three regions within Texas – San Antonio/Austin (21.9 ppb), GOM (17.0 ppb) and HGBPA (16.9 ppb) – that are higher than the local (KTF) contribution (14.6 ppb). The HGBPA nonattainment area has been shown to influence ozone at CAMS 1047 (Kemball-Cook et al., 2015). The next three largest contributions (HOTCOG, DFW and SCTX) are all equal to or exceed 10 ppb.

The NNTX region (8.2 ppb) has substantial oil and gas development and is to the east of the KTF area. West Texas (WTX) and Northeast Texas (NETX) contribute an episode maximum of 6.7 and 4.3 ppb, respectively to MDA8 ozone at CAMS 1047.

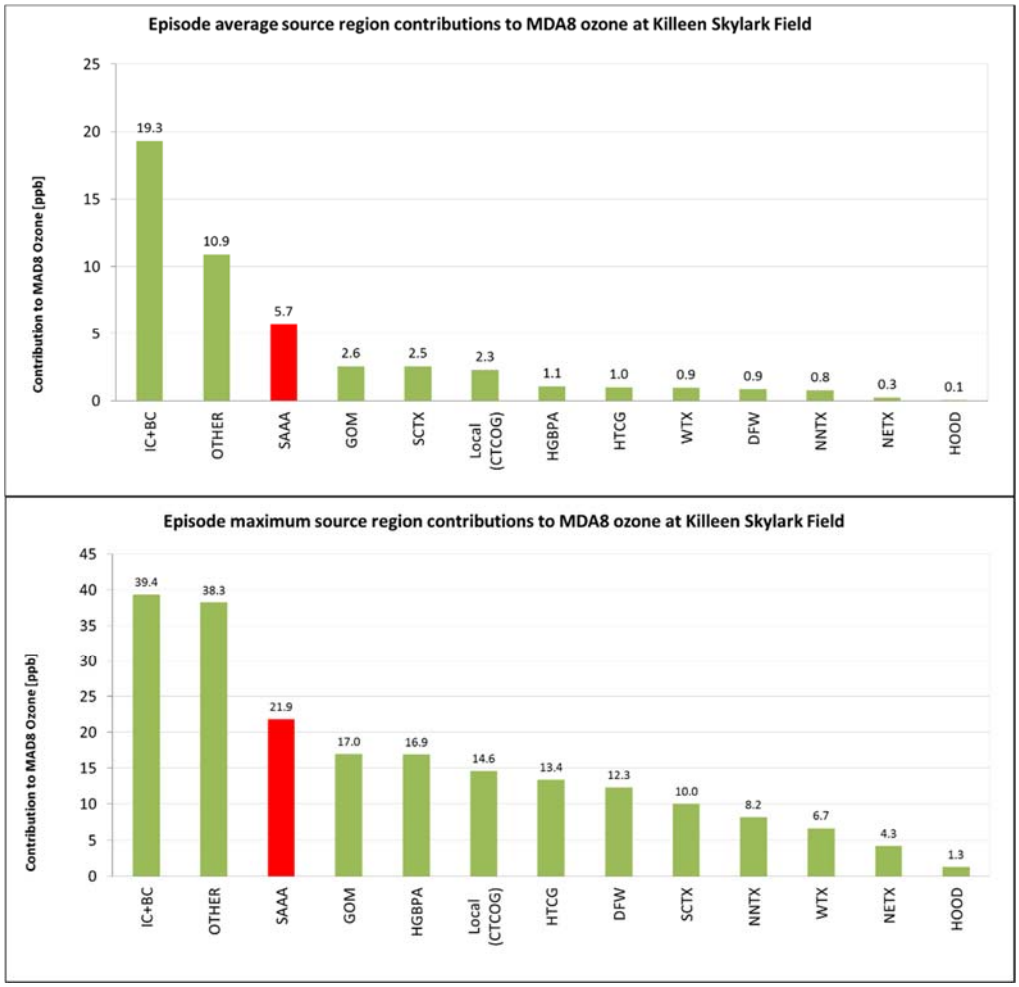

Figure 4-16. Killeen Skylark monitor detailed source apportionment by region for the May-September 2017 episode average (top) and maximum (bottom) contribution to daily maximum 8-hour ozone.

Next, we present the episode average (top panel) and maximum (bottom panel) contributions to MDA8 ozone at the CAMS 1045 monitor Figure 4-17. The episode average contributions are very similar to CAMS 1047. The largest difference is the contribution from the San Antonio/Austin area, where the episode average contribution is 4.1 ppb (CAMS 1047: 5.7 ppb). The bottom panel of Figure 4-17 shows a similar pattern – the San Antonio/Austin area contribution (highest contribution from within Texas) is lower at CAMS 1045 (17.6 ppb) compared to CAMS 1047 (21.9 ppb). The next highest contribution is the local/KTF contribution (14.8 ppb). The KTF contribution and the next five highest contributions (GOM, HOTCOG, HGBPA, DFW and SCTX) are all within 2.5 ppb. Compared to CAMS 1047, contributions from

GOM and HGBPA are higher at CAMS 1045 and contributions from HOTCOG, DFW and SCTX are lower at CAMS 1045.

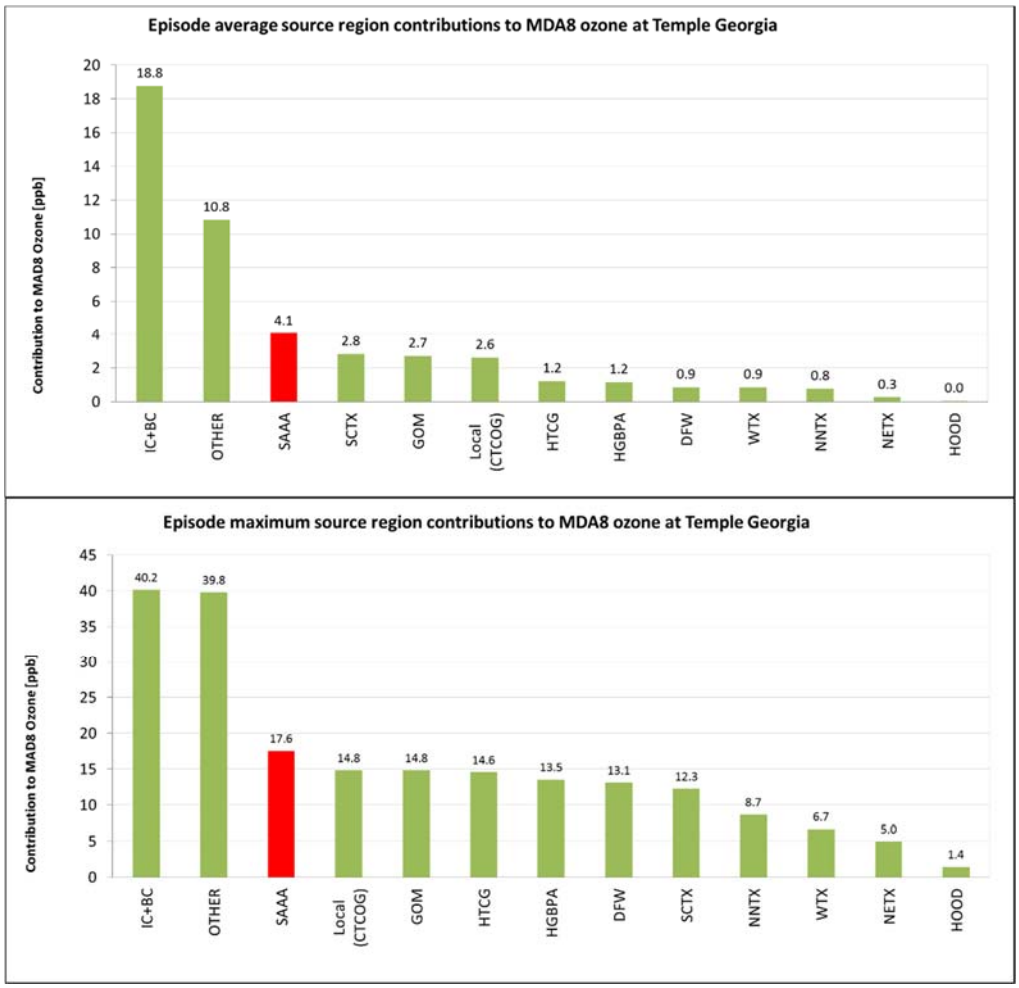

Figure 4-17. Temple Georgia monitor detailed source apportionment by region for the May-September 2017 episode average (top) and maximum (bottom) contribution to daily maximum 8-hour ozone.

Next, we examine KTF area May-September 2017 ozone contributions to other monitors in the area. The top panel of Figure 4-18 shows the contribution to MDA8 ozone at CAMS for which KTF emissions made the largest episode average ozone contributions. No MDA8 threshold was used in preparing Figure 4-18. The Temple and Killeen monitors show the largest contributions from KTF area emissions, followed by the Waco Mazanec monitor (1.3 ppb). The next 10 largest contributions from the KTF area emissions occur at monitors within the Dallas-Fort Worth region. This suggests that the DFW region is frequently downwind of the KTF region. In general, the contribution from the KTF area is largest at the monitors which are closest to the KTF area.

The bottom panel of Figure 4-18 shows the contribution to MDA8 ozone at CAMS for which KTF emissions made the largest episode maximum ozone contributions. As seen in the episode average contributions, the largest impacts are seen at the CAMS 1045 (14.8 ppb) and CAMS 1047 (14.6 ppb) monitors. The next largest contributions are seen in Austin (Austin Audubon: 8.2 ppb; Austin Northwest: 6.8 ppb). Waco Mazanec is next at 6.7 ppb, followed by 11 contributions at DFW area monitors ranging from 3.3 to 4.7 ppb.

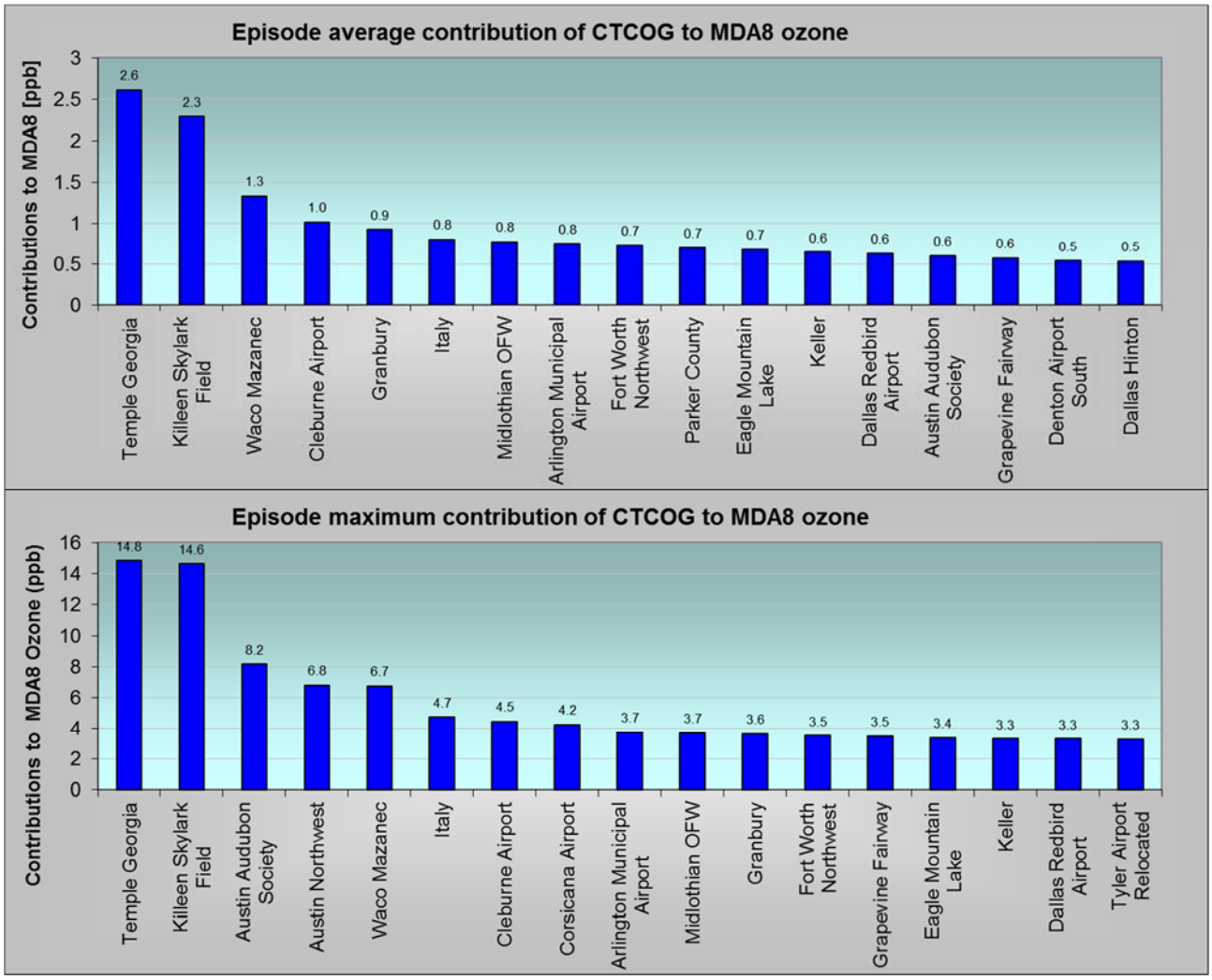

Figure 4-18. May-September 2017 episode average (top) and maximum (bottom) contributions from the 7-county KTF area to the Temple Georgia (CAMS 1045), Killeen Skylark (CAMS 1047) and other nearby monitors.

5.0 EVALUATION OF OZONE IMPACTS FROM PANDA TEMPLE POWER PLANT AND FORT HOOD IN BELL COUNTY

In this section, we apply the 2017 ozone model to evaluate ozone impacts from the Panda Temple EGU and Fort Hood military base. First, we describe the two emissions sources and explain why they are important to KTF area ozone. Next, we describe the CAMx ozone model's DDM Decoupled Direct Method (DDM) probing tool (Dunker et al., 2002) and how we applied it to evaluate ozone impacts from the two sources. Finally, we analyze the ozone sensitivities to the NOx emissions generated from the Panda Temple Power EGU and Fort Hood military base, including impacts to the 2017 ozone design values.

5.1 Panda Temple Generating Stations

The Panda Temple Power Project is a natural gas fueled combined-cycle power plant located in Temple (map shown in Figure 5-1). The facility was built in two phases, with each phase consisting of two combustion turbines and one steam turbine with total capacity of 758 MW, so that the capacity of the entire facility is 1516 MW. The TCEQ approved the permit for the Panda Temple Power Project in October 2008. Construction on the first phase of the project, the Panda Temple I Generating Station, began in 2012. Panda Temple I commenced operations in July 2014. Construction on the second phase of the Project, Panda Temple II Generating Station, began in April 2013 and Phase II became operational in 2015.

Panda Temple I and II are identical in equipment and configuration and are designed to be used as both baseload and peaking units[23]. As peaking units, they are designed to have higher power output during hot weather, when air conditioner use is high[24]. This means the facility is intended to run at high capacity on days which are most likely to have high ozone levels. Because the units generate power through combustion of natural gas, they have NOx emissions. Ozone formation in the KTF area is NOx-limited, and so an additional source of NOx in close proximity to an ozone monitoring site (~8 miles from Temple Georgia) is expected to have impacts on monitored ozone.

The Panda Temple units have NOx emissions controls consisting of dry low NOx burners and selective catalytic reduction (SCR). These controls are consistent with current practice for new combined-cycle units in Texas. The Panda Temple units were designed to come up to 60% of baseload in 20 minutes, and arrive at full power in an hour. This reduces the amount of time when the units are operating in startup mode and the temperature of the exhaust is not yet high enough for the SCR NOx emissions control equipment to function at full efficiency.[25]

The Panda Temple units came online in 2014 and were therefore not included in TCEQ's 2012 emissions inventory. The Panda Temple facility is included in TCEQ's 2017 emissions inventory,

[23] http://www.bizjournals.com/dallas/news/2013/11/21/panda-power-fired-up-about-three-new.html
[24] http://www.pandafunds.com/invest/temple/
[25] http://www.power-eng.com/articles/2014/09/texas-panda-temple-combined-cycle-plant-up-and-running.html

which allowed us to quantify the ozone impact in terms of its contribution to the 2017 ozone design value and understand the impact of this new power plant on KTF area ozone. In TCEQ's 2017 emission inventory, the Panda Temple facility had NOx emissions of 1.0 tpd, consistent with recent in-stack continuous emissions monitoring measurements shown in Figure 4-9.

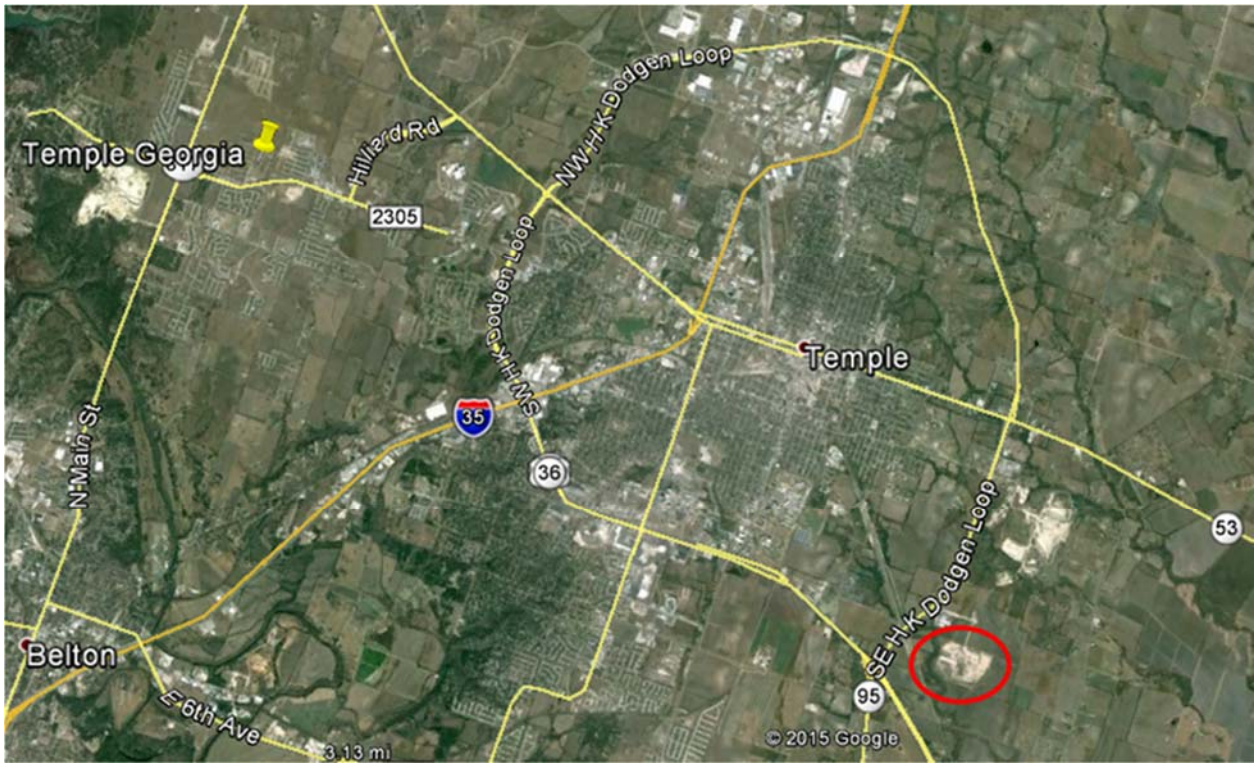

Figure 5-1. Panda Temple Power Project location. Power plant location is circled in red. Location of the Temple Georgia ozone monitor is shown in yellow.

5.2 Fort Hood Emissions

The Fort Hood military post is one of the largest military installations in the United States[26] and may have sizable emissions in all source categories of anthropogenic emissions; due to its status as a military base, Fort Hood's emissions may not be well-characterized in either the 2012 or 2017 emission inventories. Fort Hood occupies 335 square miles in Bell and Coryell Counties[26] (see Figure 5-2). Fort Hood is the only post in the United States capable of stationing and training two Armored Divisions[26]. In 2011, Fort Hood had population of 47,190 army military and army civilian personnel (United States Army Environmental Command (USAEC), 2014). Based on the army force structure realignment, there are maximum anticipated

[26] Fort Hood Fact Sheet No. 0703, http://www.hood.army.mil/facts/FS%200703%20-%20Fort%20Hood%20Overview.pdf

personnel reductions at Fort Hood of 16,000 by 2020; if the maximum personnel reductions were made, this would lead to a 2020 combined army military and army civilian personnel population at Fort Hood of 31,190[26].

Fort Hood includes the Military Equipment and Training Site (MATES) where 850 pieces of heavy equipment are stored and supported. Additionally, 1,700 pieces of equipment are stored and supported at an Equipment Concentration Site (ECS) at Fort Hood[26]. Equipment at the MATES and ECS is expected to be a source of ozone precursor emissions; the magnitude of emissions depends on equipment characteristics as well as frequency and duration of equipment use. Fort Hood off-road equipment emissions are not well-characterized and may be underestimated in both the 2012 and 2017 emissions inventories.

On-road emission inventories that TCEQ has developed rely on vehicle miles traveled (VMT) estimates from the Highway Performance Monitoring System (HPMS) managed by the Texas Department of Transportation (TxDOT) that cover public roads only. According to the Federal Highway Administration HPMS Field Manual, "All roads open to public travel are reported in HPMS regardless of ownership, including Federal, State, county, city, and privately owned roads such as toll facilities."[27] If a roadway is within the Fort Hood fence line and is not open to public travel, then the emission estimates from that roadway would not be included in the TCEQ on-road emission inventory. While the HPMS data would capture trips to/from the Fort Hood military facility, it does not capture activity that is on roads not open to the public in the facility (TCEQ, 2015). We therefore expect that on-road emissions from Fort Hood are underestimated in the TCEQ's emission inventories.

Consistent with previous KTF modeling (Kemball-Cook et al., 2015), our ozone model performance evaluation found that ozone is frequently underestimated on the highest observed ozone days at the C1047 monitor (see Appendix A). We therefore wanted to determine if the potentially underestimated Fort Hood NOx emissions could be contributing to these ozone underestimates in the model. In order to estimate the ozone sensitivity to Fort Hood NOx emissions, we estimated the missing on-road mobile and area emissions using population as a surrogate. We selected Lamar County as a surrogate for Fort Hood based on similar population (49,793 vs. 47,190) and lack of major interstate highways. We then selected three CAMx grid cells (see Figure 5-3) where emissions activity is most likely concentrated based on aerial imagery. Next, we distributed the Lamar County NOx emissions from the two sectors (on-road mobile: 2.7 tpd; area: 0.4 tpd) across the three selected CAMx grid cells. It should be emphasized that we are not suggesting that the estimates we derived accurately represent a missing amount of emissions at Fort Hood. Rather, the emissions simply allow us to calculate the ozone sensitivity of Fort Hood NOx emissions in a more accurate manner. In Section 5.5, we use the CAMx Decoupled Direct Method (DDM) probing tool to determine ozone sensitivity to these additional Fort Hood NOx emissions.

[27] http://www.fhwa.dot.gov/policyinformation/hpms/fieldmanual/

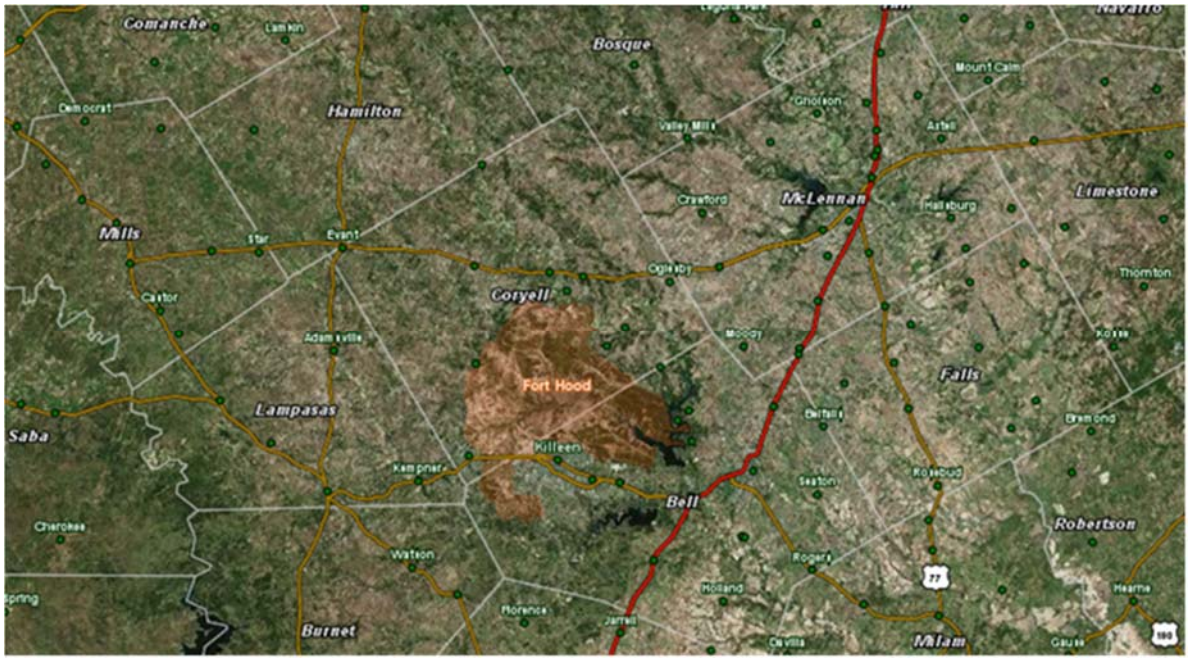

Figure 5-2. Fort Hood area (shaded brown) with county boundaries[28]. I-35 is shown in red.

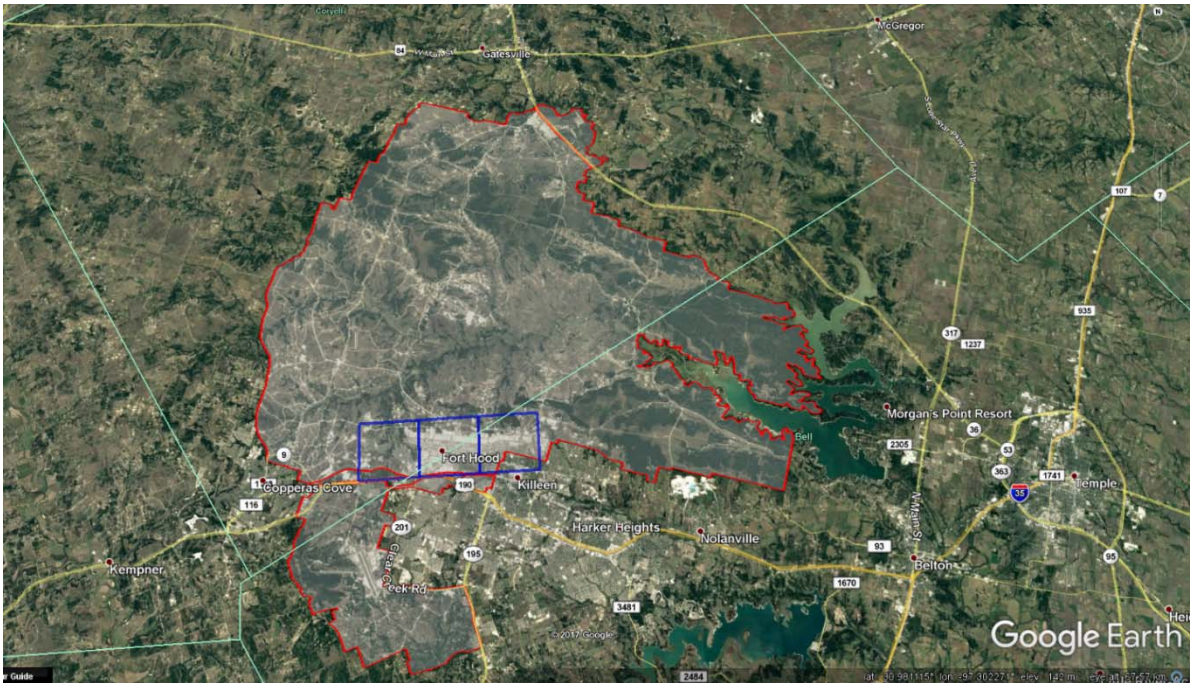

Figure 5-3. Fort Hood (red boundary) with CAMx grid cells (outlined in blue).

[28] http://websoilsurvey.nrcs.usda.gov/app/WebSoilSurvey.aspx

5.3 CAMx Direct Decoupled Method Probing Tool

The CAMx ozone model DDM probing tool (Dunker et al., 2002) was used to determine ozone impacts of the Panda Temple EGU facility and Fort Hood military base by calculating the sensitivity of modeled ozone to the NOx emissions from each source. We focused on the sensitivity of ozone to NOx emissions because ozone formation in the KTF area is NOx-limited (Grant et al., 2017; Kemball-Cook et al., 2015). The CAMx DDM probing tool can calculate the sensitivity of predicted concentrations to pollutant sources (e.g., emissions, initial conditions, boundary conditions). Sensitivities are calculated explicitly by specialized algorithms implemented in the host CAMx model. The DDM probing tool is described in Appendix B and in greater detail in Ramboll Environ (2016).

5.4 Panda Temple EGU Impact on 2017 Ozone DVF

We adopted a similar procedure for the DDM MATS analysis as the APCA MATS analysis described in Section 4.3.1. We evaluated the ozone impact of the Panda Temple EGU using DDM together with MATS produce a spatial map that represents the 2017 DVF ozone impact from the Panda Temple EGU units (Figure 5-4). Within Bell County, the impact from Panda Temple NOx emissions on 2017 ozone DVF ranges from less than 0.025 ppb (west of Killeen) to about 0.2 ppb (just south of the Temple Georgia CAMS monitor). The impacts at Temple Georgia and Killeen Skylark are both less than 0.1 ppb. Impacts outside Bell County are also less than 0.1 ppb. We note that the largest impacts from power plants on a given day are typically seen within relatively narrow plumes downwind of the emissions source on that day. Therefore, the results shown here are highly dependent on wind direction on the highest ozone days selected by the MATS software and do not necessarily reflect the spatial pattern of ozone impacts that might occur during a different ozone season with different wind patterns.

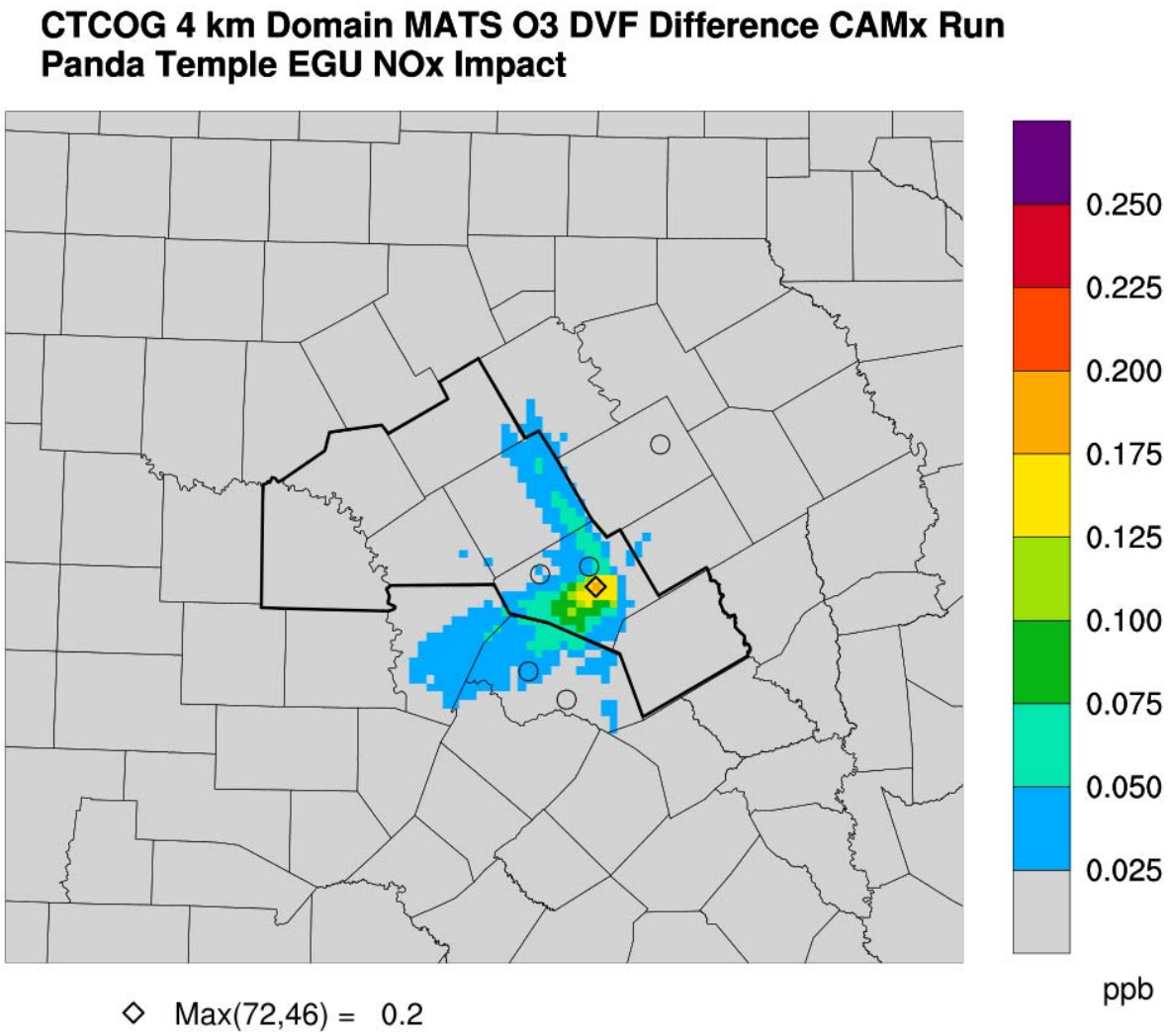

Figure 5-4. Panda Temple EGU NOx emissions contribution to 2017 ozone DVF.

We take a closer look at the Panda Temple EGU impacts in Figure 5-5. This time series chart shows the sensitivity of MDA8 ozone to Panda Temple NOx emissions (red) and MDA8 ozone (blue) for the entire May-September modeling episode for the 2017 model simulation. In the top panel (C1047), we find an episode maximum MDA8 ozone sensitivity of 0.6 ppb per tpd of NOx emissions from the plant, which occurs on May 11. We note that the sign of the ozone sensitivity can sometimes be negative (e.g. May 21-22) and represents decreases in MDA8 ozone resulting from ozone titration by the NOx emitted by the power plant. The model predicted an MDA8 ozone concentration of 58.3 ppb on May 11, which is in the top 10% of all days in the episode. The bottom panel (C1045) shows a slightly lower episode maximum sensitivity (0.5 ppb per tpd of NOx emissions) than C1047, but shows a higher frequency of impacts in the 0.25-0.50 ppb/tpd range, both positive and negative. This result is expected because the Panda Temple power plant is closer to the Temple Georgia monitor.

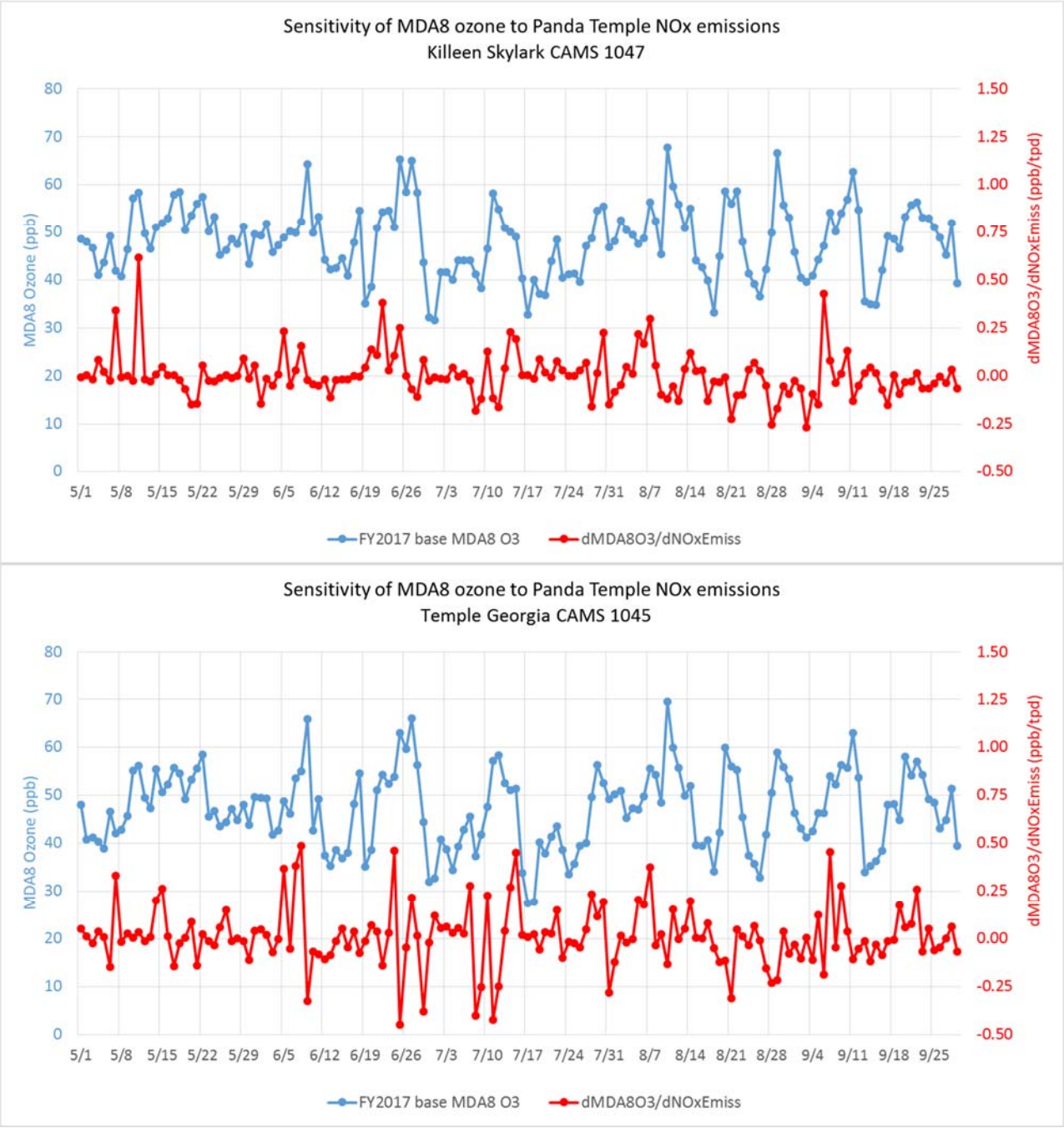

Figure 5-5. Sensitivity of MDA8 ozone to Panda Temple NOx emissions (red; plotted on secondary axis) and MDA8 ozone (blue; plotted on primary axis) at CAMS 1047 (top) and CAMS 1045 (bottom) for the 2017 ozone model.

5.5 Fort Hood Impact on 2017 Ozone DVF

We evaluated the 2017 ozone DVF impact for additional Fort Hood NOx emissions using the same procedure applied in the previous section to the Panda Temple EGU. As discussed in Section 5.2, we supplemented the TCEQ 2017 emissions inventory with additional NOx emissions in Fort Hood to address an anticipated underestimation of Fort Hood emissions.

We present a spatial map that represents the 2017 DVF ozone impact from the additional Fort Hood NOx emissions in Figure 5-6. The largest impact is 0.7 ppb and occurs directly over the Fort Hood military base along the border of Bell and Coryell counties. The impact at Killeen Skylark is 0.4 ppb and less than 0.1 ppb at Temple Georgia. Areas of impacts exceeding 0.5 ppb occur just to the west and south of Fort Hood within Bell County and in southeast Lampasas County. Impacts outside the KTF area exceed 0.2 ppb across the northern half of Burnet County and smaller portions of Llano and Williamson counties. We note that the additional NOx emissions added are only a rough estimate of the actual emissions and therefore the associated ozone impacts from additional Fort Hood emissions could be smaller or larger than shown here.

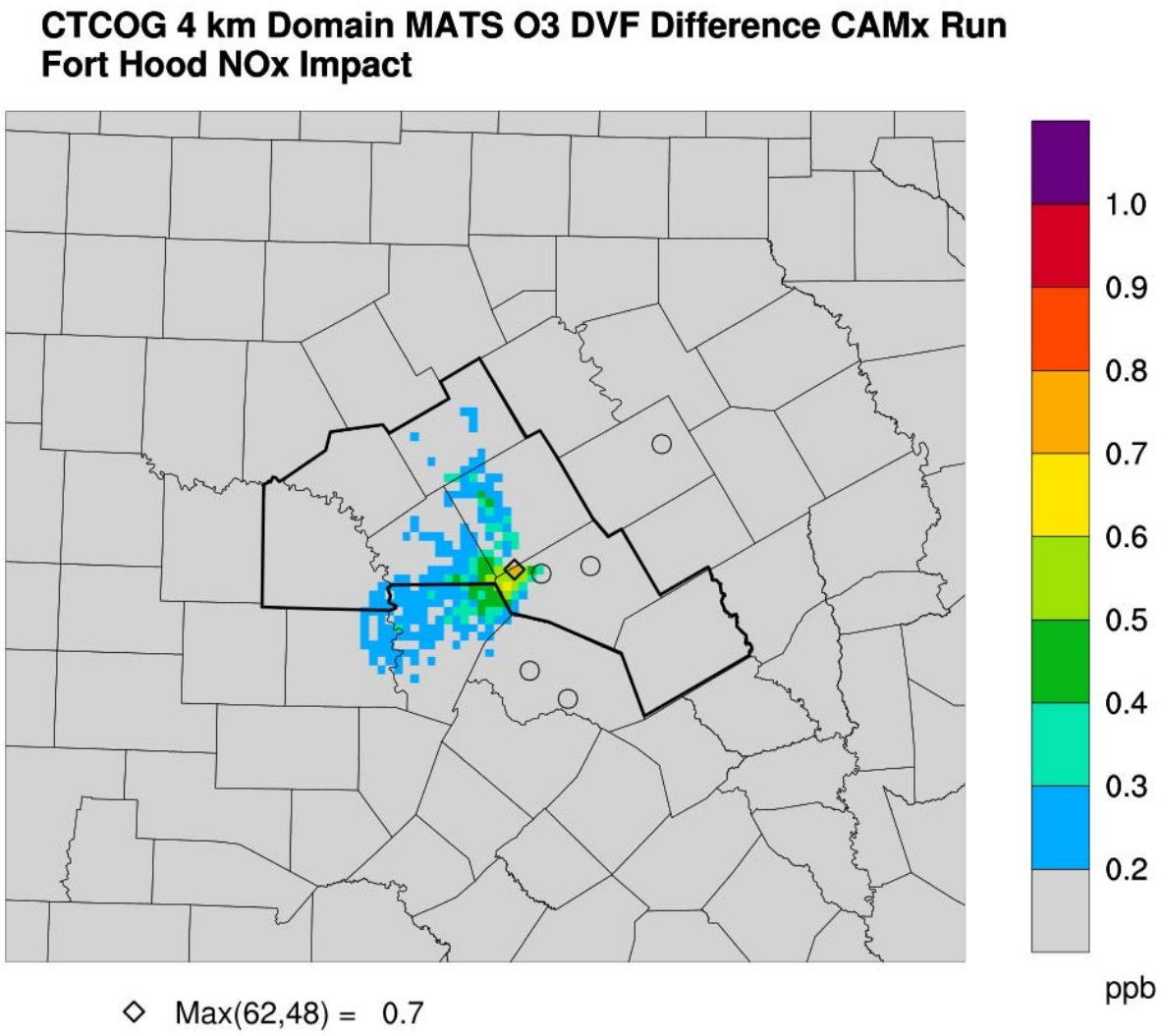

Figure 5-6. Fort Hood military base additional NOx emissions contribution to 2017 ozone DVF.

We present time series of the sensitivity of MDA8 ozone to the Fort Hood NOx emissions in Figure 5-7. Due to the close proximity of the Fort Hood military base to the Killeen monitor, we find that relatively larger impacts (outside the ±0.25 ppb/tpd range) are much more frequent at C1047 (top panel) than at C1045 (bottom panel). In addition, the episode maximum sensitivity at C1047 (1.2 ppb/tpd) is twice the episode maximum sensitivity at C1045 (0.6 ppb/tpd). The uncertainty in the Fort Hood NOx emissions has the potential to contribute to poor ozone model performance at the Killeen and (to a lesser extent) Temple monitors.

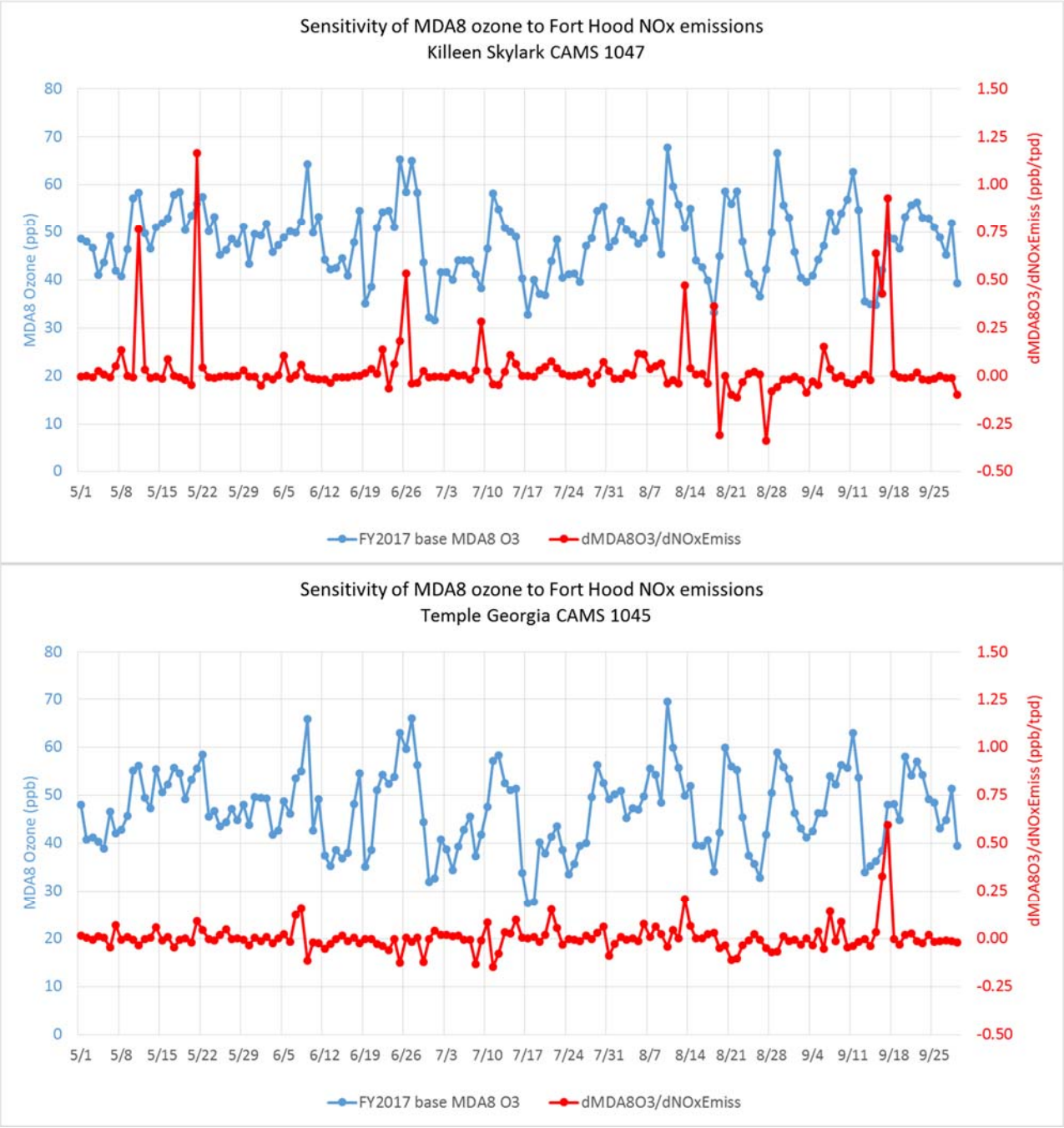

Figure 5-7. Sensitivity of MDA8 ozone to Fort Hood NOx emissions (red; plotted on secondary axis) and MDA8 ozone (blue; plotted on primary axis) at CAMS 1047 (top) and CAMS 1045 (bottom) for the 2017 ozone model.

6.0 SUMMARY OF MODELING RESULTS AND RECOMMENDATIONS FOR IMPROVEMENTS

The main results of the CAMx modeling of 2017 were:

- KTF area emissions of ozone precursors (oxides of nitrogen [NOx] and volatile organic compounds [VOC]) are projected to decrease between 2012 and 2017.
- KTF area ozone design values are projected to decrease between 2012 and 2017.
- The Killeen Skylark monitor (CAMS 1047) model-projected design value for 2017 is 67.5 ppb, which attains the 2015 NAAQS of 70 ppb.
- For CAMS 1047, the contribution of ozone and ozone precursors transported into the KTF area (63.9 ppb) to the 2017 design value is far larger than the contribution of ozone from local KTF emissions sources (3.6 ppb).
- The largest contributions to CAMS 1047 design value from local KTF area emissions are from on-road mobile sources such as cars and trucks (1.3 ppb).
- The combined contribution from Eagle Ford, Haynesville and Barnett Shale O&G sources to the 2017 Killeen monitor ozone design value is 0.9 ppb, which exceeds the contribution of KTF Area O&G emissions sources (0.1 ppb).
- The impact of the Panda Temple EGU on the 2017 design value at CAMS 1047 is less than 0.1 ppb. The maximum impact on KTF area ozone design values is 0.2 ppb near Belton.
- The impact of the Fort Hood military base on the 2017 design value at CAMS 1047 is 0.1 ppb. The maximum impact on KTF area ozone design values is 0.7 ppb near Fort Hood.
- The 2017 modeling showed ozone formation in the KTF area is limited by the amount of available NOx. This finding is consistent with previous KTF studies.
- KTF area emission reduction efforts should continue to focus on NOx reductions rather than VOC reductions.

6.1 Recommendations for Future KTF Area Ozone Modeling

We recognize that Rider 7 funding is no longer available for photochemical modeling to support future air quality planning and make no recommendations for further model development at this time. However, the 2017 modeling platform uses an emission inventory that is applicable to the present day and could be used in the near term by CTAIR for air quality planning.

- We recommend using the 2017 ozone model to quantify ozone impacts of new/proposed emissions sources or changes in emissions from existing sources.
- Analysis of high ozone days when monitored ozone at CAMS 1047 and CAMS 1045 exceed the 2015 National Ambient Air Quality Standard for ozone (70 ppb) continues to be important in understanding the causes of high ozone at the monitor. High ozone day analysis can also identify days which may be excluded from the design value calculation

under the EPA's Exceptional Events Rule[29], potentially lowering the design values at the Killeen Skylark and Temple Georgia monitors.

- As of the writing of this report, the 2017 design value for CAMS 1047 stands at 67 ppb. The 2017 design value for CAMS 1045 stands at 69 ppb. Both design values are below the 2015 National Ambient Air Quality Standard for ozone (70 ppb). If design values in the KTF area were to approach 70 ppb in the future, routine daily photochemical modeling designed to identify the influence of exceptional events on KTF area ozone would be important. Ozone impacts from wildfires, stratospheric ozone or international transport could all be modeled with a short lag time (on the order of 2-3 days) and could be used as a possible screening tool for exceptional events. Ramboll Environ has developed a modeling platform for TCEQ to support this type of analysis.

[29] The Exceptional Events Rule states that if an exceedance of the ozone NAAQS can be shown to be caused by an uncontrollable, unusual event such as a wildfire or stratospheric ozone intrusion, the exceedance day may be excluded from the calculation of the monitor's ozone design value, potentially lowering the design value and even changing nonattainment status to attainment.

7.0 REFERENCES

Dunker A.M., G. Yarwood, J.P. Ortmann, G.M. Wilson. 2002. The decoupled direct method for sensitivity analysis in a three-dimensional air quality model – implementation, accuracy and efficiency. *Environ. Sci. Technol.*, **36,** 2965-2976.

Emery, C., Z. Liu, B. Koo and G. Yarwood, 2016. "Improved Halogen Chemistry for CAMx Modeling." Prepared for the TCEQ, Austin, TX. May.

EPA. 2014. Draft Modeling Guidance for Demonstrating Attainment of Air Quality Goals for Ozone, PM2.5, and Regional Haze http://www.epa.gov/ttn/scram/guidance/guide/Draft_O3-PM-RH_Modeling_Guidance-2014.pdf.

Grant, J., J. King, S. Kemball-Cook and G. Yarwood. 2015. Review of Killeen-Temple-Fort Hood Area Ozone Precursor Emission Inventory for Point, Off-road and Area Sources. Prepared for Ian McCaffrey, TCEQ. May.

Grant, J., L. Huang and S. Kemball-Cook. 2017. Final Report: Emission Inventory Evaluation and Improvement for the Killeen-Temple-Fort Hood Area. Prepared for Jennifer Lawyer, Central Texas Council of Governments. June.

Johnson, J., E. Tai, P. Karamchandani, G. Wilson, and G. Yarwood. 2013. TCEQ Ozone Forecasting System. Prepared for Mark Estes, TCEQ. November.

Johnson, J., G. Wilson, A. Wentland, W. C. Hsieh and G. Yarwood. 2016. Daily Near Real-Time Ozone Modeling for Texas. Prepared for Mark Estes, TCEQ. December.

Kemball-Cook, S., J. Johnson, J. Grant, L. Parker, J. King, W. C. Hsieh and G. Yarwood. 2015. Conceptual Model of Ozone Formation in the Killeen-Temple-Fort Hood Area. Prepared for Ian McCaffrey, TCEQ. September.

Kemball-Cook, S., J. Grant, J. Johnson, L. Parker and G. Yarwood. 2017. Central Texas Council of Governments Ozone Advance Action Plan. Prepared for Jennifer Lawyer, Central Texas Council of Governments. July.

Parker, L., S. Kemball-Cook, G. Yarwood. 2013. "Evaluation of High Ozone Days in Waco and Killeen". Environ International Corporation. Prepared for Heart of Texas Council of Governments. December, 2013.

Parrish, D., S. Kemball-Cook, J. Grant and G. Yarwood. 2017. "Science Synthesis Report: Atmospheric Impacts of Oil and Gas Development in Texas." Prepared for Texas Commission on Environmental Quality, Austin, TX. June.

Ramboll Environ. 2016. User's Guide to The Comprehensive Air quality Model with extensions version 6.40. ENVIRON International Corporation, Novato, CA. March. Available at www.camx.com.

Skamarock, W.C., J.B. Klemp, J. Dudhia, D.O. Gill, D.M. Barker, M.G. Duda, X-Y Huang, W. Wang, J.G. Powers. 2008. "A Description of the Advanced Research WRF Version 3." NCAR Technical Note, NCAR/TN-45+STR (June 2008). http://www.mmm.ucar.edu/wrf/users/.

Texas Commission on Environmental Quality (TCEQ). 2015. Personal Communication with TCEQ staff (Chris Kite). April.

United States Army Environmental Command (USAEC). 2014. "Supplemental Programmatic Environmental Assessment for Army 2020 Force Structure Realignment". June.

Wesely, M. L.: Parameterization of surface resistances to gaseous dry deposition in regional-scale numerical models, Atmos. Environ., 23, 1293–1304, 1989.

Yantosca, B., Long, M., Payer, M., Cooper, M. 2013. GEOS-Chem v9-01-03 Online User's Guide, http://acmg.seas.harvard.edu/geos/doc/man/.

Yarwood, G., B. Koo, 2015. "Improved OSAT, APCA and PSAT Algorithms for CAMx". Prepared for Jim Price, TCEQ. August.

Zhang, L., Brook, J.R. and Vet, R., 2003. A revised parameterization for gaseous dry deposition in air-quality models. Atmospheric Chemistry and Physics, 3(6), pp.2067-2.

APPENDIX A

2012 Model Performance Evaluation

Appendix A 2012 Model Performance Evaluation

A.1 Summer 2012 Ozone Modeling Platform

In this Appendix, we present the Weather Research and Forecasting (WRF; Skamarock et al., 208) model and Comprehensive Air quality Model with Extensions (CAMx; Ramboll Environ, 2016) modeling domains and vertical layer structure. Then we present an overview of the development of the summer 2012 ozone modeling platform and efforts to improve model performance at Killeen Skylark CAMS 1047.

A.1.1 Modeling Domains

Figure A-1 presents the 36/12/4 km WRF and CAMx modeling domains used for the ozone modeling platform. These domains are the TCEQ State Implementation Plan (SIP) modeling domains and are defined on a Lambert Conformal Conic (LCC) map projection identical to that used in the Regional Planning Organization (RPO) modeling[30]. The RPO projection is defined to have true latitudes of 33°N and 45°N and central latitude and longitude point (97°W, 40°N). The 36 km WRF modeling domain encompasses the continental U.S. and parts of Canada and Mexico. The 12 km grid includes Texas and adjacent states and the 4 km grid is centered on East Texas. WRF 36, 12 and 4 km grids are slightly larger than the corresponding CAMx grids to remove any artifacts (i.e., numerical noise) that can arise in WRF adjacent to fine grid boundaries.

The vertical layer mapping table from lowest 42 layers (43 total) in WRF to 29 layers in CAMx, is presented in Figure A-2. As with the modeling domains, this layer mapping is based on the TCEQ SIP modeling and other recent modeling work performed by Ramboll Environ.

[30] http://www.epa.gov/visibility/regional.html

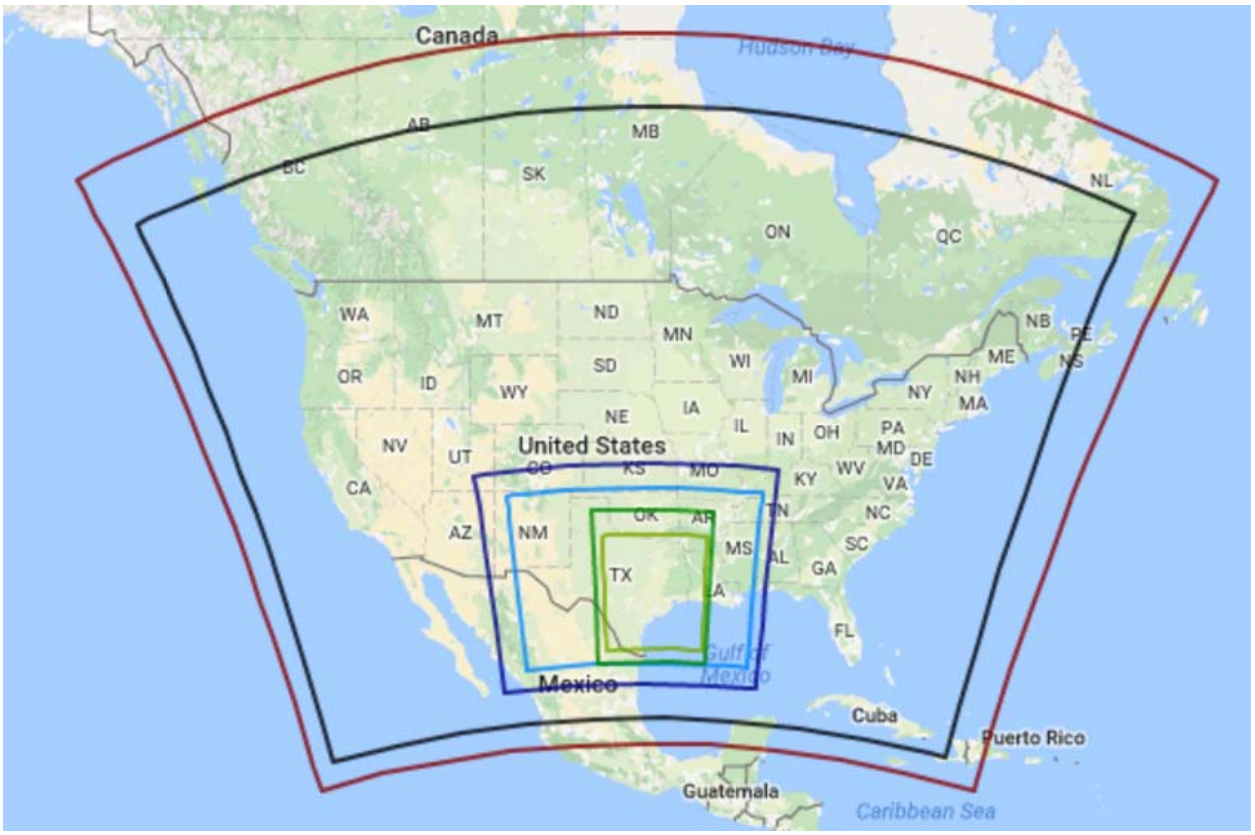

WRF Domain	Range (km)		Number of Cells		Cell Size (km)	
	Easting	Northing	Easting	Northing	Easting	Northing
North America Domain	(-2916,2916)	(-2304,2304)	163	129	36	36
South US Domain	(-1188,900)	(-1800,-144)	175	139	12	12
Texas Domain	(-396,468)	(-1620,-468)	217	289	4	4
CAMx Domain	**Range (km)**		**Number of Cells**		**Cell Size (km)**	
	Easting	**Northing**	**Easting**	**Northing**	**Easting**	**Northing**
RPO 36km Domain	(-2736,2592)	(-2088,1944)	148	112	36	36
Texas 12km Domain	(-984,804)	(-1632,-312)	149	110	12	12
Texas 4km Domain	(-328,436)	(-1516,-644)	191	218	4	4

Figure A-1. WRF and CAMx 36/12/4 km modeling domains developed by TCEQ.

2012 MAY - SEP

WRF Layer	CAMx Layer	Top (m AGL)	Center (m AGL)	Thickness (m)
42	29	18250	16445	3611
39	28	14639	13632	2015
37	27	12624	10786	3675
33	26	8949	7891	2115
30	25	6833	6289	1088
28	24	5746	5290	911
26	23	4835	4449	772
24	22	4063	3704	717
22	21	3346	3175	341
21	20	3005	2840	330
20	19	2675	2515	320
19	18	2355	2225	259
18	17	2096	1969	253
17	16	1842	1718	248
16	15	1595	1474	242
15	14	1353	1281	143
14	13	1210	1140	141
13	12	1069	1000	139
12	11	930	861	138
11	10	792	747	91
10	9	702	656	90
9	8	612	567	89
8	7	522	478	89
7	6	433	389	88
6	5	345	302	87
5	4	258	215	87
4	3	171	128	86
3	2	85	60	51
2	1	34	17	34

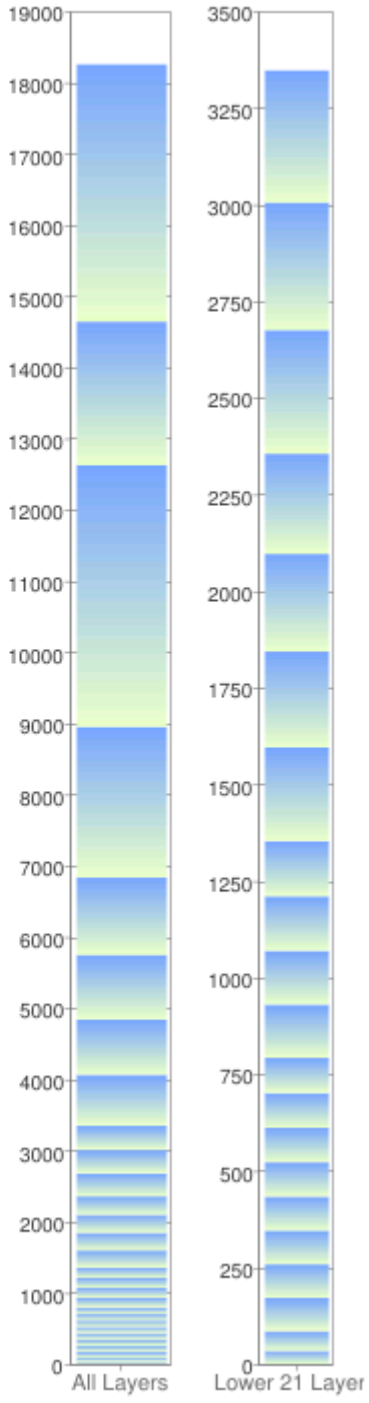

Figure A-2. CAMx Model Layer Structure. TCEQ figure from [http://www.tceq.texas.gov/airquality/airmod/rider8/modeling/domain.](http://www.tceq.texas.gov/airquality/airmod/rider8/modeling/domain)

A.1.2 Overview of Modeling Platform Development for 2012

Background on Ozone Model Development for KTF Area

In March 2015, the TCEQ completed development of a June 2012 modeling episode for use by the Texas NNAs. The TCEQ developed episode-specific weather data as well as a June 2012 emission inventory. This 2012 episode replaced the TCEQ's older June 2006 modeling episode. Ramboll Environ evaluated the 2012 ozone model (Kemball-Cook et al., 2015) and found persistent ozone overestimates at the Killeen Skylark (CAMS 1047) monitor on most days of the episode. However, substantial ozone underestimates were found when observed ozone exceeded 70 ppb. Evaluation of ozone source apportionment results found that transported ozone contributed far more than local emissions sources to ozone at CAMS 1047 and that ozone formed almost exclusively under NOx-limited conditions. Based on the results of the model performance evaluation, Ramboll Environ recommended taking steps to improve model performance at CAMS 1047 and revisiting the ozone source apportionment modeling after 2012 model performance had improved.

Updated KTF Ozone Model

In early 2016, TCEQ made available an ozone modeling platform for the June 2012 modeling episode for the Texas NNAs. This release was an updated version of the platform that was released in 2015. This platform includes all the model inputs (including meteorology, emissions and initial/boundary conditions), model source code and scripts needed to run the CAMx photochemical grid model for a given episode. Relative to the original June 2012 modeling platform released in 2015, the updates were relatively minor and included minor model source code updates. TCEQ's ultimate goal was to develop a modeling platform for the May – September 2012 modeling episode – which includes a 2017 future year scenario for attainment demonstration purposes – that was to be used for the Houston SIP.

Ramboll Environ evaluated TCEQ's June 2012 ozone modeling platform, including an evaluation of WRF meteorological performance. Hereafter, we refer to this modeling platform as TCEQ_r0. In Table A-1, we present the WRF meteorological configuration details for TCEQ_r0 as well as subsequent WRF simulations performed by TCEQ (TCEQ_r1 and TCEQ_r2) and Ramboll Environ (REWRF) described below.

Evaluation of the TCEQ_r0 simulation revealed substantial ozone overestimations at many East Texas locations including the Killeen Skylark (CAMS 1047) monitor. We present measured and modeled MDA8 ozone time series during the June 2012 period at CAMS 1047 for the TCEQ_r0 simulation in Figure A-3. The persistent positive ozone bias is evident throughout the modeling period and results in a mean bias of 3.8 ppb and mean error of 6.6 ppb (Root Mean Squared Error, RMSE: 7.77 ppb). However, the day of the highest observed MDA8 ozone – June 26 – showed a substantial underestimate at CAMS 1047. These model performance results at CAMS 1047 are consistent with our analysis of the previous June 2012 TCEQ platform released by TCEQ and evaluated by Ramboll Environ in 2015 (Kemball-Cook et al., 2015).

A WRF meteorological model performance evaluation conducted for the same TCEQ_r0 June 2012 modeling platform revealed significant humidity and precipitation errors in the model. In

Figure A-4, we present June 2012 monthly total precipitation for the PRISM (Parameter-elevation Relationships on Independent Slopes Model[31]) analysis fields (left) versus WRF modeled precipitation (right) for the 36 km (top), 12 km (middle) and 4 km (bottom) domains. The PRISM analysis fields are based on precipitation observations from U.S. monitoring sites and cover the continental United States and do not extend into Canada or over the ocean. The WRF simulation shows large overestimations of precipitation (wet bias) across the Eastern U.S. for the 36 and 12 km domains coupled with substantial underestimations of precipitation (dry bias) for most of East Texas within the 4 km domain. We note that a lack of feedback from the cumulus parameterization to the radiation scheme and/or use of large moisture nudging coefficients (see Table A-1) may have contributed to these model issues.

All meteorological models have trouble consistently simulating the timing and location of sub-grid scale convective features that produce precipitation from thunderstorms. These models typically show much better reproduction of synoptic scale features that also produce precipitation. However, the extreme underestimations of precipitation from the WRF simulation across East Texas shown in Figure A-4 suggest the presence of a systematic bias that may be related to a general lack of cloud cover and/or other model features (e.g. changes in wind speed and direction, mixing depths and temperature) that are associated with precipitation. All of these factors have the potential to substantially impact ozone concentrations in the ozone model. Therefore, it is reasonable to expect that the poor precipitation performance may be indicative of degraded ozone performance in CAMx. The relatively poor CAMx ozone and WRF humidity/precipitation performance guided Ramboll Environ to develop a new WRF modeling platform for June 2012 to determine if ozone performance could be improved. While RE was in the process of evaluating this new modeling platform in August 2016, TCEQ released a new ozone model (TCEQ_r1) covering the May – September 2012 ozone season which included an updated WRF simulation. RE then extended its WRF modeling episode to match the May – September 2012 modeling period (REWRF). After RE completed seasonal 2012 CAMx ozone model simulations using this new WRF simulation in December 2016, TCEQ released an updated version of their modeling platform (TCEQ_r2) used for the Houston SIP. Throughout this process, major issues with WRF meteorological performance were addressed and resolved through collaboration between the TCEQ and RE.

Table A-1. WRF configuration details for TCEQ and RE WRF simulations.

	TCEQ_r0 (June 2012; released early 2016)	TCEQ_r1 (May-Sep 2012; released Aug 2016)	TCEQ_r2 (May-Sep 2012; HGB SIP released Dec 2016)	REWRF (May-Sep 2012)
		(Differences from TCEQ_r0)	(Differences from TCEQ_r0)	
WRF version	3.6.1	3.7.1	3.7.1	3.7.1
Horizontal Resolution	36/12/4 km			36/12/4 km
Vertical Resolution	43 layers	44 layers	44 layers	36 layers

[31] ftp://rattus.nacse.org/pub/prism/docs/appclim97-prismapproach-daly.pdf

	TCEQ_r0 (June 2012; released early 2016)	TCEQ_r1 (May-Sep 2012; released Aug 2016)	TCEQ_r2 (May-Sep 2012; HGB SIP released Dec 2016)	REWRF (May-Sep 2012)
Microphysics	36/12 km: WSM5 4 km: WSM6			Thompson
Longwave Radiation	RRTM			RRTMG
Shortwave Radiation	Dudhia			RRTMG
Surface Layer Physics	Revised MM5 similarity			Monin-Obukhov
LSM	Pleim-Xiu			Noah
PBL scheme	Yonsei University (YSU)			Yonsei University (YSU)
Cumulus parameterization	Kain-Fritsch on 36/12 km grids; None on 4 km	Kain-Fritsch on 36/12 km grids; Multi-scale Kain-Fritsch on 4 km	Kain-Fritsch on 36/12 km grids; Multi-scale Kain-Fritsch on 4 km	Kain-Fritsch on 36/12 km grids; None on 4 km
Cumulus feedback to radiation scheme	Off	On	On	On
Boundary and Initial Conditions Data Source	40 km NAM/Eta analysis			12 km NAM analysis
Analysis Nudging Coefficients (s-1)	36/12 km: 3-D 4 km: 3-D and surface			36/12 km: 3-D 4 km: none
Winds	36/12/4 km: $3x10^{-4}$			36 km: $5x10^{-4}$; 12km: $3x10^{-4}$
Temperature	36/12/4 km: $3x10^{-4}$ (above PBL only for 3-D)			36 km: $5x10^{-4}$; 12km: $3x10^{-4}$ (above PBL only)
Mixing Ratio	36/12/4 km: $3x10^{-4}$ (above PBL only for 3-D)		None	36/12 km: $1x10^{-5}$ (above PBL only)
Observation Nudging Coefficients (s-1)	4 km only (MADIS profiler/sodar ONLY)			None
Winds	$6x10^{-4}$			None
Temperature	None			None
Mixing Ratio	None			None
Urban Canopy Model	4 km: 1-layer UCM		None	None

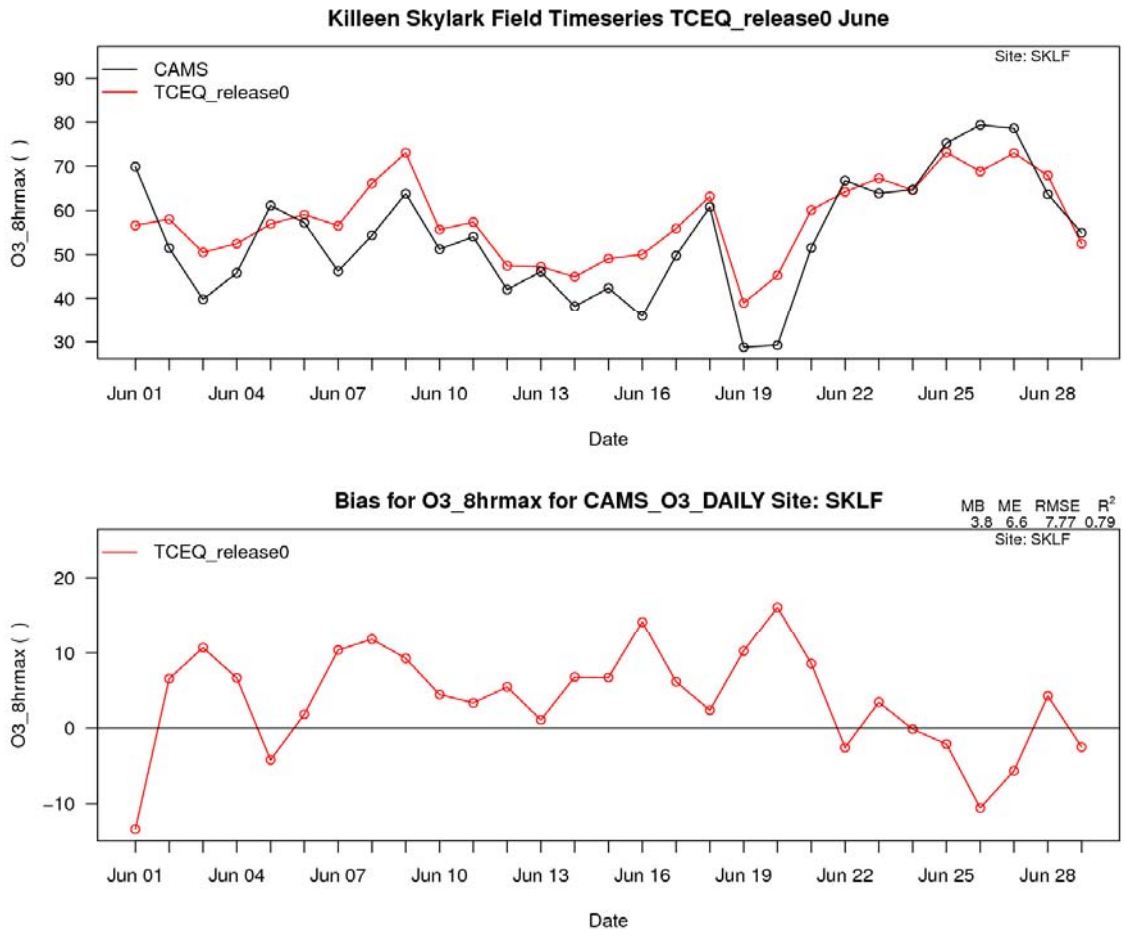

Figure A-3. Top panel: observed MDA8 ozone (black) at Waco Mazanec C1037 monitor versus TCEQ_r0 modeled MDA8 surface layer ozone (red) for the June 2012 modeling episode. Bottom panel: MDA8 ozone bias (model-observed) at the Killeen Skylark C1047 monitor for the June 2012 modeling episode.

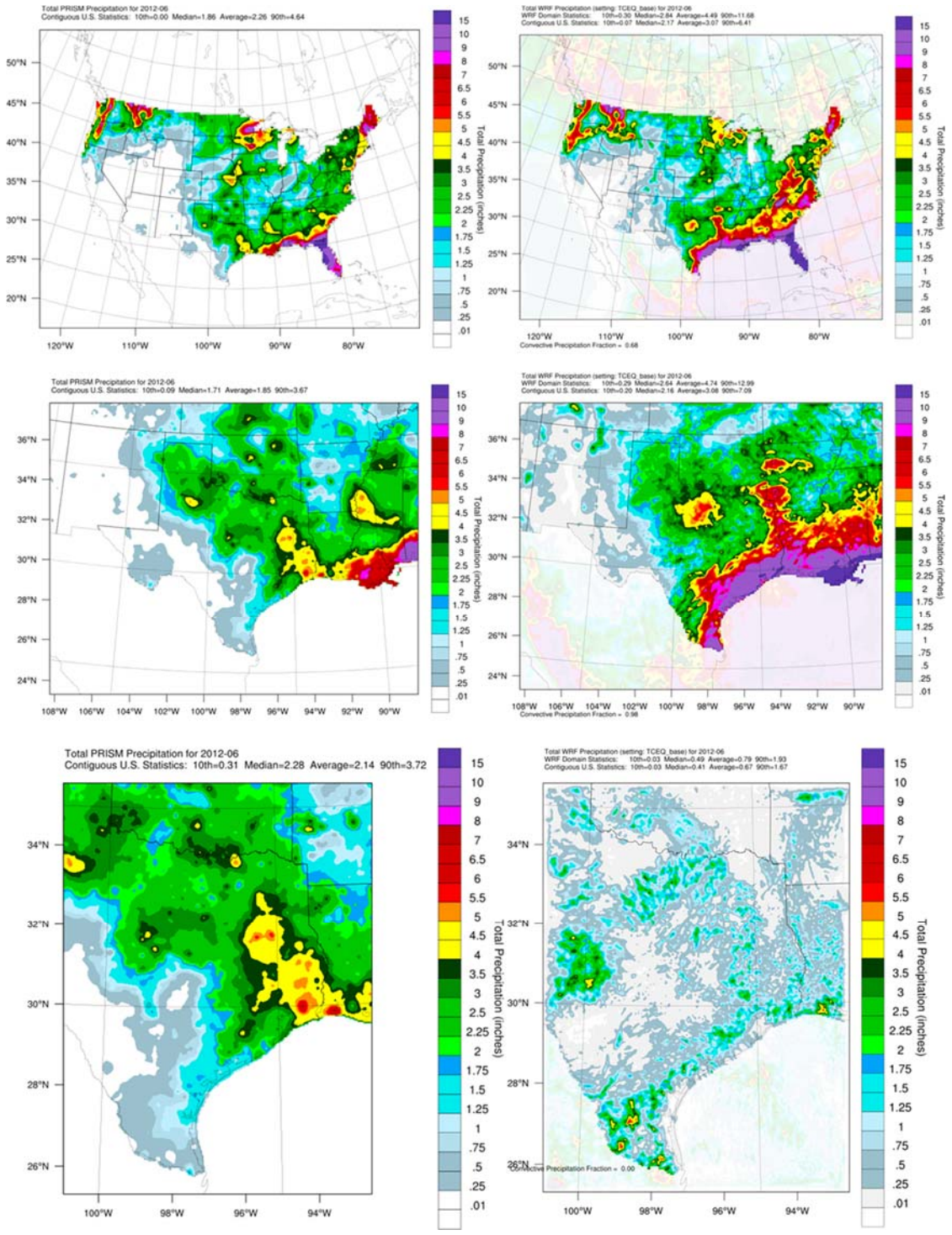

Figure A-4. June 2012 monthly total precipitation comparison for the 36 km (top), 12 km (middle) and 4 km (bottom) for PRISM (left) and WRF modeled precipitation (right).

Table A-2 describes the CAMx ozone model configurations used by TCEQ and RE between late 2015 and early 2017. TCEQ_r0, TCEQ_r1 and TCEQ_r2 were all released by TCEQ and each utilized unique WRF meteorological simulations.

RE developed a new CAMx ozone modeling platform in early 2017 (REWRF) that combined REWRF meteorology, the emissions inventory developed by the TCEQ for the HGB SIP and the latest CAMx updates available at the time of modeling (model version 6.40, Carbon Bond 6 release 4 [CB6r4; Emery et al., 2016] chemical mechanism and new Asymmetric Convective Model version 2 [ACM2; Pleim, 2007] vertical diffusion scheme). The CB6r4 chemical mechanism combines a condensed set of reactions involving ocean-borne inorganic iodine from the full halogen mechanism with temperature- and pressure-dependent organic nitrate branching. This mechanism also provides a more realistic characterization of ozone deposition to seawater (Ramboll Environ, 2016). Ozone is frequently transported from the Gulf of Mexico to Central and East Texas. By including more ozone destruction pathways over the Gulf via the halogen chemical mechanism, we reduced widespread high ozone bias (Emery et al., 2016; Johnson et al., 2016). The ACM2 vertical diffusion scheme is considered more accurate than the default K-theory scheme utilized in CAMx, but has historically run much slower than K-theory, limiting its usefulness for most applications. The latest update to the ACM2 scheme results in much faster runtime (Ramboll Environ, 2016) so that it can be used for a wide range of applications.

Finally, RE developed a new CAMx sensitivity (TCEQWRF) that was identical to the REWRF configuration, but substituted REWRF for TCEQ_r2 WRF meteorological inputs. This run was designed to be able to isolate the impact of WRF meteorology in the REWRF simulation. This also allowed comparison with the TCEQ_r2 run to evaluate the impact of the CAMx model updates introduced in REWRF separately.

The primary focus for this application is 2017 ozone source apportionment and source sensitivity analyses, so a complete meteorological model performance evaluation for summer 2012 is not presented here. Instead, resulting ozone model performance for the 2012 ozone season that compares performance across the TCEQ_r2, TCEQWRF and REWRF CAMx simulations is presented in the next section. Ramboll Environ determined from this evaluation that the TCEQWRF simulation demonstrated the best overall ozone model performance. We used this TCEQWRF configuration for 2017 ozone source apportionment and source sensitivity modeling that is presented in Sections 5 and 6, respectively.

Table A-2. CAMx configuration options for TCEQ and RE CAMx simulations.

	TCEQ_r0 (June 2012; released early 2016)	TCEQ_r1 (May-Sep 2012; released Aug 2016)	TCEQ_r2 (May-Sep 2012; HGB SIP released Dec 2016)	REWRF (May-Sep 2012)	TCEQWRF (May-Sep 2012)
		(Differences from TCEQ_r0)	(Differences from TCEQ_r0)		(Differences from REWRF)
Model Code	v6.11	v6.30	v6.31	v6.40	
Vertical Layers	28 layers (model top ~14.5 km)	29 layers (model top ~18 km)	29 layers (model top ~18 km)	29 layers (model top ~18 km)	
Chemistry					
Gas Phase Chemistry	CB6r2	CB6r2h (CB6r2 + streamlined halogen chemistry)	CB6r2h (CB6r2 + halogen chemistry); includes in-line sea salt emissions	CB6r4 (CB6r3 + i16b iodine chemistry + INTR hydrolysis rxn + hetero SO2 rxn; deleted O + organics)	
Aerosol Chemistry	None			None	
Plume-in-Grid	GREASD			GREASD	
Photolysis Rate Adjustment	In-line TUV			In-line TUV	
Meteorological Processor	WRFCAMx			WRFCAMx	
Subgrid Cloud Diagnosis	CMAQ-based			CMAQ-based	
Horizontal and Vertical Transport					
Eddy Diffusivity Scheme	ACM2	K-Theory	K-Theory	ACM2 (new formulation from v6.40)	
Diffusivity Lower Limit	Kz_min = 0.1 m^2/s			Kz_min = 0.1 m^2/s	
Dry Deposition	Zhang et al. (2003)	Wesely (1989)	Wesely (1989)	Wesely (1989)	
Numerical schemes					
Gas Phase Chemistry Solver	Euler Backward Iterative (EBI)			Euler Backward Iterative (EBI)	
Horizontal Advection Scheme	Piecewise Parabolic Method (PPM) scheme			Piecewise Parabolic Method (PPM) scheme	
Inputs					
WRF Meteorology	TCEQ_r0 (June 2012; released 2015)	TCEQ_r1 (May-Sep 2012; released Aug 2016)	TCEQ_r2 (May-Sep 2012; HGB SIP released Dec 2015)	REWRF (May-Sep 2012)	TCEQ_r2 (May-Sep 2012; HGB SIP released Dec 2015)
IC/BCs	GEOS-Chem	GEOS-Chem	GEOS-Chem with halogens	GEOS-Chem with halogens	

	TCEQ_r0 (June 2012; released early 2016)	TCEQ_r1 (May-Sep 2012; released Aug 2016)	TCEQ_r2 (May-Sep 2012; HGB SIP released Dec 2016)	REWRF (May-Sep 2012)	TCEQWRF (May-Sep 2012)
Top Concentrations	None		GEOS-Chem with halogens	GEOS-Chem with halogens	
Biogenic Emissions	MEGAN v2.10	MEGAN v2.10 (Isoprene EF adjusted to reflect aircraft measurements; LAI and PFT updates)	BEIS v3.61	BEIS v3.61	
Anthropogenic Emissions	Developed by TCEQ	Various updates to anthropogenic EI from TCEQ_r0	HGB SIP[32]	HGB SIP	

A.2 Model Performance Evaluation

A.2.1 Model Performance Evaluation Approach

We present results from the model performance evaluation (MPE) in this section. The goal was to identify the best performing model among TCEQ_r2, TCEQWRF, and REWRF, which would then be used in the source apportionment and source sensitivity modeling and analysis for the KTF area. We used ground level ozone observations from rural and suburban Air Quality System (AQS) and Clean Air Status And Trends Network (CASTNET) monitors outside Texas and TCEQ CAMS monitors within Texas for the MPE. Accurate model source apportionment relies on adequate model performance not only at the receptor sites of interest, but also along the transport paths from the sources. With such consideration, our comparative MPE entails three types of analyses as follows.

We first examine the overall model performance on regional scale at CAMS monitors in and around Dallas-Fort Worth region as well as in the entire 4 km modeling domain covering the state of Texas, to assess the models' capabilities in reproducing the background conditions; model performance outside Texas in the outer 36 km domain is also examined to evaluate model representation of long range ozone transport.

We recognize that the KTF area monitoring network is too sparse to perform a complete model performance evaluation across the region. The Dallas-Fort Worth area however, offers several advantages for evaluating ozone model performance:

[32] https://www.tceq.texas.gov/assets/public/implementation/air/sip/hgb/HGB_2016_AD_RFP/AD_Adoption/HGB_AD_SIP_Appendix_B_Adoption.pdf

- Relatively dense monitoring network
- Rural/suburban monitors form a "ring" around the DFW region that are distinct from urban monitors
- Nearby and frequently upwind of KTF region

We performed a detailed evaluation of ozone transport and the local production of ozone for the dense monitoring network in Dallas-Fort Worth, with the assumption that the model performance results are representative of ozone transport and urban ozone production in East Texas and in the KTF area in particular. One way to evaluate ozone model performance across an area such as Dallas-Fort Worth is to calculate the MDA8 ozone Local Increment (LI), which is defined as the difference between median MDA8 ozone concentration across rural/suburban monitors and the maximum MDA8 ozone concentration across all monitors in the same region. Observed MDA8 LI are classified into different ranges and compared with model simulations, to evaluate model skill of reproducing urban ozone production and enhancements. This approach also has the benefit of not penalizing the model for slight displacements or misalignments of ozone plumes within a metropolitan area.

Finally, we examine the model performance at monitors in and around the KTF area, the region of interest for this study. Results from the above three types of comparisons provide a comprehensive perspective of the relative model performance of the three different CAMx simulations.

Table A-3 lists statistical metrics considered in the MPE. These metrics quantitatively assess the agreement between model simulations and the observations in terms of model bias (NMB and MB), model error in absolute (ppb) (ME, RMSE) or relative (%) (NME) sense, as well as pattern variability (R^2).

Table A-3. Definition of statistical metrics used in model performance evaluation.

Statistical Measure	Mathematical Expression	Notes
Coefficient of determination (R^2)	$\frac{\left[\sum_{i=1}^{N}(P_i-\overline{P})(O_i-\overline{O})\right]^2}{\sum_{i=1}^{N}(P_i-\overline{P})^2\sum_{i=1}^{N}(O_i-\overline{O})^2}$	P_i = prediction at time and location i; O_i = observation at time and location i; $\overline{P}$ = arithmetic average of Pi, i=1,2,…, N; $\overline{O}$ = arithmetic average of Oi, i=1,2,…,N
Normalized Mean Error (NME)	$\frac{\sum_{i=1}^{N}\lvert P_i-O_i\rvert}{\sum_{i=1}^{N}O_i}$	Reported as %
Mean Error (ME) (also known as Mean Absolute Gross Error)	$\frac{1}{N}\sum_{i=1}^{N}\lvert P_i-O_i\rvert$	Reported as concentration (e.g., ppb)

Statistical Measure	Mathematical Expression	Notes
Normalized Mean Bias (NMB)	$\frac{\sum_{i=1}^{N}(P_i - O_i)}{\sum_{i=1}^{N} O_i}$	Reported as %
Mean Bias (MB)	$\frac{1}{N}\sum_{i=1}^{N}(P_i - O_i)$	Reported as concentration (e.g., ppb)
Root Mean Square Error (RMSE)	$\sqrt{\frac{1}{N}\sum(P_j - O_j)^2}$	Reported as concentration (e.g., ppb)

In addition to time series plots of observed and modeled MDA8 ozone pairs at individual sites, quantile-quantile (Q-Q) plots are employed to compare observed versus modeled statistical distributions of hourly and MDA8 ozone. Density scatter plots are used to visualize the clustering of modeled and observed data pairs at different concentration ranges. The plots are described in the next section.

A.3 Overall Regional Level Ozone Model Performance

Figure A-5 and Figure A-6 present the density scatter plots and quantile-quantile (Q-Q) plots of observed versus modeled hourly (top) and MDA8 (bottom) ozone for all CAMS sites in the Dallas-Fort Worth region. Both products are types of scatter plots that show observed ozone on the x-axis and modeled ozone on the y-axis. Density scatter plots use colored contouring to display the number of points in a given area of the plot. In the density scatter plots in this section, blue represents the lowest concentration or density of points, while dark red represents the highest density of points.

Q-Q plots sort model/observed pairs by the observed values (called quantile pairing) in order to better understand how well the model performs for different ranges of observed ozone. The Q-Q plots in this section include a solid red line that indicates the linear regression for the quantile-paired points and the black dashed line is the 1:1 line. For both plots, the closer the points align with the 1:1 line, the better the model agrees with the observations.

For hourly ozone, all three model runs have the vast majority of predictions fall between the 1:2 and 2:1 to the observed concentrations, as well as highest density of data points along 1:1 line (Figure A-5). All three models tend to overestimate ozone when observed concentrations are below 20 ppb. Distinct differences between REWRF and TCEQ_r2/TCEQWRF exist when observed concentrations are between 20 and 40 ppb, with a higher tendency of overestimation by REWRF than TCEQ_r2/TCEQWRF. The best agreement is seen in 60-80 ppb concentration range for both models. When observed concentrations are above 80 ppb, all three model runs tend to underestimate ozone, while the bias is slightly worse with REWRF.

The high bias of REWRF below 40 ppb is also apparent in the Q-Q plots (Figure A-6), where individual quantile points and the linear regression line of REWRF are consistently above the 1:1 line. For MDA8 ozone, all model runs show a substantial positive bias when observed concentrations are below 60 ppb, and a negative bias when observed concentrations are higher than 60 ppb. The difference between the three model runs are not as distinct as for hourly ozone, with TCEQ_r2 and TCEQWRF showing tighter clustering of data points along the 1:1 line in the density scatter plots (Figure A-5) and smaller magnitudes of model biases in the Q-Q plots (Figure A-6). Overall, for both hourly and MDA8 ozone, the TCEQ_r2 and TCEQWRF runs outperform REWRF at monitoring sites in the Dallas-Fort Worth region.

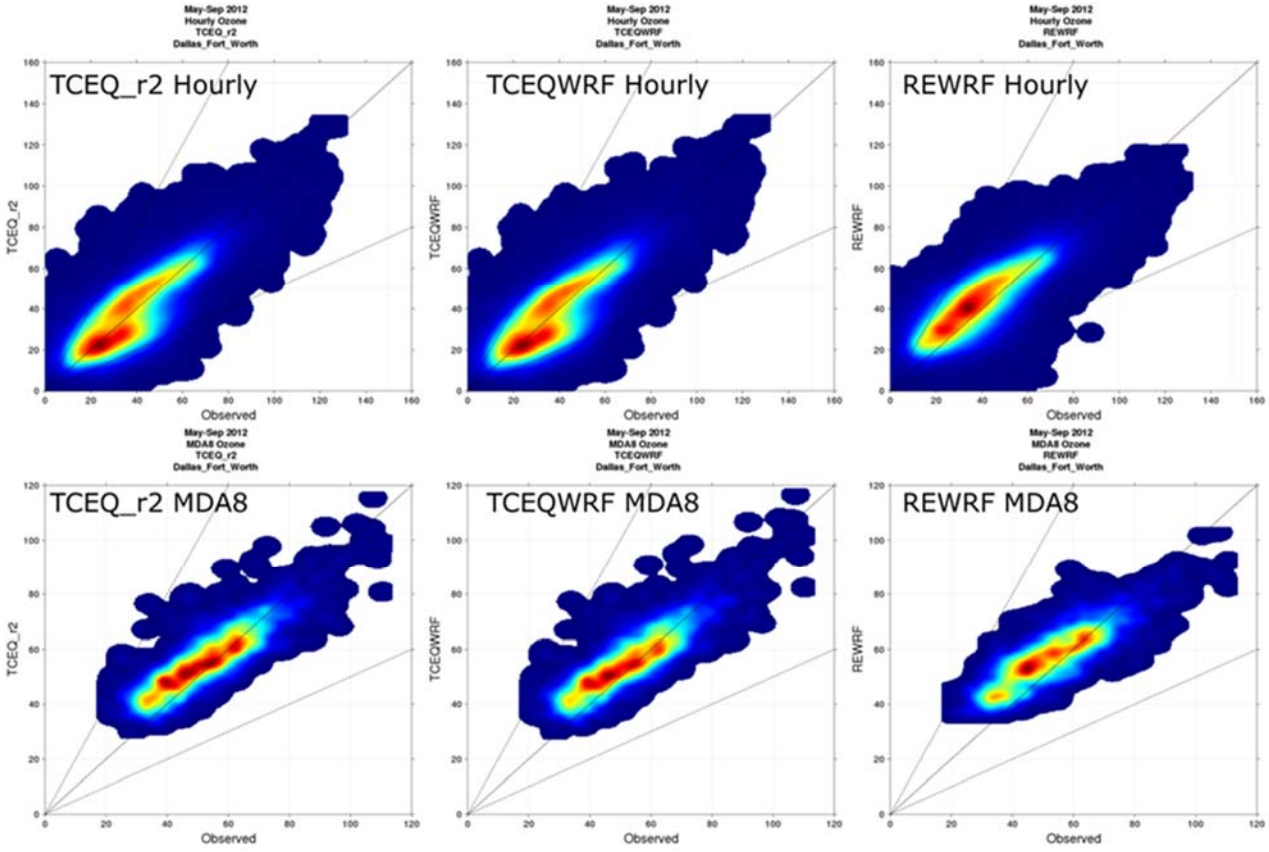

Figure A-5. Density scatter plots of observed and modeled hourly (top) and MDA8 ozone (bottom) at CAMS monitors in the Dallas-Fort Worth region during May – September 2012 for the TCEQ_r2 (left), TCEQWRF (middle) and REWRF (right) CAMx simulations.

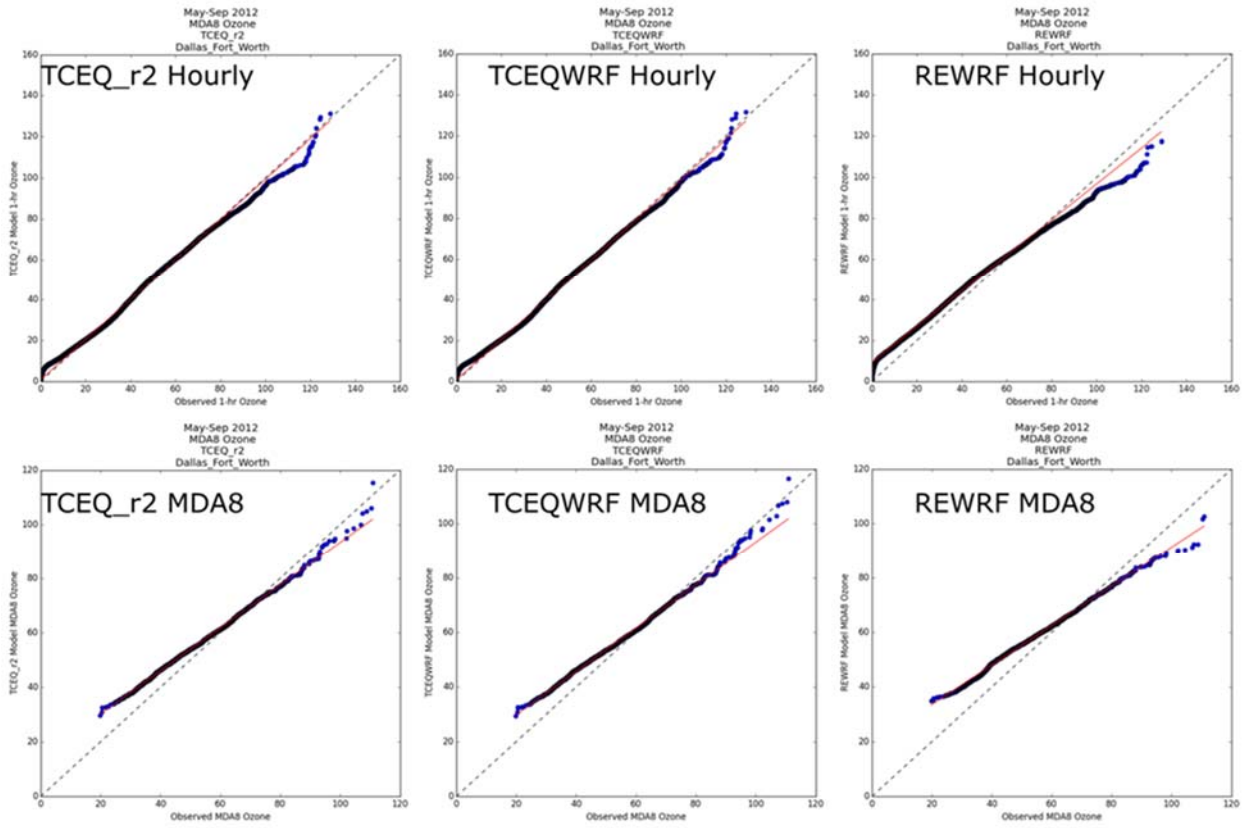

Figure A-6. Quantile-Quantile (Q-Q) plots of observed and modeled hourly (top) and MDA8 (bottom) ozone at CAMS monitors in the Dallas-Fort Worth region during May – September 2012 for the TCEQ_r2 (left), TCEQWRF (middle) and REWRF (right) CAMx simulations. Red straight lines are from linear regression using the quantile-paired points.

Figure A-7 and Figure A-8 suggest that qualitative findings above hold true when the comparison is extended to all CAMS sites within the Texas 4 km modeling domain. Although the quantitative range of model biases changes by some extent, the relative performance revealed by Q-Q plots and density scatter plots still suggest that the TCEQ_r2 and TCEQWRF runs outperform REWRF.

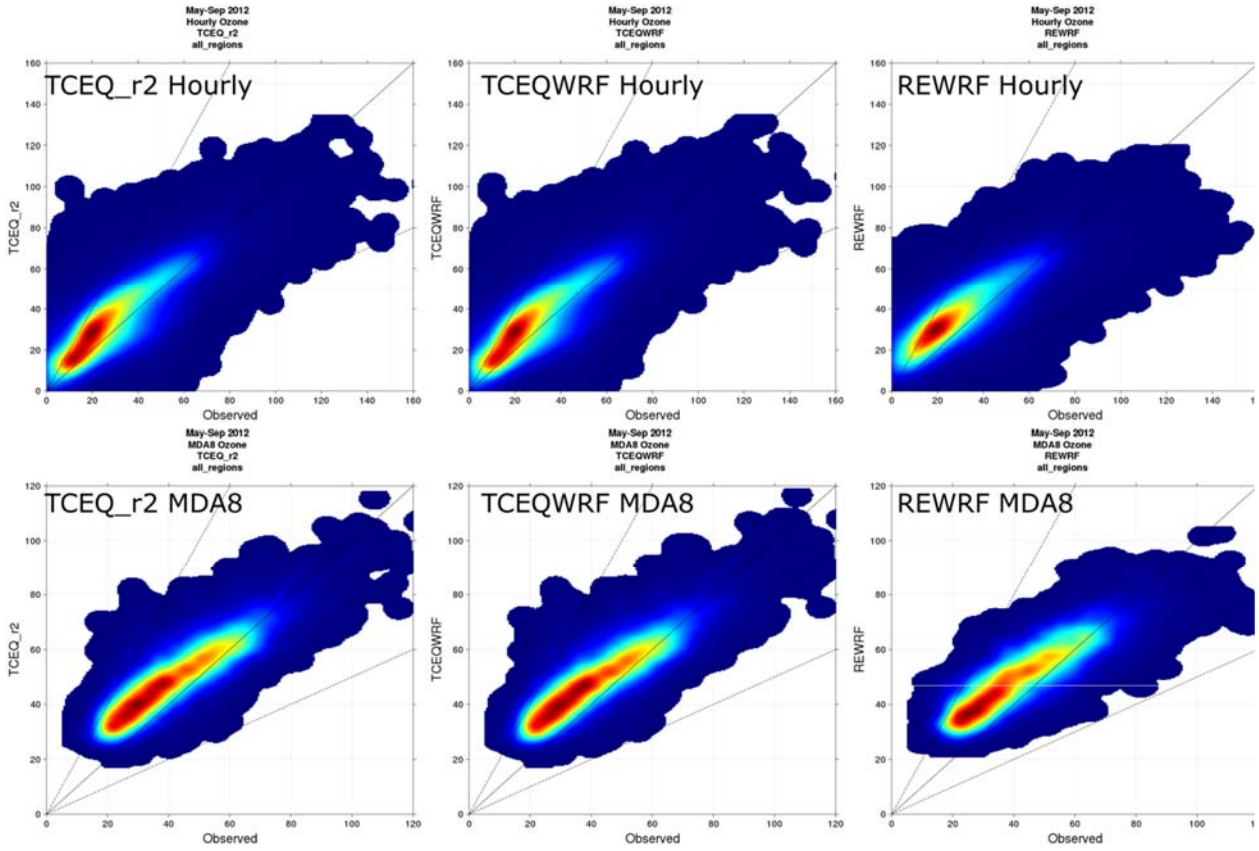

Figure A-7. Density scatter plots of observed and modeled hourly (top) and MDA8 (bottom) ozone at all CAMS monitors in the Texas 4 km CAMx modeling domain during May – September 2012 for the TCEQ_r2 (left), TCEQWRF (middle) and REWRF (right) CAMx simulations.

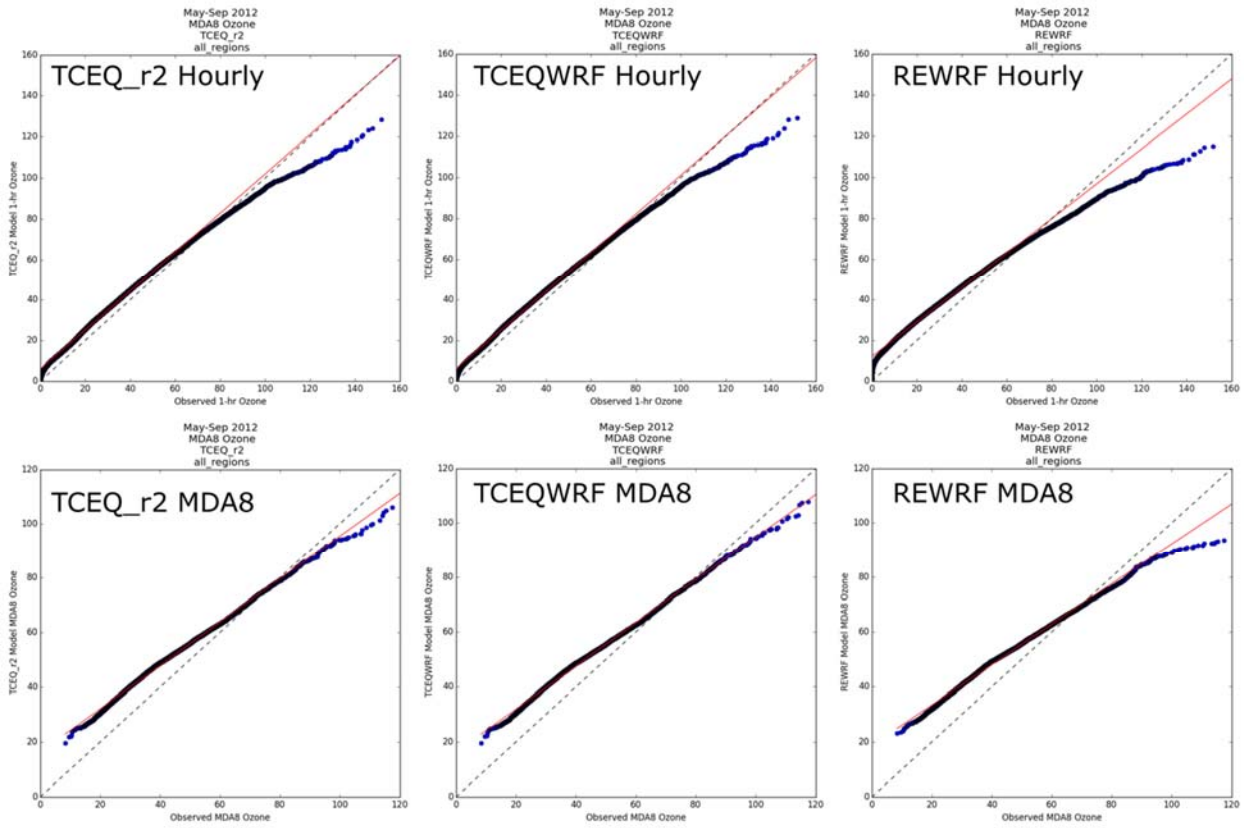

Figure A-8. Quantile-Quantile (Q-Q) plots of observed and modeled hourly (top) and MDA8 (bottom) ozone at all CAMS monitors in the 4 km CAMx modeling domain during May – September 2012 for the TCEQ_r2 (left), TCEQWRF (middle) and REWRF (right) CAMx simulations. Red straight lines are from linear regression using the quantile-paired points.

In summary, on a regional level within Texas, the nearly indistinguishable performance of TCEQ_r2 and TCEQWRF suggests minor impact due to changes of model configuration in chemical mechanism, vertical diffusion and other minor changes introduced by updated model version. In contrast, different meteorological inputs lead to notable better ozone model performance in the TCEQ_r2/TCEQWRF runs compared to REWRF. Compared to TCEQ_r2 and TCEQWRF, the regional background ozone in REWRF may be too high due to misrepresented meteorology.

Next, we examine ozone performance at broader regions upwind of Texas in the 36 km domain in order to understand potential impact of long range transport on ozone model performance within the 4 km domain. Figure A-9 shows spatial maps of Mean Bias (MB) of MDA8 ozone for TCEQ_r2 (upper), TCEQWRF (middle) and REWRF (lower) at rural AQS and CASTNET monitoring sites in the Ohio/Tennessee Valley region during May – September 2012. TCEQ_r2 and TCEQWRF show similar performance. All three simulations have a tendency to overestimate ozone in the southern states in this region while underestimating ozone in the northern sites. REWRF demonstrates a consistently higher bias than the other two simulations. These differences are also illustrated from a statistical perspective in Figure A-10. In terms of quantile

distributions, REWRF is more deviated from the 1:1 line with respect to observation than the other two simulations by overestimating lower quantiles of ozone while underestimating higher quantiles of ozone.

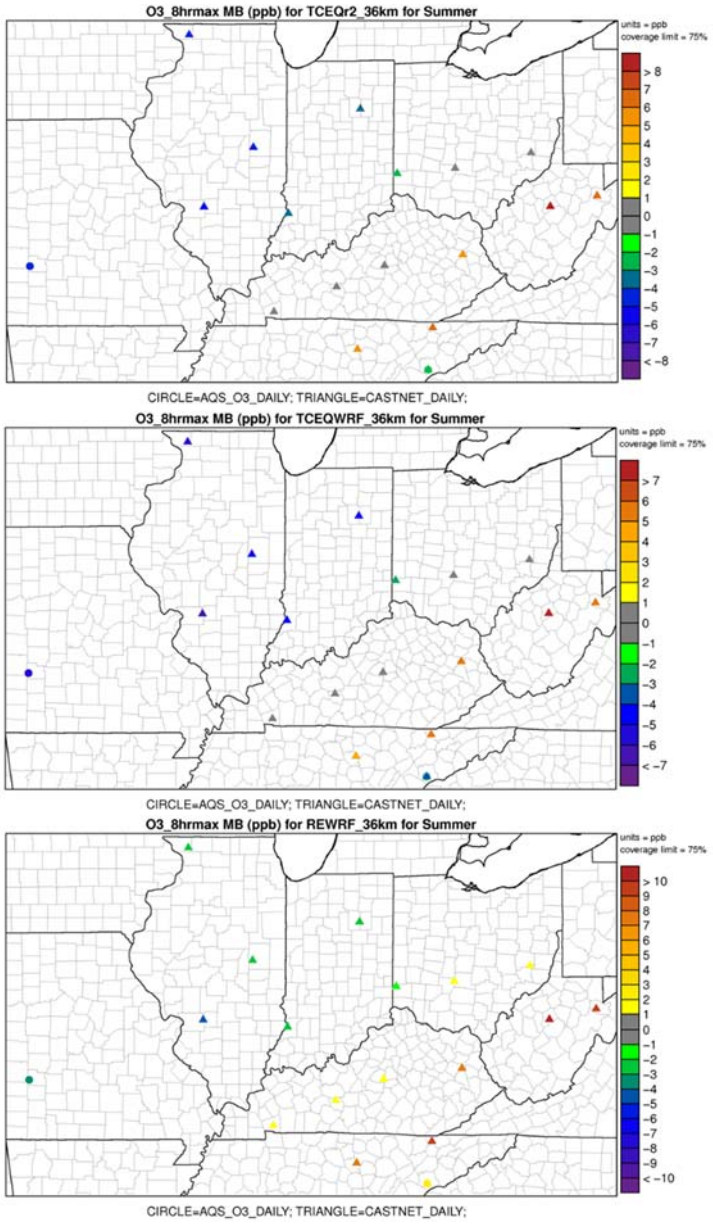

Figure A-9. MDA8 ozone Mean Bias (MB) for TCEQ_r2 (top), TCEQWRF (middle) and REWRF (bottom) at rural AQS and CASTNET monitoring sites in the Ohio/Tennessee Valley region during May – September 2012.

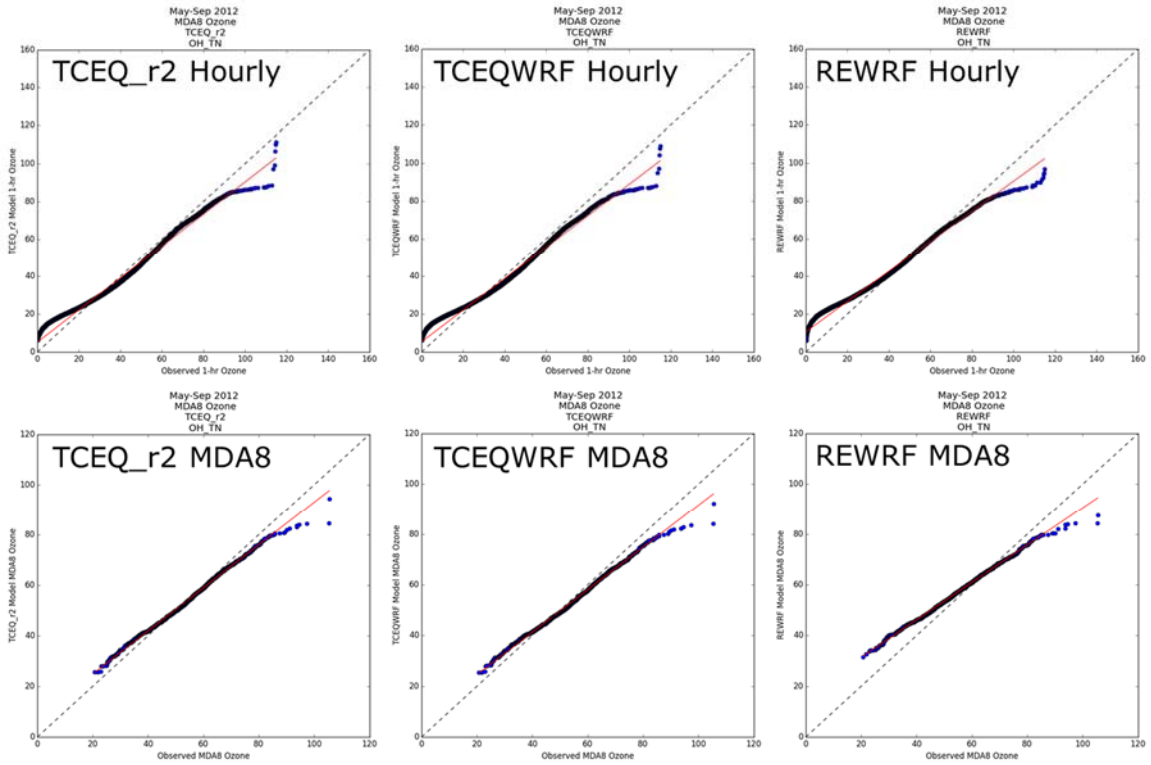

Figure A-10. Quantile-Quantile (Q-Q) plots of observed and modeled hourly (top) and MDA8 (bottom) ozone at AQS and CASTNET monitors in the Ohio/Tennessee Valley region in the 36 km CAMx modeling domain during May – September 2012. Red straight lines are from linear regression using the quantile-paired points.

Figure A-11 shows MDA8 ozone mean bias at rural AQS and CASTNET sites in the Southeastern U.S. All three simulations tend to overestimate MDA8 ozone in the Southeast US with a positive mean bias. Similar to findings in the Ohio/Tennessee Valleys, REWRF has higher ozone

concentrations than TCEQWRF.

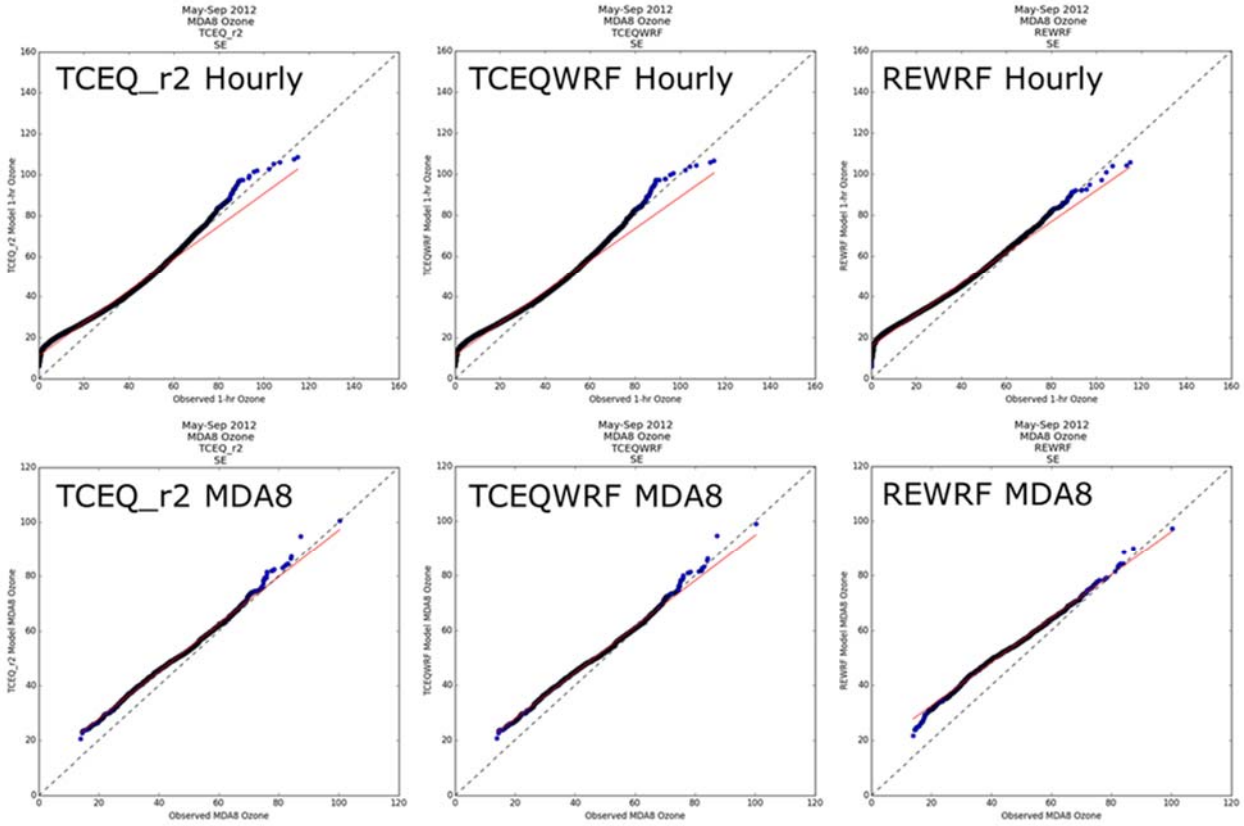

Figure A-12 presents the MDA8 ozone Q-Q plots for the same Southeastern U.S. monitors shown in Figure A-11. While the REWRF simulation still shows a pronounced positive bias for low observed ozone, performance is quite similar among the three simulations when for higher quantiles.

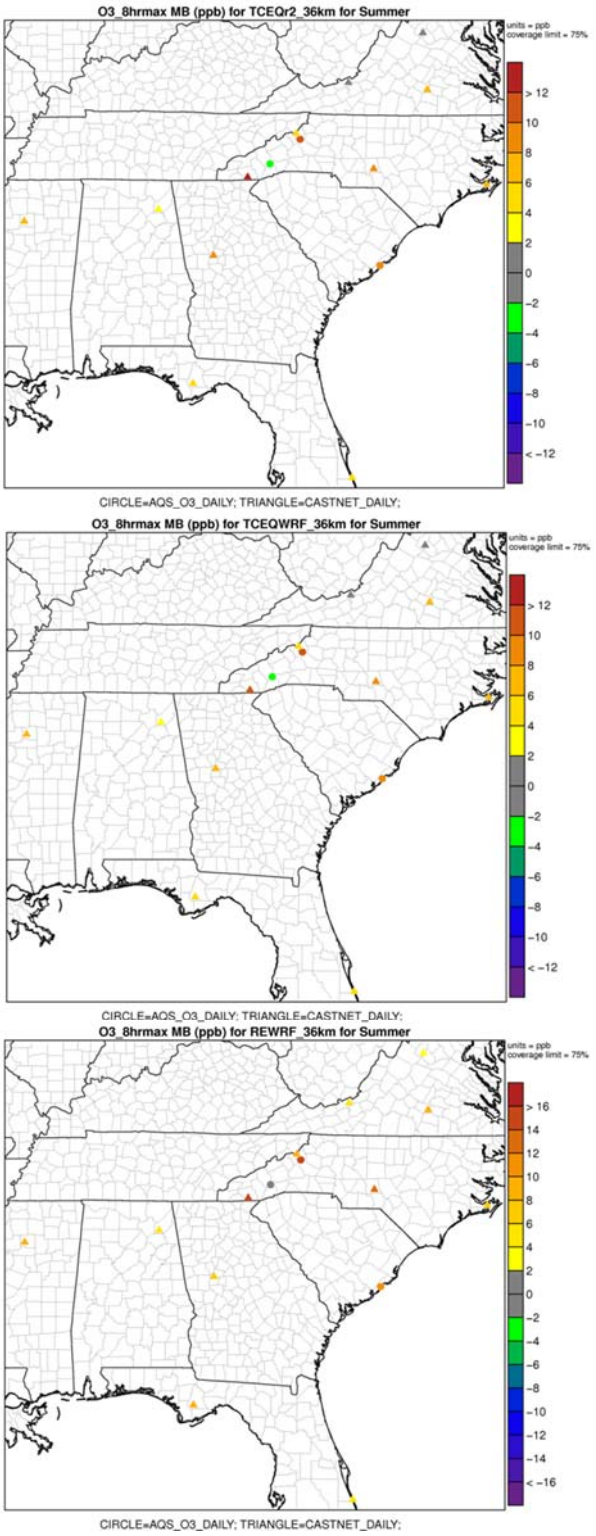

Figure A-11. MDA8 ozone Mean Bias (MB) for TCEQ_r2 (top), TCEQWRF (middle) and REWRF (bottom) at rural AQS and CASTNET sites in the Southeastern U.S. during May – September 2012.

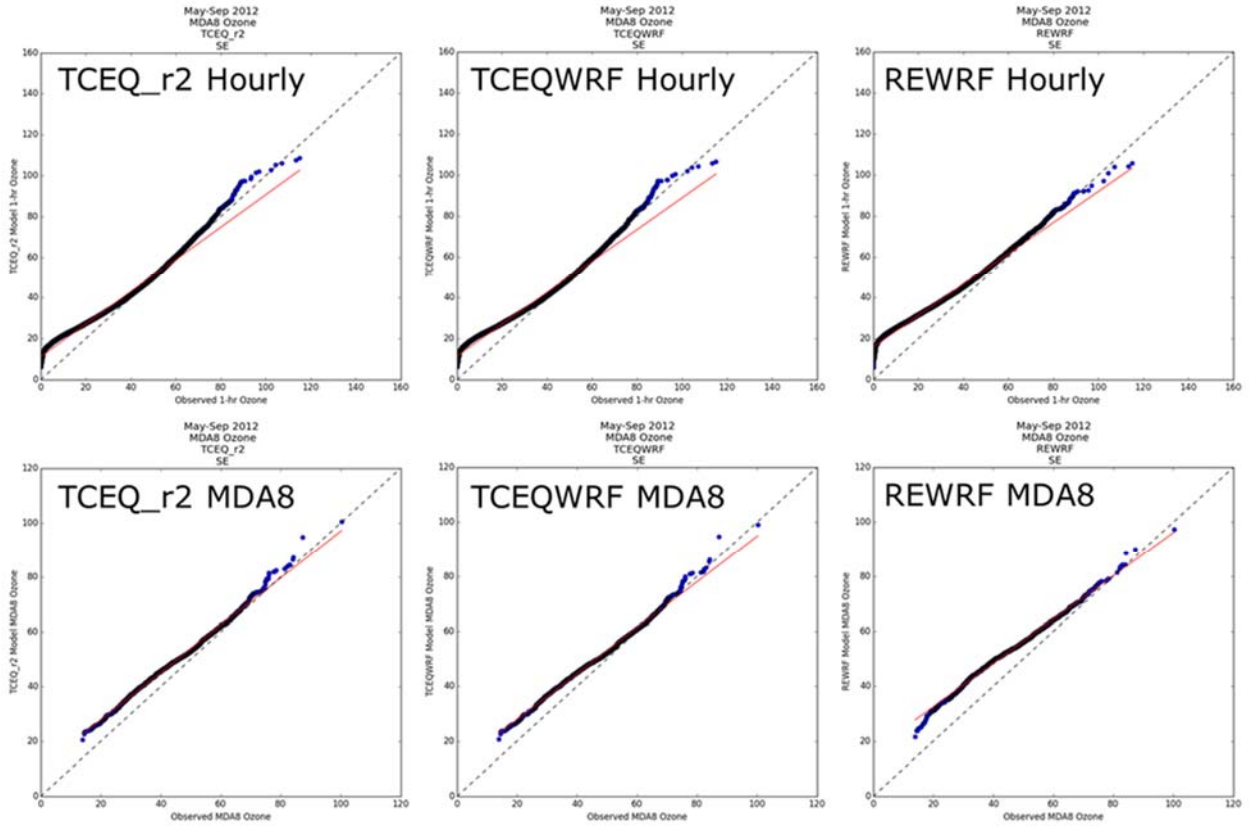

Figure A-12. Quantile-Quantile (Q-Q) plots of observed and modeled hourly (top) and MDA8 (bottom) ozone at rural AQS and CASTNET monitors in the Southeastern U.S. in the 36 km CAMx modeling domain during May – September 2012. Red straight lines are from linear regression using the quantile-paired points.

In summary, results from the ozone model performance evaluation at rural AQS and CASTNET sites in the Ohio/Tennessee Valleys and the Southeastern U.S. in the 36 km domain suggest that, compared to TCEQ_r2 and TCEQWRF, REWRF has the highest positive ozone biases in these potential source regions of ozone long range transport to Texas. This finding appears to be consistent with the largest positive biases of REWRF at lower quantiles in the regional MPE analysis for Texas and Dallas.

A.4 MDA8 Ozone Local Increment in and around Dallas

In this section, we analyze the MDA8 ozone LI produced by the Dallas-Fort Worth area to evaluate the model's ability to reproduce ozone enhancement due to photochemical production of ozone in the Dallas-Fort Worth region.

Figure A-13 displays a map of all Dallas-Fort Worth CAMS monitoring stations that are used in MDA8 ozone LI analysis. We classify the monitors with green pushpins as potential background sites (meaning that when they are upwind of the urban area they are indicative of rural/suburban ozone and not enhanced by urban photochemical production). To estimate background ozone, we calculate the median MDA8 ozone concentration across these monitors for each day. Because we expect only a few of these background monitors to be impacted by urban ozone on a particular day, the median should effectively screen out the influences of urban photochemical production. Then we find the difference between this median value and the maximum MDA8 ozone concentration across all monitors (red and green pushpins in Figure A-13) in the same region. We refer to this difference as the MDA8 ozone LI.

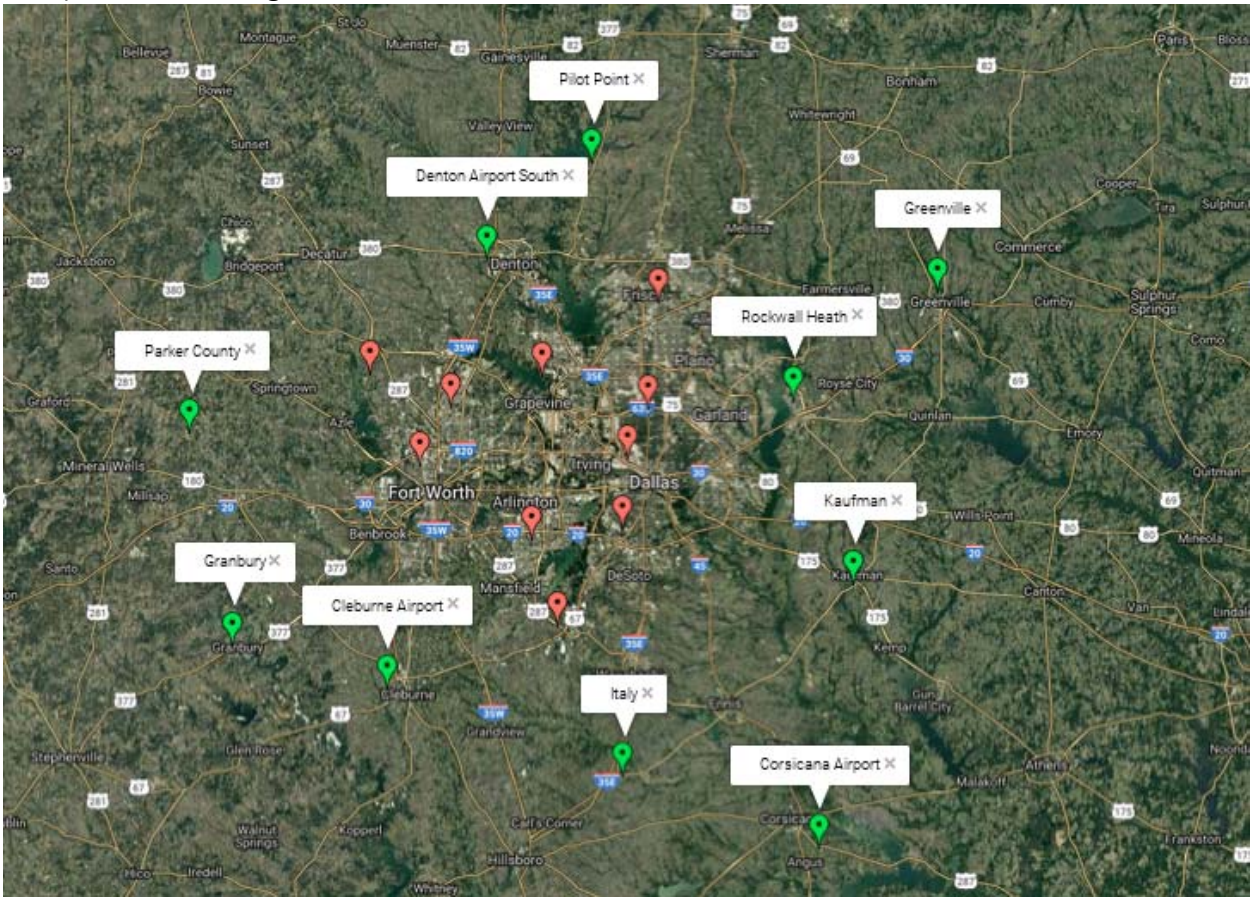

Figure A-13. Map of Dallas-Fort Worth CAMS monitoring locations. The 10 background sites used for the local increment analysis have green markers and are labeled.

Figure A-14 compares observed versus modeled MDA8 ozone Local Increment (LI) in the Dallas-Fort Worth region during May – September 2012, for the TCEQ_r2 and REWRF CAMx simulations. The comparisons are done separately for three observed LI ranges, i.e., when LI is not higher than 15 ppb (left), between 15 ppb and 25 ppb, and not lower than 25 ppb. The values of mean biases and errors for all three simulations are shown in Figure A-15.

When observed LI is lower than 15 ppb, REWRF shows good agreement with observations with a mean bias of 0.5 ppb and error of 3.1 ppb. TCEQ_r2 overestimates the mean LI by 1.9 ppb and has a slightly larger error of 3.5 ppb. We find slightly worse performance for the TCEQWRF simulation (MB: +2.6 ppb; ME: 3.8 ppb). Therefore, for LI less than 15 ppb, REWRF performs better than either TCEQ_r2 or TCEQWRF. When observed LI is between 15 and 25 ppb or larger than 25 ppb, all three simulations have negative LI biases. While TCEQ_r2 and TCEQ_WRF show similar performance, REWRF shows substantially worse mean bias and error values for these two LI ranges. The comparisons for the three LI ranges combined appears to point to a systematic underestimation of strong ozone production/enhancement events by REWRF, i.e., when observed LI is higher than 15 ppb. TCEQ_r2 and TCEQWRF agree with the observed LI better in spite of a slight positive bias when observed LI is lower than 15 ppb. The Q-Q plots in

Figure A-16 statistically illustrates REWRF's systematic low LI bias with its quantile points constantly below the 1:1 line, and the better agreement of TCEQ_r2 with almost all quantiles of observed LI than REWRF.

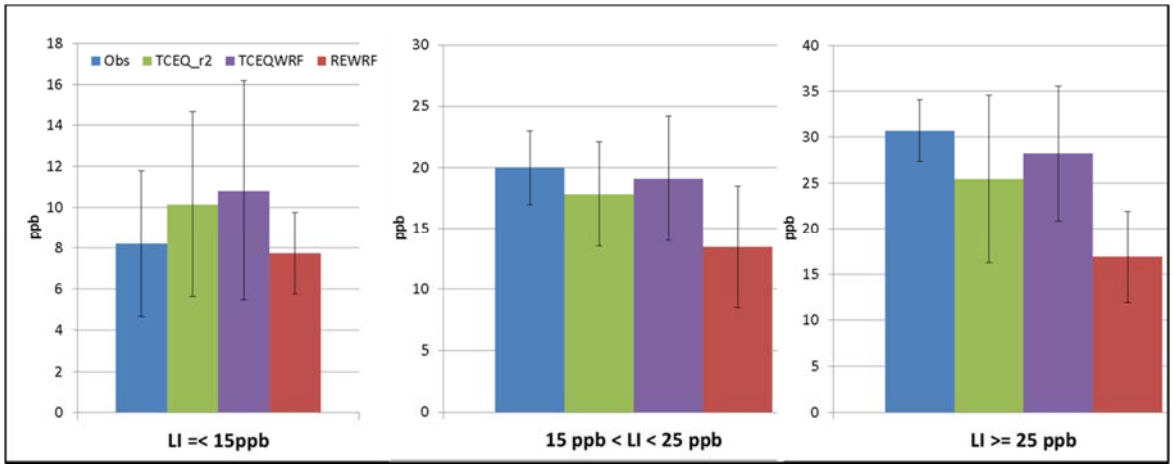

Figure A-14. Observed versus modeled MDA8 ozone Local Increment (LI) in the Dallas-Fort Worth region during May – September 2012 for the TCEQ_r2 (green), TCEQWRF (purple) and REWRF (red) CAMx simulations, when LI is less than 15 ppb (left), between 15 ppb and 25 ppb, and greater than 25 ppb. Black centered bars represent +/- 1 standard deviation.

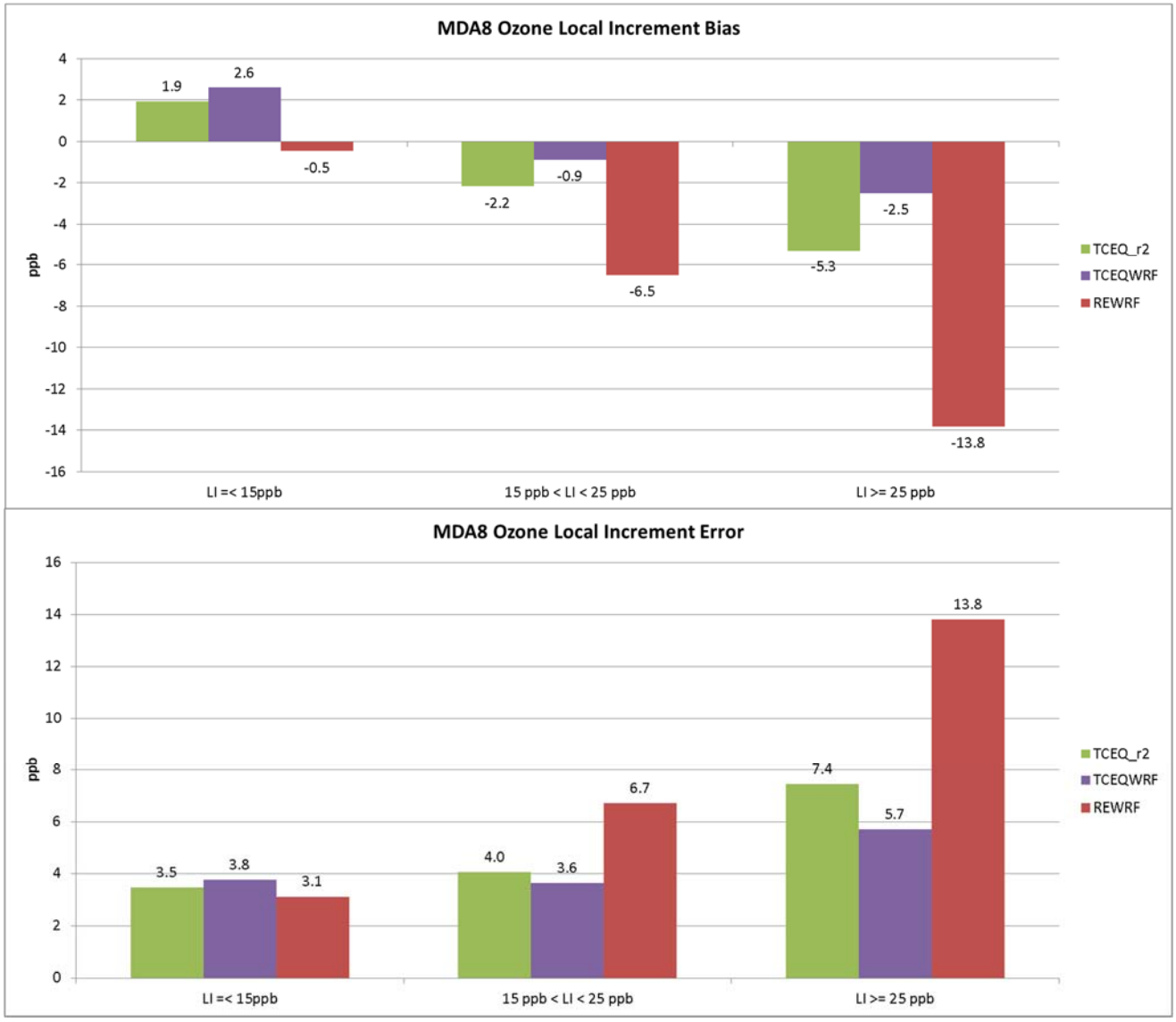

Figure A-15. MDA8 ozone Local Increment (LI) mean bias (upper) and mean error (lower) in and around the Dallas-Fort Worth region during May – September 2012 for the TCEQ_r2 (green), TCEQWRF (purple) and REWRF (red) CAMx simulations.

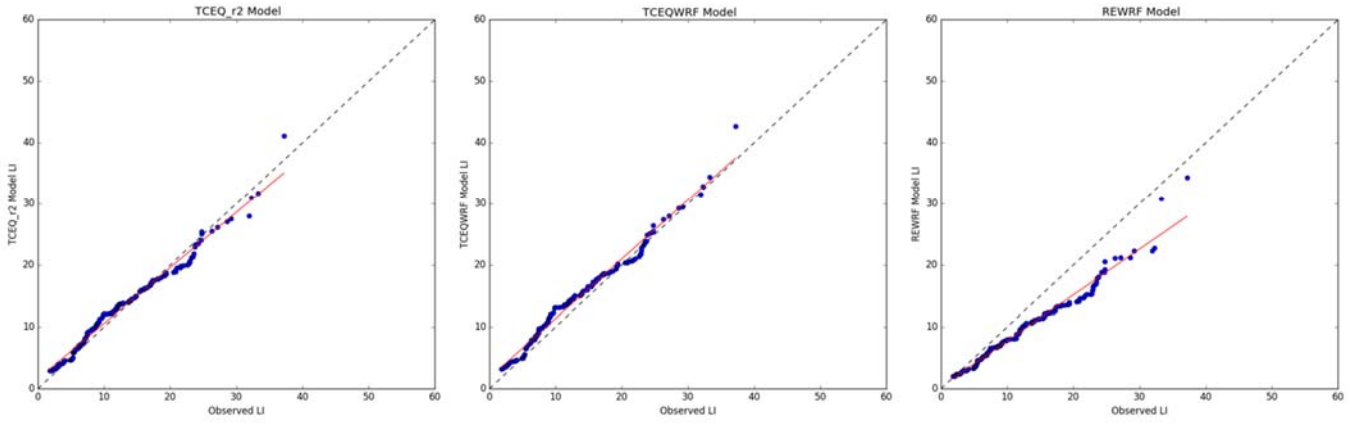

Figure A-16. Quantile-Quantile (Q-Q) plots of observed and modeled MDA8 ozone Local Increment (LI) in and around the Dallas-Fort Worth region during May – September 2012 for the TCEQ_r2 (left), TCEQWRF (middle) and REWRF (right) CAMx simulations. Red straight lines are from linear regression using the quantile-paired points.

In summary, MDA8 ozone local increment (LI) analysis for the Dallas-Fort Worth region suggests that the TCEQ_r2 and TCEQWRF simulations perform better than REWRF in reproducing observed local enhancement of ozone due to photochemical production when the observed LI is greater than 15 ppb. REWRF slightly outperforms the other two simulations when observed LI is lower than 15 ppb.

A.5 Ozone Performance in and around the Killeen-Temple-Fort Hood (KTF) Area

In this section, we examine and compare model performance at individual CAMS monitors in the 7-county KTF Area as well as its upwind areas. Figure A-17 shows the locations of the five CAMS monitors used in the model performance evaluation. Killeen Skylark Field (CAMS 1047) is in Bell County in the KTF area; Waco Mazanec (CAMS 1037) lies to the northeast of the Waco city center; Hutto College Street (CAMS 6602) and Lake Georgetown (CAMS 690) are in the Austin area, which are upwind of the KTF area during southerly winds; the Northwest Harris County monitor (CAMS 26) is in the Houston area, which is upwind of the KTF area during southeasterly winds.

We present time series of observed versus modeled MDA8 ozone individually at all five sites, and compare the model performance by TCEQ_r2, TCEQWRF, and REWRF using quantitative metrics of model bias and error, as well as correlation with observed concentrations. In addition, Q-Q plots are also presented to assess the overall pattern of modeled concentrations against the observations.

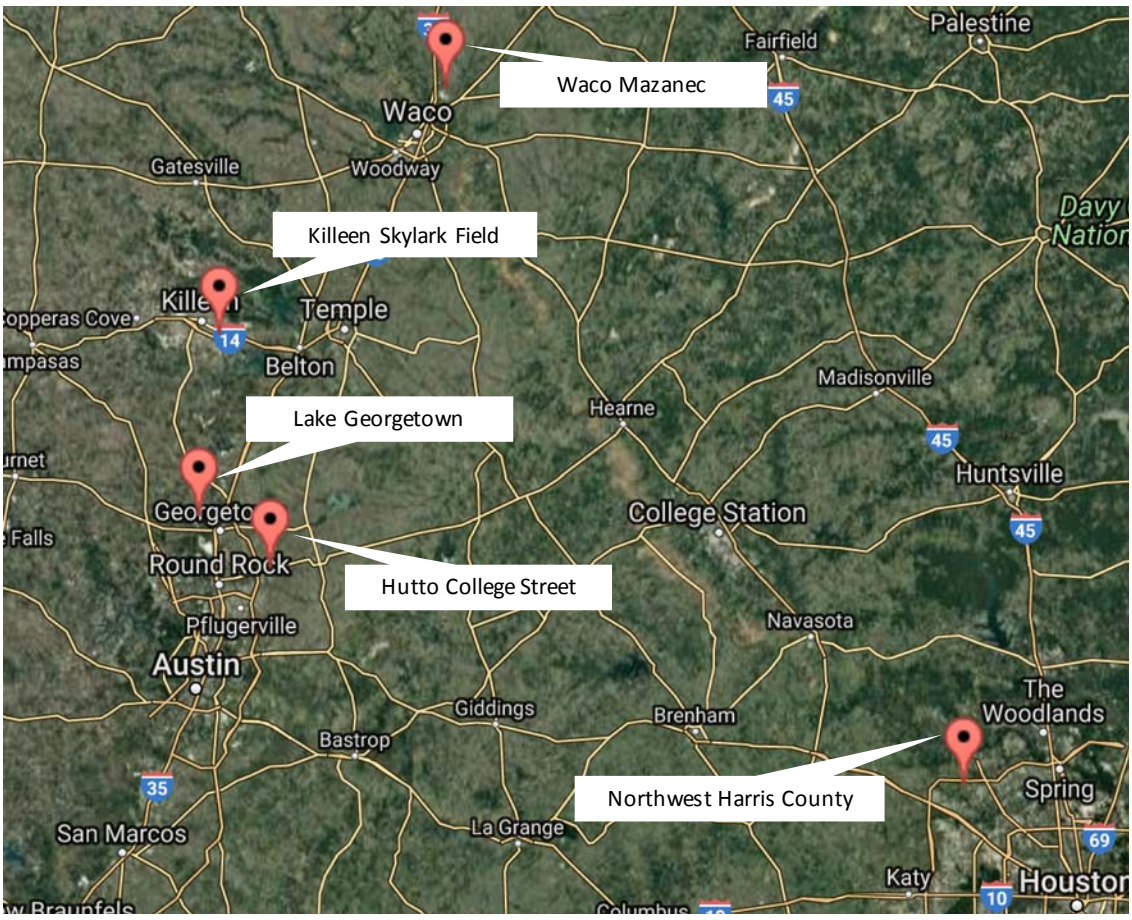

Figure A-17. Map of monitoring sites in and around the KTF area.

Figure A-18 shows time series of observed versus modeled MDA8 ozone (upper) and model biases (lower) at the Killeen Skylark Field (CAMS 1047) monitor for all three model simulations. Observed MDA8 ozone spans from 20 ppb to slightly above 80 ppb (only one instance). Each of the three model simulations largely captures the overall observed trend and range of MDA8 ozone. Among the three simulations, REWRF is markedly different from TCEQ_r2 and TCEQWRF, while the latter two closely track each other. In terms of quantitative performance metrics, TCEQ_r2 and TCEQWRF have the same NME, RMSE and R^2, while TCEQWRF has slightly lower NMB (2.5 ppb) than TCEQ_r2 (3.3 ppb); in comparison, REWRF has higher NMB, larger RMSE and NME, but lower R^2, suggesting inferior performance to these two models. Figure A-19 shows Q-Q plots of observed versus modeled hourly (upper) and MDA8 (lower) ozone for the three models. TCEQ_r2 and TCEQWRF exhibit very similar statistical distributions for both hourly and MDA8 ozone. For hourly ozone, both models agree with the observed quantile distribution in the 30 – 60 ppb range, but have a low bias when observed ozone is above 60 ppb and a high bias when observed ozone is below 30 ppb. For MDA8 ozone, TCEQ_r2 and TCEQWRF have a high bias for observed quantiles lower than 60 ppb, and a low bias for observed quantiles higher than 60 ppb. REWRF is distinctly different from TCEQ_r2 and TCEQWRF, with larger overestimate for both hourly and MDA8 ozone for observed quantiles lower than 60 ppb. In sum, quantitative MPE metrics and Q-Q plots suggest very similar

performance between TCEQ_r2 and TCEQWRF, and inferior performance of REWRF to these two models.

Ozone time series (Figure A-20) and Q-Q plots (Figure A-21) for the Waco Mazanec (CAMS 1037) site exhibit very similar features to those found at Killeen Skylark Field. TCEQ_r2 and TCEQWRF have the same R^2 (0.69) while TCEQWRF has smaller NMB, NME, and RMSE than TCEQ_r2. Compared to these two models, REWRF has larger NMB, NME, and RMSE, but lower R^2. Q-Q plots also reveal a stronger tendency to overestimate ozone by REWRF than TCEQ_r2 and TCEQWRF when the observed concentrations are lower than 60 ppb.

Figure A-22 through Figure A-25 show MPE results for the Hutto College Street site (CAMS 6602) and Lake Georgetown site (CAMS 690) in the Austin area. Overall, all three models tend to overestimate MDA8 ozone at these two sites, with the minimum NMB of the three being higher than 18% and 10% for the two sites, respectively, which suggest stronger overestimating tendency than at the two sites in the KTF area discussed above, where the maximum NMB among the three models is only 8.1%. Confidingly, the Q-Q plots also reveal a high bias in MDA8 ozone for all three models, which is seen at almost all quantiles at Hutto College Street and at all quantiles lower than 70 ppb at Lake Georgetown. Q-Q plots for hourly ozone suggest a slight overestimation in the 30-60 ppb quantiles by the three models. Compared to the other two models, for both MDA8 and hourly ozone, REWRF has a strong tendency to overestimate at quantiles lower than 60 ppb, while underestimating concentrations above 60 ppb, constituting a flatter slope on the Q-Q plots than the other two models. A quantitative comparison of MPE metrics in the time series plots (Figure A-22 and Figure A-24) suggests that TCEQ_r2 and TCEQWRF are very similar with better performance than REWRF with respect to all metrics; in particular, REWRF exhibits a larger high bias (3 – 4 ppb of NMB) than the other two models.

Figure A-26 and Figure A-27 show MPE results for the Northwest Harris County monitor in the Houston area. Compared to the other sites discussed so far, the observed ozone concentrations at this site has a larger range that extends to above 100 ppb. While all three models show a tendency to overestimate ozone, TCEQ_r2 and TCEQWRF exhibit lower biases during the high ozone episodes than REWRF. Overall, compared to TCEQ_r2 and TCEQWRF, REWRF shows a flatter regression slope in the Q-Q plots and inferior performance with respect to all metrics. TCEQWRF has slightly smaller bias and error than TCEQ_r2.

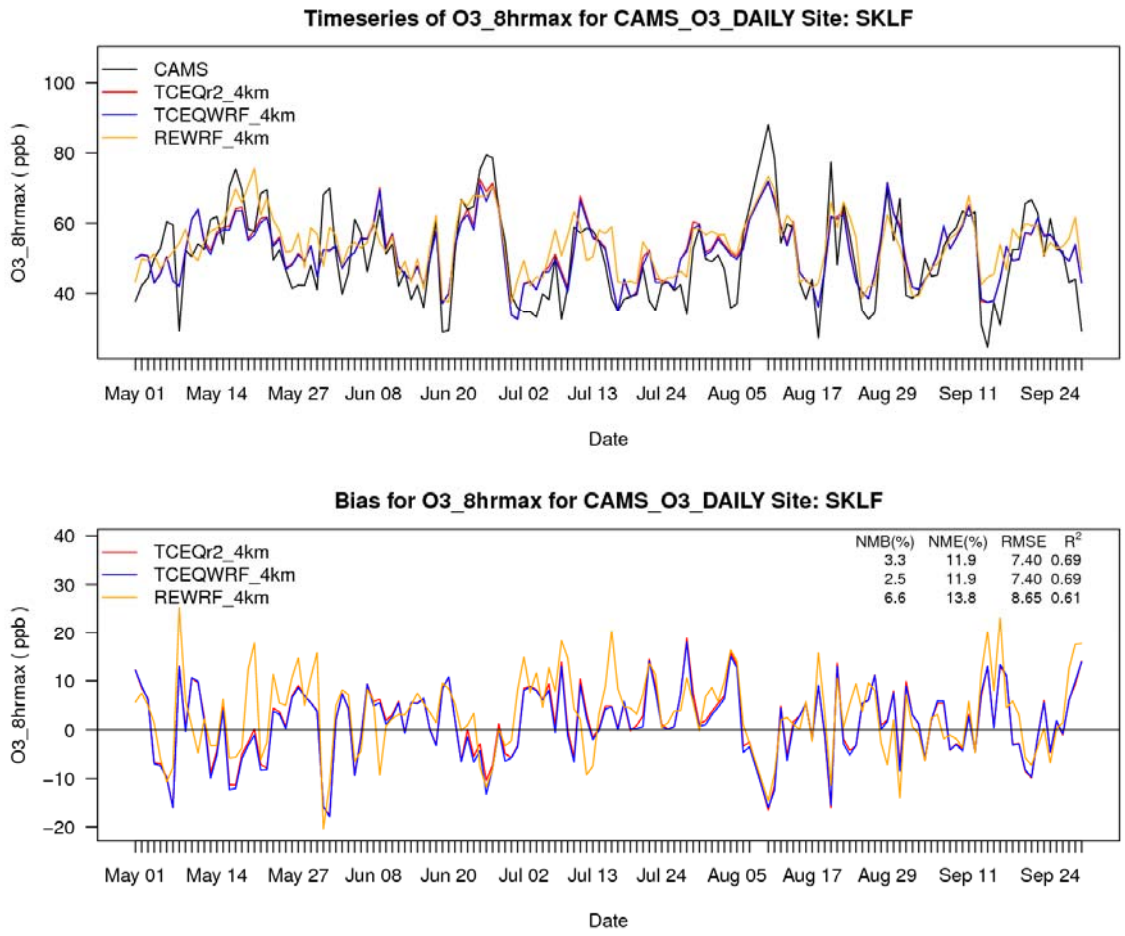

Figure A-18. Time series of observed versus modeled (upper) MDA8 ozone and model biases (lower) at the Killeen Skylark (CAMS 1047) monitor for May – September 2012.

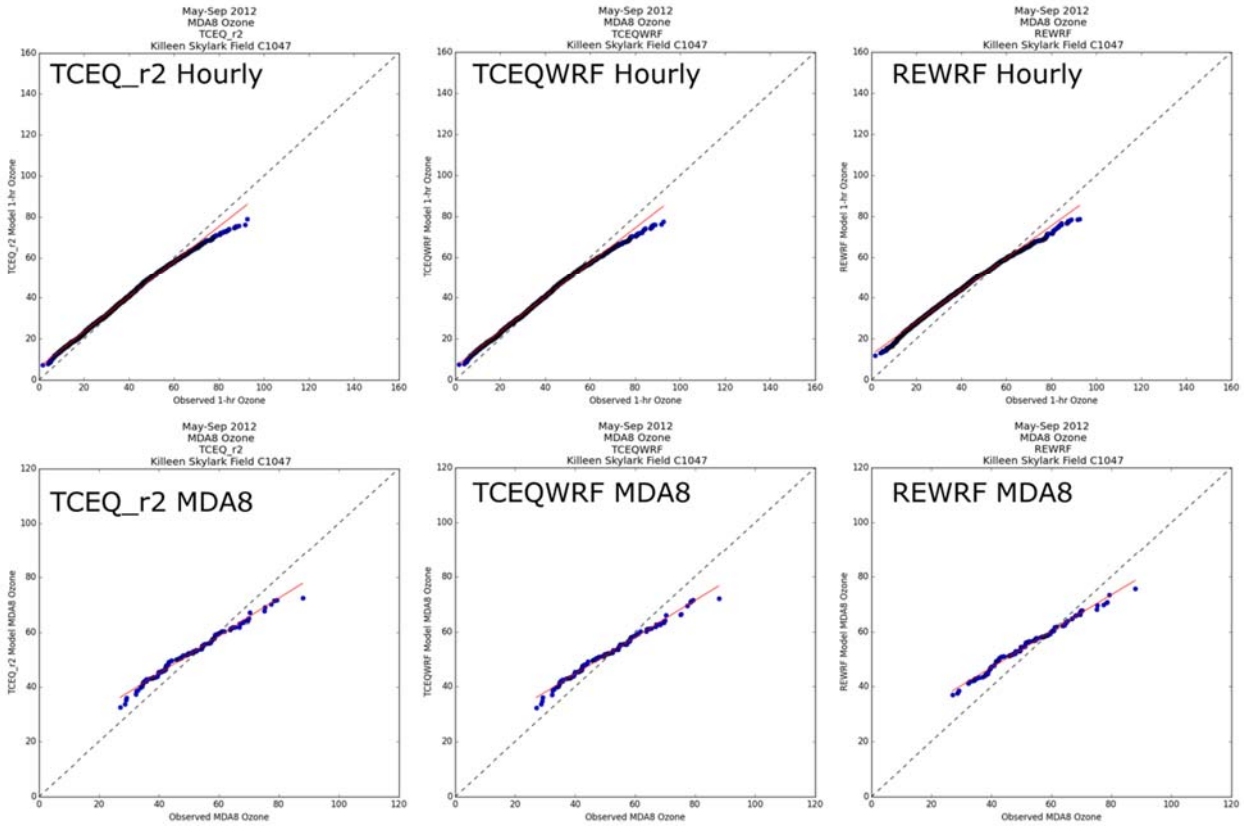

Figure A-19. Quantile-Quantile (Q-Q) plots of observed versus modeled hourly (upper) and MDA8 (lower) ozone for the TCEQ_r2 (left), TCEQWRF (middle) and REWRF (right) CAMx simulations at the Killeen Skylark (CAMS 1047) monitor for May – September 2012.

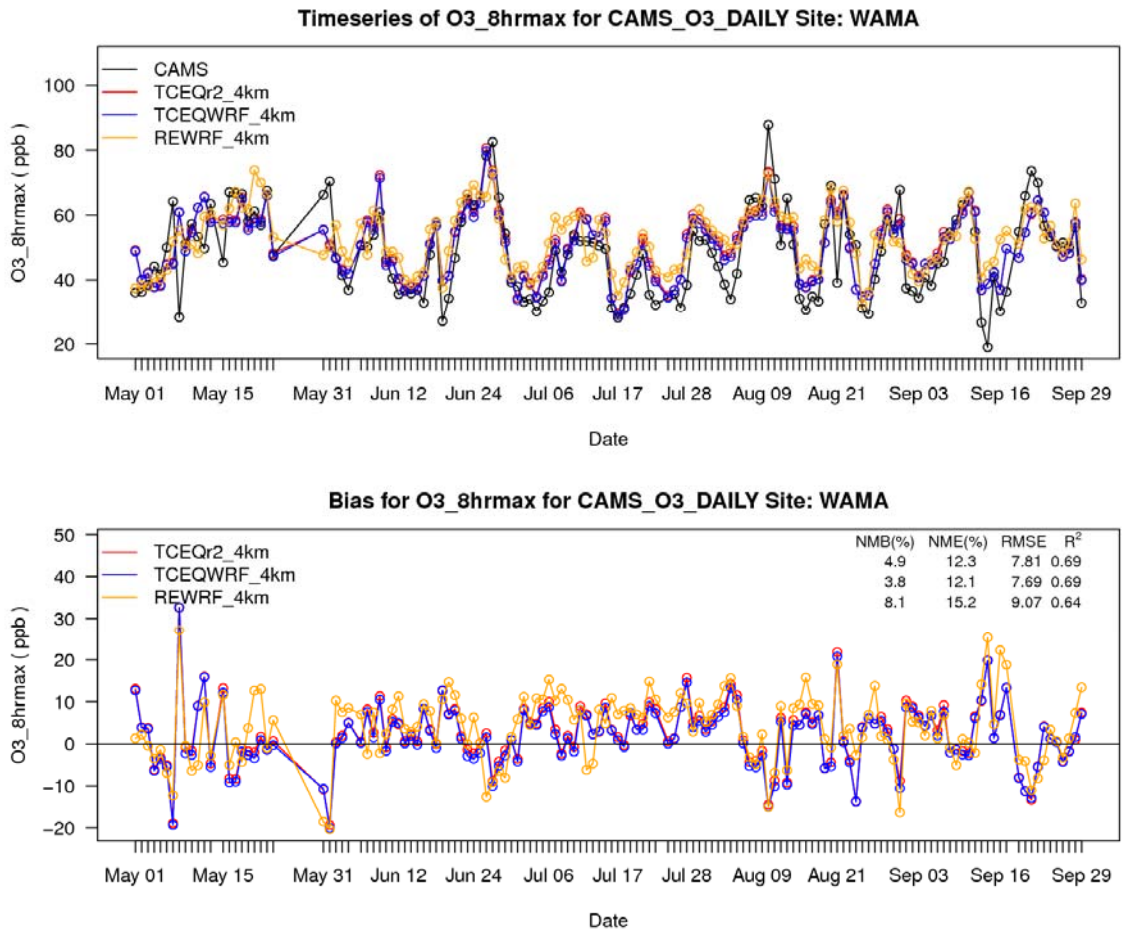

Figure A-20. Time series of observed versus modeled (upper) MDA8 ozone and model biases (lower) at Waco Mazanec (CAMS 1037) for May – September 2012.

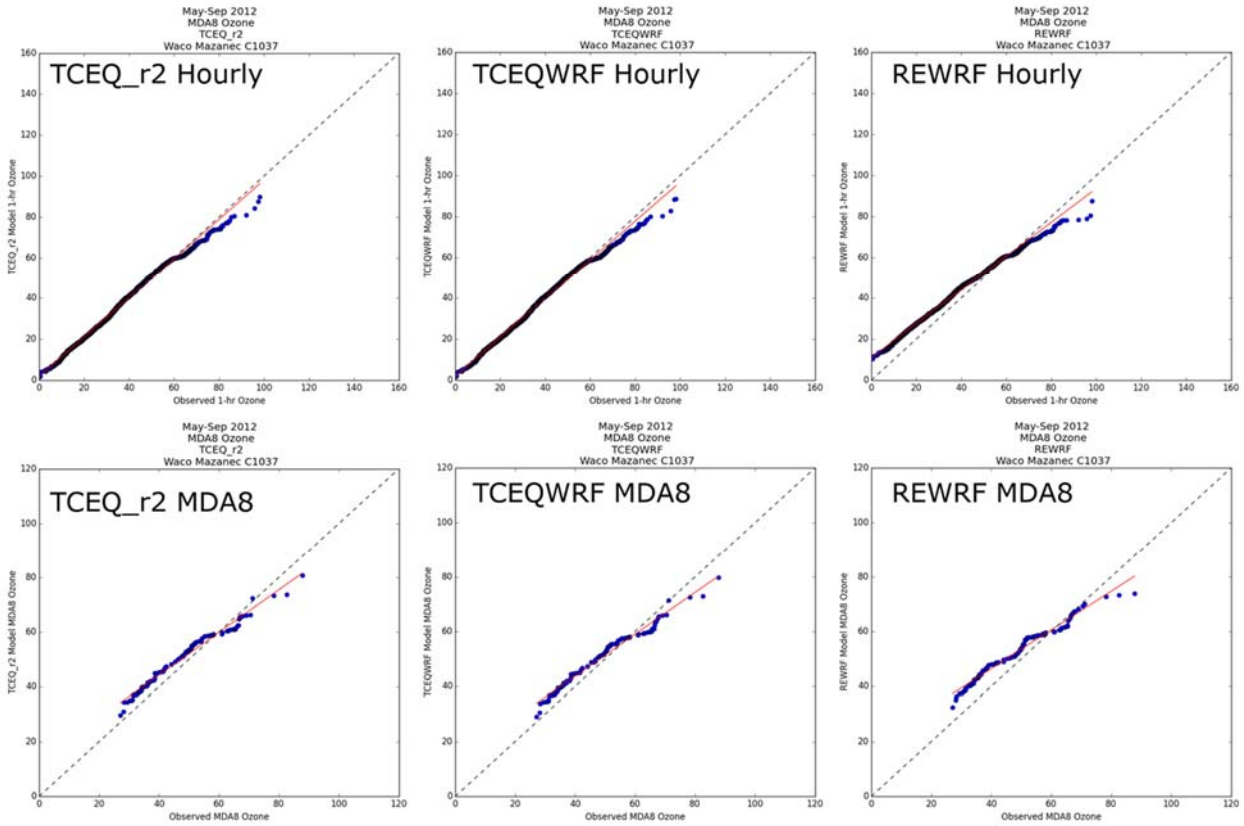

Figure A-21. Quantile-Quantile (Q-Q) plots of observed versus modeled hourly (upper) and MDA8 (lower) ozone for the TCEQ_r2 (left), TCEQWRF (middle) and REWRF (right) CAMx simulations at Waco Mazanec (CAMS 1037) for May – September 2012.

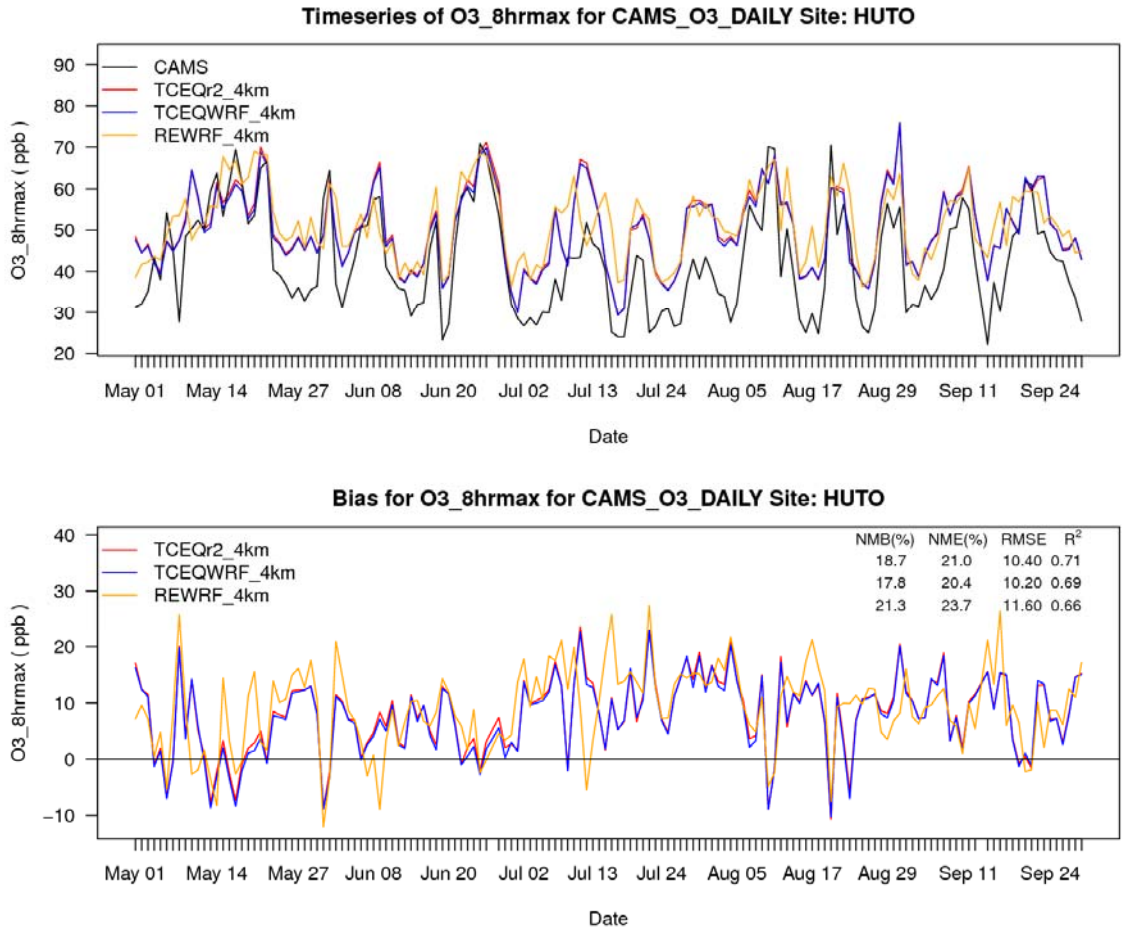

Figure A-22. Time series of observed versus modeled (upper) MDA8 ozone and model biases (lower) at the Hutto College Street (CAMS 6602) monitor for May – September 2012.

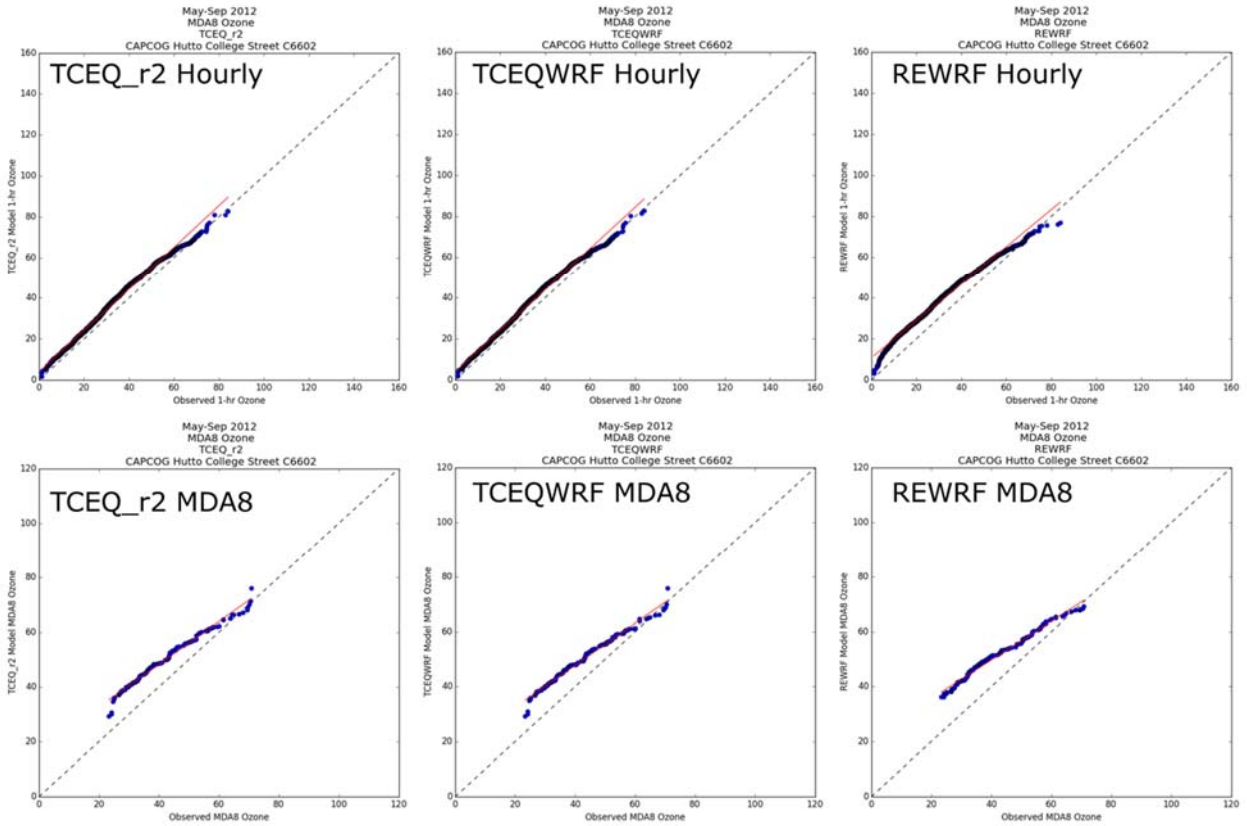

Figure A-23. Quantile-Quantile (Q-Q) plots of observed versus modeled hourly (upper) and MDA8 (lower) ozone for the TCEQ_r2 (left), TCEQWRF (middle) and REWRF (right) CAMx simulations at the Hutto College Street (CAMS 6602) monitor for May – September 2012.

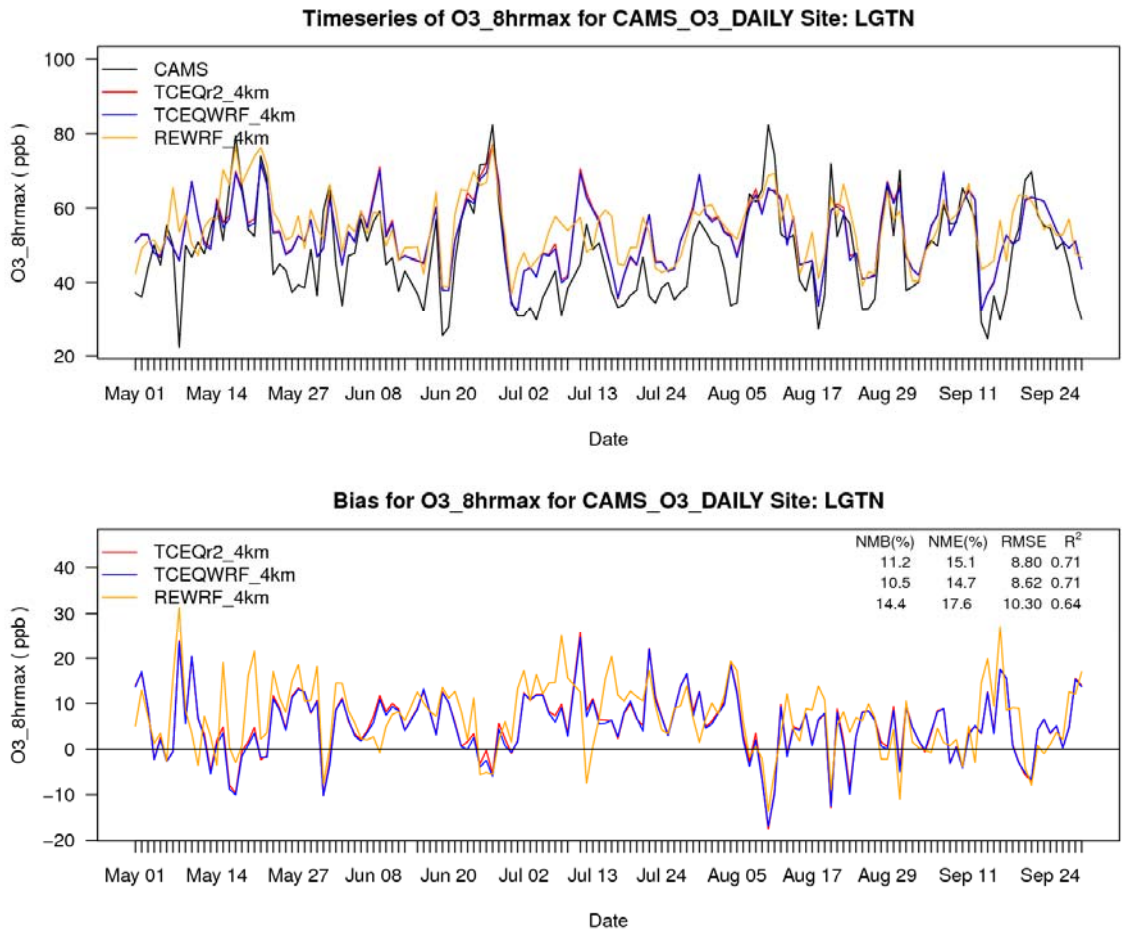

Figure A-24. Time series of observed versus modeled (upper) MDA8 ozone and model biases (lower) at the Lake Georgetown (CAMS 690) monitor for May – September 2012.

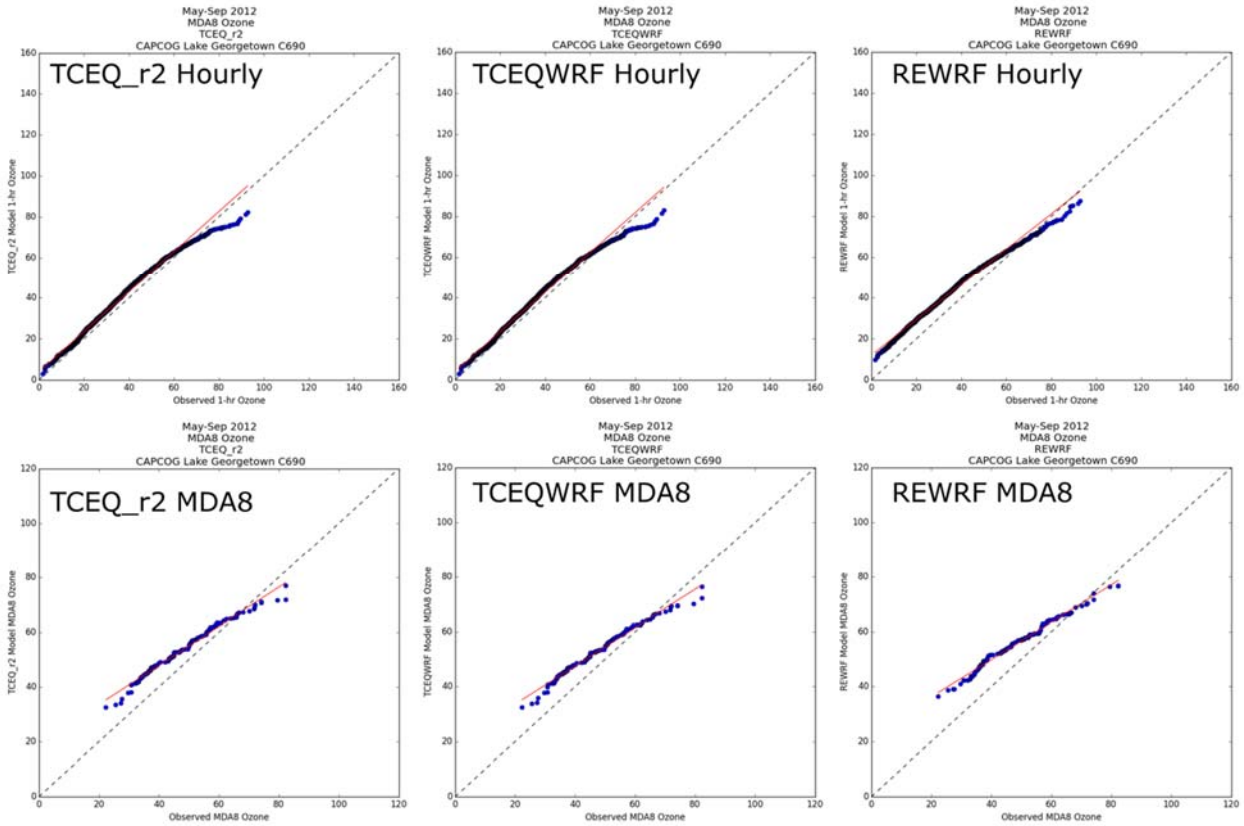

Figure A-25. Quantile-Quantile (Q-Q) plots of observed versus modeled hourly (upper) and MDA8 (lower) ozone for the TCEQ_r2 (left), TCEQWRF (middle) and REWRF (right) CAMx simulations at the Lake Georgetown (CAMS 690) monitor for May – September 2012.

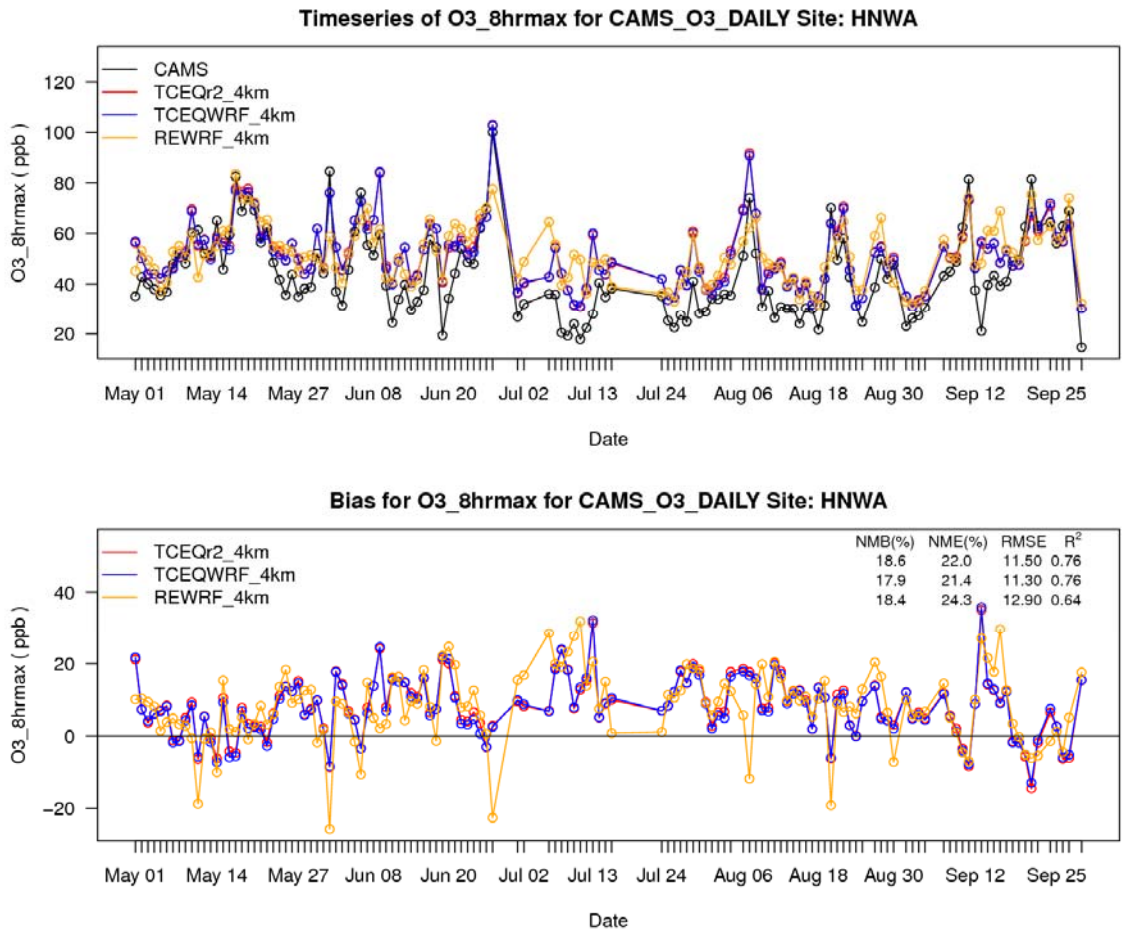

Figure A-26. Time series of observed versus modeled (upper) MDA8 ozone and model biases (lower) at the Northwest Harris County (CAMS 26) monitor for May – September 2012.

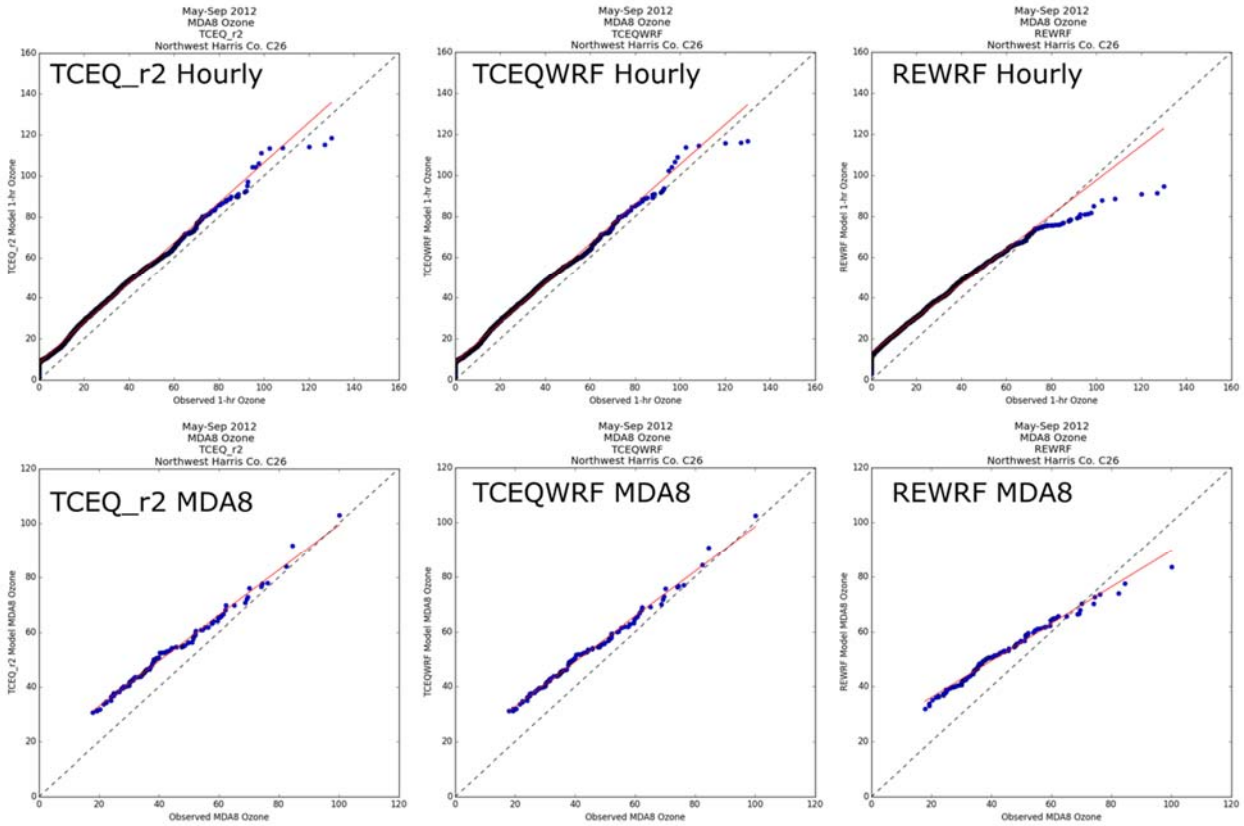

Figure A-27. Quantile-Quantile (Q-Q) plots of observed versus modeled hourly (upper) and MDA8 (lower) ozone for the TCEQ_r2 (left), TCEQWRF (middle) and REWRF (right) CAMx simulations at the Northwest Harris County (CAMS 26) monitor for May – September 2012.

A.6 Overall Assessment

Our 2012 ozone model performance evaluation shows that the TCEQWRF simulation demonstrates the best overall performance. In particular, the REWRF simulation has higher biases (modeled ozone is too high when observed ozone is low and too low when observed ozone is high) than the other two simulations. We therefore used the TCEQWRF ozone model for the ozone source apportionment and source sensitivity analyses. While we do note a negative bias for higher observed ozone measurements, especially at sites outside the urban areas, we do not anticipate substantial impacts to the analyses performed in Section 4 and 5. Overall, we find improved ozone model performance compared to previous KTF modeling efforts. In particular, we observe better ozone model performance at the Killeen monitor during the June 2012 high ozone period.

We summarize key findings from our evaluation as follows:

- MPE results on a regional level using all CAMS sites in the Dallas-Fort Worth region and the Texas 4 km modeling domain suggest that TCEQ_r2, TCEQWRF, and REWRF share a systematic high bias of ozone at lower quantiles when observed concentrations are under about 60 ppb, and a systematic low bias at higher quantiles when observed concentrations are above about 60 ppb. Previous KTF modeling of June 2012 found persistent positive ozone biases at the Killeen monitor throughout the modeling episodes with substantial negative biases when observed ozone was highest (Kemball-Cook et al., 2015). This study finds that the model still shows negative ozone biases during periods of high ozone in June 2012, but the persistent positive ozone biases are substantially reduced. While TCEQ_r2 and TCEQWRF exhibit comparable performance, REWRF has larger positive biases at lower quantiles. Results from the ozone evaluation at rural AQS and CASTNET sites in the Ohio/Tennessee Valley regions and the Southeastern U.S. in the 36 km domain suggest that, among the three models, REWRF has the largest positive bias at lower observed ozone concentrations in these potential source regions of ozone long-range transport to Texas.
- MDA8 ozone local increment (LI) analysis in the Dallas-Fort Worth region shows that TCEQ_r2 (and TCEQWRF) perform better than REWRF in reproducing observed local enhancement of ozone due to photochemical production when the observed LI is greater than 15 ppb; REWRF performs the best with a small negative bias when observed LI is lower than 15 ppb, while TCEQ_r2 and TCEQWRF have small positive biases.
- When the performance at five individual sites in and upwind of the KTF area is compared, TCEQ_r2 and TCEQWRF share very similar modeled time series, quantile distributions, and overall model performance, while the use of updated CAMx chemical mechanism and physics options by TCEQWRF led to improved performance at all six sites, in terms of most but not all MPE metrics. Compared to TCEQ_r2 and TCEQWRF, REWRF exhibits inferior performance at all five sites; it also exhibits flatter Q-Q statistical distribution that suggests its weaker skill in capturing the observed dynamical range of ozone.

- Results from MPE analysis on a regional level, LI analysis in the Dallas-Fort Worth region, and MPE at individual sites in and around the KTF area combined highlight a systematic ozone overestimation with all three models when observed ozone is below around 60 ppb. This positive bias points to an overestimated background concentration on a regional level.
- The use of the most updated CAMx chemical mechanism and physics options by TCEQWRF leads to small but consistent improvement in performance. The different meteorological input utilized by REWRF causes modeled background ozone to deviate from observed ozone relative to the other two model simulations. The cause of such a modeled high bias in background ozone is not known.

APPENDIX B

CAMx Decoupled Direct Method Probing Tool

Appendix B 2012 CAMx Decoupled Direct Method Probing Tool

B.1 Overview of CAMx Decoupled Direct Method

The DDM probing tool (Dunker et al., 2002) was used to determine ozone impacts of the Panda Temple EGU facility and Fort Hood military base by calculating the sensitivity of modeled ozone to the NOx emissions of the two sources. We focused on the sensitivity of ozone to NOx emissions because ozone formation in the KTF area is NOx-limited (Grant et al., 2017; Kemball-Cook et al., 2015). The CAMx DDM probing tool can calculate the sensitivity of predicted concentrations to pollutant sources (e.g., emissions, initial conditions, boundary conditions) and to chemical rate constants. Sensitivities are calculated explicitly by specialized algorithms implemented in the host CAMx model.

We define a "sensitivity coefficient" (s) which represents the change in concentration (c) of a modeled chemical species with respect to some input parameter (λ), evaluated relative to the base state ($\lambda=\lambda_0$),

$$s = \left.\frac{\partial c}{\partial \lambda}\right|_{\lambda_o}$$

In general, λ can be a vector (denoted $\underline{\lambda}$), which contains multiple parameters related to processes in the model (e.g., chemical rate constants) or inputs to the model (e.g., emissions). In this study, "c" is the ground level ozone concentration (in ppb) and λ corresponds to the NOx emissions (in tpd) from the Panda Temple EGU facility. The base state λ_0 is the TCEQ 2017 emission inventory that does not contain emissions from the Panda Temple facility. (The same procedure was applied to the Fort Hood NOx emissions.)

The response of concentration to a change in $\underline{\lambda}$ about the base state λ_0 can be represented by a Taylor series of sensitivity coefficients:

$$c(\underline{x},t;\underline{\lambda}) = c(\underline{x},t;\underline{\lambda}_0) + \sum_{i=1}^{n} \left.\frac{\partial c}{\partial \lambda_i}\right|_{\underline{\lambda}_o} (\lambda_i - \lambda_{i0}) + \ldots (higher\ \ order\ \ terms)$$

where n is the number of $\underline{\lambda}$ vector elements, $\underline{x}$ is the spatial dimension vector, and t is time. If the magnitude of the input perturbation is small, the output response will become dominated by the first-order sensitivity. This is the case in the present study, where the perturbations are the NOx emissions from Panda Temple EGU and Fort Hood military base, which have emissions of 1.0 tpd and 3.1 tpd, respectively, while the entire NOx emission inventory for the KTF area is approximately 43.6 tpd (see Figure 4-1). The increased NOx emissions from the Panda Temple

facility represents a perturbation of approximately 2.3% to the KTF area NOx emission inventory and the additional Fort Hood emissions represents a 7.1% perturbation. Therefore it is reasonable to expect that the output ozone response will be linear and dominated by the linear first-order sensitivity term.

The DDM calculates the first-order sensitivity $s_i^{(1)}(\underline{x},t)$ with respect to the scalar parameter λ_i. The Taylor series to first order then gives the estimate:

$$c_l\left(\underline{x},t;\lambda_i\right) \quad = \quad c_l\left(\underline{x},t;\lambda_i=0\right)+\lambda_i\times s_i^{(1)}\left(\underline{x},t\right)$$

where $c_l(\underline{x};t;\lambda_i)$ is the estimated model result for species *l* when the perturbed emission inventory (e.g. TCEQ base case 2017 inventory + Panda Temple EGU emissions) is used as input, and $c_l(\underline{x},t;\lambda_i=0)$ is the base case model result when only the base case TCEQ 2017 emission inventory is used as input.

APPENDIX C

Model Attainment Test Software (MATS) Ozone Design Value Analysis Method

Appendix C MATS Ozone Design Value Analysis Method

C.1 Overview of MATS Modeling Method

For ozone analysis, EPA's current recommended procedures for making future year ozone projections involve use of the model in a relative sense to scale observed site-specific current year 8-hour ozone Design Value Concentrations (DVCs) based on the relative changes in the modeled 8-hour ozone concentrations between the current year and the future year. The model-derived scaling factors are called Relative Response Factors (RRFs), and are based on the relative changes in the modeling results between the current year base case (2012) and the future-year (2017) emission scenarios. These EPA guidance procedures for performing 8-hour ozone DV projections have been codified in the MATS tool.

MATS performs two types of 8-hour ozone DV projections:

1. Projections at monitoring sites using observed 8-hour ozone Design Values.

2. Unmonitored area analysis (UAA) 8-hour ozone projections based on interpolation of the observed 8-hour ozone DVCs across the modeling domain to obtain gridded fields of 8-hour ozone projections.

The following general procedure was employed for projecting 2012 8-hour ozone Design Values (DVCs) at a monitoring site to 2017 future year DVFs:

1. The 2012 DVCs were obtained by averaging 8-hour ozone DVs for 2012 (average of 2010-2013 4th highest annual 8-hr daily max) through 2014 (average of 2012-2015 4th highest annual 8-hr daily maximum).
2. The RRFs, defined as the ratio of the average of modeled 8-hour daily maximum ozone concentrations for the 2017 future year emission scenario to the modeled 2012 base value "near" each monitor were developed for all days in which the 2012 base case ozone values are above a "threshold" value:
    - Here, "near" the monitor is defined as a grid cell size dependent array of cells centered on a monitor. As per EPA guidance, for 4 km grid cells, arrays of 3 x 3 grid cells were used.
    - RRFs were calculated using all days with base-year ozone concentrations near the monitor greater than or equal to 60 ppb, with the restriction that at least 1 modeling day should be included.
3. Apply the model-derived RRFs to the DVC to obtain a projected future year 8-hour ozone DV (DVF)
4. Truncate the future-year DVF to the nearest ppb.

The unmonitored area analysis feature of MATS is used to test for potential 8-hour ozone hotspots away from the monitors where Design Values are unavailable. The MATS procedure for conducting the unmonitored area attainment test consists of the following steps:

1. Interpolate the DVCs from the monitoring sites to each grid cell in the modeling domain.
2. Calculate gridded RRFs for each grid cell using the ratio of the average modeled future-year to current-year concentrations in each grid cell for all days in which the current-year daily maximum 8-hour ozone concentrations exceeds a threshold value.
3. The gridded RRFs are applied to the gridded DVCs to obtain an array of gridded future-year projected DVs (DVFs). Note that it is likely that portions of the modeling domain will have no projected DVFs because there were insufficient ozone days above 60 ppb to construct an RRF.

The MATS tool can also be supplied with ozone source apportionment model output to estimate relative contributions from emissions source regions and source categories to ozone DVFs. We utilized this technique in order to estimate each source category's impact on 2017 design values.

For the Panda Temple EGU analysis, we adopted a similar procedure for the DDM MATS analysis as the APCA MATS analysis described in Section 4.3.1. First, we applied a 100% decrease ($\lambda_i = -1$) to Panda Temple EGU NOx emissions sensitivities to generate a new set of gridded ozone model concentrations. These ozone concentrations, along with the base model 2017 ozone concentrations, were then provided to MATS in a similar manner to the APCA ozone contributions. We then used the MATS outputs to produce a spatial map that represents the 2017 DVF ozone impact from the Panda Temple EGU (Figure 5-4). We applied the same procedure to Fort Hood NOx emissions sensitivities to determine the 2017 DVF ozone impacts (map shown in Figure 5-6).